THE UNIVERSITY OF NORTH CAROLINA AT CHAPEL HILL

Institute of Marine Science, Morehead City Field Site
Fall 2018 Capstone Project

A Multifaceted Analysis of Processes Influencing Water Quality within the Atlantic Beach, NC Canal System

Aisha Booze-hall, Chelsea Brown, Rebecca Cooper, Allison Duprey, Avia Dolberry, Felix Evans, Jake Malone, Emily McGuirt, Carly Richardson, Zack Saklad, Suzie Schoolfield, Savannah Swinea, EmmaLi Tsai

Course Instructors: Dr. Stephen Fegley and Dr. Johanna Rosman
Field Site Director: Dr. Rachel Noble

TABLE OF CONTENTS

Abstract

Recreational waterways and related tourism are economically integral aspects of coastal communities but can harbor environmental challenges, such as degraded water quality. To characterize the water quality within the Atlantic Beach canal system, our study focused on two main canals, which are representative of both the simple and geometrically complex canals within this system. Water quality can be influenced by stormwater runoff introducing excess nutrients and septic waste into the system, generating phytoplankton blooms and increased bacterial concentrations. Our study found that nutrients, phytoplankton, and bacterial concentrations were highest at the end of the longer, more geometrically complex canal where flushing was minimal and residence time was longer. Sites with better water quality had high flushing and short residence times. Therefore, locations with potential water quality concerns would be present at the ends of the canals within the system. There is a need to investigate these parameters during other seasons in order to better characterize the water quality in the canal system to ensure continued economic contributions, promote human health, and sustain ecosystem services provided by these recreational waterways.

Introduction

As coastal development continues to expand, knowledge about the ways in which infrastructure impacts water systems is increasingly important. In North Carolina (NC), understanding the influences of development on water quality is critical given predicted population growth. Nationally, coastal counties make up 10% of land mass, but accommodate 39% of the population (NOAA, 2013). According to the North Carolina Office of State Budget and Management, the NC coastline is projected to experience population growth of 26% by 2020, and Carteret County, the broader region around the site of our study, is projected to grow by 12.9% (OSBM, 2017).

The focus of our study is the Atlantic Beach canal system. Historically, the canals offered waterfront real estate in a desirable location creating opportunity for waterfront access and tourism. In the summer months the local population of around 1,495 people can expand to roughly 45,000 individuals (HCP, 2008). This influx of people emphasizes the importance of maintaining high water quality. Anthropogenic runoff can have adverse effects on recreational waters typically used for swimming, kayaking, paddle boarding, boating, etc.

Two sites within the canal system were assumed representative of the differential tidal exposure and flushing dynamics within the canal system (Fig. 0.1). Site 1, the shorter canal, is representative of canals that are presumably more directly influenced by tides. Site 1 is approximately 238.0 m in length, 21.0-29.0 m wide, and 1.5 m deep at mean tide, and provides insight regarding short, near-sound canals. Site 2, the longer canal, is approximately 688 m in length, 30.0-73.0 m wide, and 1.5-4.5 m deep at mean tide, and is representative of a larger canal that is more geometrically complex and further from the sound relative to canals like Site 1. The study period occurred after Hurricane Florence made landfall in North Carolina on 9 September 2018, and both before and after Tropical Storm Michael made landfall on 11 October 2018. The influence of these weather events and antecedent rainfall were considered and incorporated into the interpretations.

The town of Atlantic Beach contacted the University of North Carolina at Chapel Hill Institute of Marine Science to assist in the assessment of water quality within the Atlantic Beach residential canal system. The purpose of this study was to determine the current state of water quality in the Atlantic Beach canal system and develop a better understanding of factors influencing water quality in the canals. This study was divided into six sections: (1) spatial analysis, (2) circulation and flushing, (3) nutrients, (4) primary production, (5) filtration, and (6) bacteria. Water samples were taken around two major storm events, Hurricane Florence and Tropical Storm Michael, that occurred during Fall 2018. These samples were used to identify nutrients, bacteria, and chlorophyll-a levels. The primary objective was to equip the town of Atlantic Beach with the appropriate water quality information to assist in management efforts associated with the canal system.

Figure 0.1 *(right)* Map of the section of the Atlantic Beach Canal System that was analyzed. The canals are positioned north of Atlantic Beach and south of Bogue Sound. For the purpose of this paper, Site 1 will refer to the shorter canal and Site 2 will refer to the larger, bent canal. Each canal was further divided into subsections, labeled 1A-B and 2A-C accordingly.

Chapter 1: Spatial Analysis

1. INTRODUCTION

The Atlantic Beach canal system may be vulnerable to water quality impairment due to runoff (Duda & Cromartie, 1982). Previous studies have shown that impervious surface cover promotes runoff and can result in increased microbial contaminant and nutrient loading in receiving water bodies (Glasoe & Christy, 2004). Impervious surface has further been verified as a quantifiable land-use indicator correlated closely with polluted runoff (Arnold & Gibbons, 2007). Given the known potential impacts of impervious surfaces (Duda and Cromartie, 1982), the canal system within Atlantic Beach should be assessed for its vulnerability to such impacts. An increase in population and subsequent development will intensify the human impacts of urbanization on water quality, largely seen through widespread landscape modifications, such as increased impervious surfaces and the utilization of septic tank systems. These landscape components may help identify potential water quality hazards associated with coastal development and inform the development and implementation of interventions, such as effective land use planning and management. Dependence on septic tank systems, also known as onsite wastewater treatment systems (OWTS), is prevalent in residential areas along the waterfront. Research has demonstrated that under certain conditions these systems can introduce bacteria and nutrients in both

surface and ground waters (Parker et al., 2010). Because the North Carolina coast is characterized by a narrow vadose zone and a high water table, it is especially important to consider the risk of contamination of the groundwater due to the prevalence of OWTS (USGS, 2018; Mallin, 2013). Evaluating the presence of OWTS is important in this study as the canal system was constructed on top of existing marshes and wetlands, using dredged salt marsh fill as a foundation (HCP, 2008). Understanding the prevalence of impervious surfaces and the potential for groundwater inputs is imperative in order to promote the health of residential and recreational waterways. Runoff has been shown to be a major contributor of contaminants; therefore, addressing overland flow can be helpful in promoting overall water quality (Selvakumar and Borst, 2006). Groundwater inputs, the distribution and role of impervious surfaces, and OWTS can be used to infer over-land and subsurface water movement and their relative magnitude of impact on water quality in the canal system. Investigation of these measures may help identify potential water quality hazards associated with coastal development, and orient development towards restorative interventions to maintain and ensure the health and longevity of NC coastlines.

Using aerial and land-based observations translated into statistical mapping methods in a Geographic Information System (QGIS) we identified pervious and impervious surface coverage to indicate the potential pathways of surface runoff. We utilized spatial analyses of houses and septic tanks along with construction permits to calculate residential density and determine OWTS location and age. We conducted storm drain surveys and compiled slope elevation data to make inferences regarding the amount and direction of surface runoff potentially captured or directed into the waterway.

2. METHODS

To emplace the aerial imagery into a coordinate system, we used the georeference plugin in QGIS. We merged high-resolution orthoimages from 2012 (USGS, 2009) to illustrate the full extent of the area that was sampled. We computed all layers and analysis using the georeferenced imagery and Universal Transverse Mercator (UTM) zone 18S projection.

2.1 Land Cover

Normalized Difference Vegetation Index (NDVI) is a quantifiable land-use indicator, and is calculated using the ratio of the near infrared (NIR) to red (RED) bands within a four-band raster image obtained from USGS EarthExplorer (EE).

$$NDVI = \frac{NIR-}{NIR+} \tag{1.1}$$

NDVI values range from -1 to 1 and represent non-vegetated to densely vegetated areas, respectively. Using raster algebra, we reclassified each type of land cover and assigned categories as either homes, pavements, or shrubs/grass. Both homes and pavement were considered impervious surfaces in calculations. We used the Clipper tool to delineate the canal land area of interest to obtain canal-specific coverage statistics that effectively cropped out the surrounding area as much as possible. The water surfaces that were not completely removed using the Clipper tool were excluded from calculations of percent area coverage. The Zonal Statistics plugin was used to compute the number of raster grid cells that contained the reclassified values for the respective categories. Raster grid cells represented 1 m^2. The number of raster cells within each land category was compared to the total number of raster cells within the clip to obtain the percentage of total vegetative cover and total impervious cover.

2.2 Stormwater and Slope Elevation

We measured and recorded the dimensions of storm drains throughout the entire canal system. Ratios relating the total area of all storm drains to the total land area and to the total area of impervious surfaces were calculated in order to make inferences about the effectiveness of the storm water capture system. Storm drain surveys were compared to slope elevation data from LiDAR-derived imagery data

obtained from the USGS National Map Viewer (TNM Viewer). We outlined the canal system within Atlantic Beach using a site-specific search and a fine scale magnification feature (1:9028). An elevation SlopeMap layer was selected to provide a visualization of slope intensity within the canal system. A color gradient displays the degree of slope with flat surfaces as gray, shallow as yellow, moderate as orange, and steep surfaces as red. The location of flat to intense degrees of slope allows for inferences to be made about flow direction of stormwater across the land surface.

2.3 Development

The density distribution of houses and the age of the associated wastewater treatment systems are relevant for estimating anthropogenic influences on the canal system. We created a point layer to delineate each housing location and used a heatmap plugin to visualize areas of higher housing density. Permit and construction documentation for all homes within the canal system was formally requested from the town of Atlantic Beach from the Carteret County official website. We created a point layer to mark the location of septic tanks for which there were data, added a field for the connection or installation date recorded in the permits. We also compiled relevant written statements found within septic system permit records. Graduated categorization was used to classify those dates using a color gradient, and a histogram was created to display the canal OWTS age distribution. The heatmap plugin was used to simultaneously observe housing development and septic tank densities within the entire canal system using the aforementioned point vector layer.

3. RESULTS

3.1 NDVI and Physical Characteristics

NDVI values >0.1, from 0.2 to 0.5, or from 0.6 to 0.9 are typically classified as barren rock/sand/water, shrubs and grass, or dense vegetation cover types respectively (Palanisamy & Gurugnanam, 2014). The NDVI analysis (Fig. 1.1) illustrates that the dominant land cover around the canal system is pervious surface, identified here as shrubs/grass. This was further verified via qualitative field surveys of the area, as the majority of properties have sodded grass lawns with generally low plant diversity. It is noteworthy that just over half of the total land area within the canal is sparse (Fig. 1.2; NDVI: *-0.015 - 0.278*). The impervious cover accounts for ~60% of the land area (*203,038 m^2*), exceeding pervious surface by ~20% (*or ~123,200 m^2*).

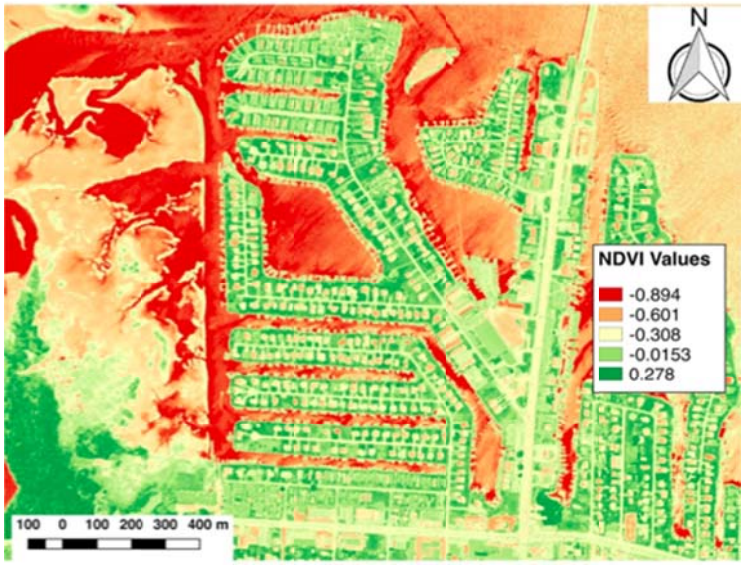

Figure 1.1 NDVI values.

3.2 Runoff

Surveys reveal that the total storm drain areas made up less than 1% (*33.49 m^2*) of both the total land area and the total impervious surface area (Table 1.1). Qualitative field surveys conducted after Hurricane Florence also revealed that many storm drains were covered by natural and household debris, likely due to the storm. Further, the storm drains were not typically located in shallow depressions that would direct stormwater towards the drain.

Slope elevation shows flat areas (*gray*) are most prevalent along the centerline of the canal arms, creating a convex shape that slopes towards the receiving water body (Fig. 1.3). Shallow slope (*yellow*) is

concentrated around canal edges while moderate and steep slopes (*orange to red*) are found along the complete western edge of the canal system.

Table 1.1 Surface area coverage for each land category.

Land Category	Surface Area (m^2)	% Cover
Homes/Pavement	203,038	38.36%
Vegetation	326,319	61.64%
Total	529,357	100%

Figure 1.2. NDVI Reclassification for Atlantic Beach Canal System. The "other" category includes roofs of homes and areas of water that are not relevant to impervious and pervious surface cover.

Figure 1.3. Degree of slope.

Table 1.2 Storm drain area ratios to total land area and impervious land area.

Storm drain area (m2)	Total Land Area	% of Area Serviced
33.49	529,357	>0.001%
Storm drain area (m2)	**Total Impervious Land Area**	**% of Area Serviced**
33.49	203,038	>0.015%

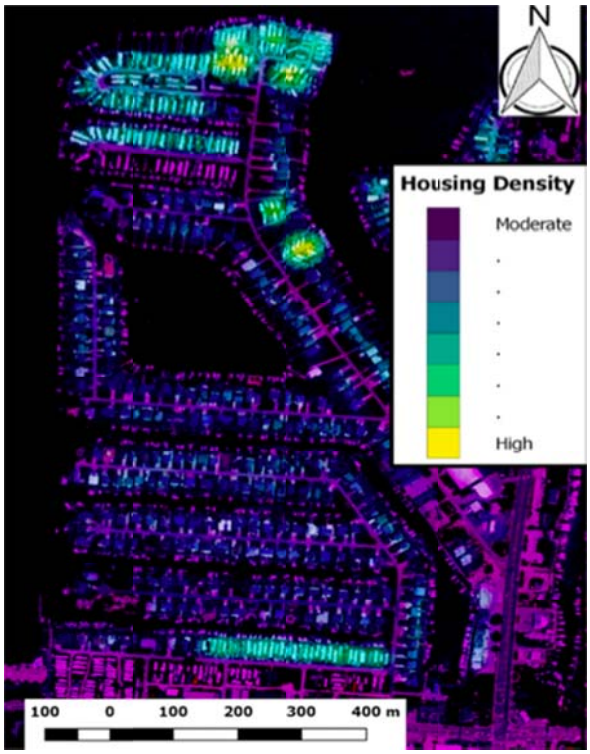

Figure 1.4. Housing density within the canal system.

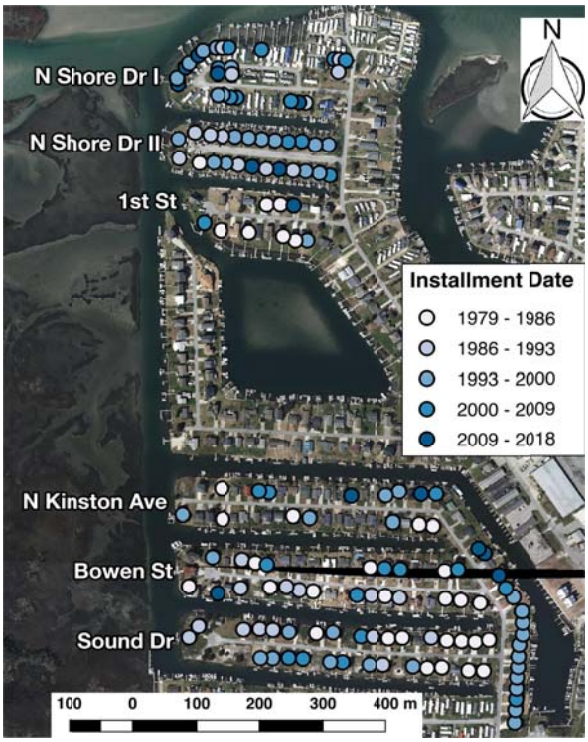

Figure 1.5. Categorization of septic tanks by installment date.

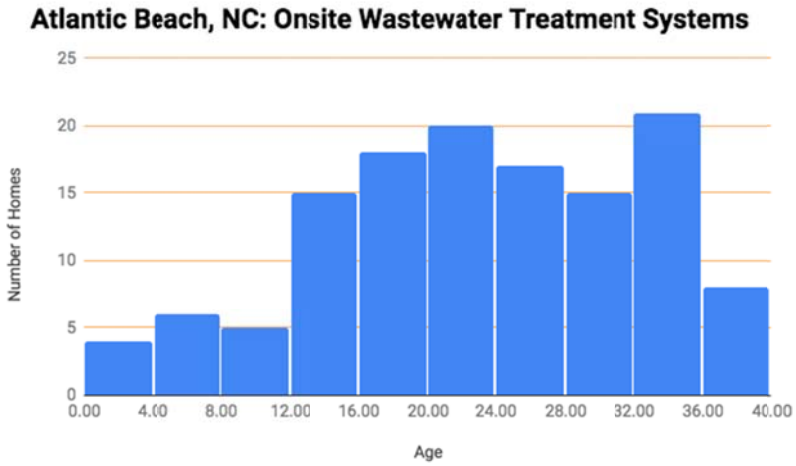

Figure 1.6. Histogram of OWTS age within the canal system.

3.3 Infrastructure

There were 565 distinct vector points plotted to represent development throughout the canal. The heatmap illustrates a higher density near the entrance of the canal system at the top portion of the image and along the bottom of the image (Fig. 1.4). These areas are largely occupied by trailer homes that were densely packed (approximately 1 trailer home/290 m^2), often times onto one property plot (Table 1.3). Outside of these high-density areas, development is relatively uniform throughout the canal system. According to the 2012 aerial imagery (USGS, 2009), only three lots within the canal are presently vacant, thus it is not expected that the non-vegetative, impervious land cover will change significantly in the future. Therefore, the data are representative of the state of the canal system at present, and can be considered representative of the future.

Records regarding septic tank installations were obtained for seven streets and 129 houses in the canal system (Figs. 1.4 & 1.5). The average installation date was 1994. The majority of the septic systems were 1,000 gallon tanks approved for a single home installed 5-10 ft from the home. Out of the subset of 38 trailer homes for which there were relevant records, 14 shared a septic system (*40%*) that was 1,000-1,500 gallons on average.

Table 1.3. Excerpts of written statements from permitting and construction documents received from the town. Permission granted by the town of Atlantic Beach.

Housing Unit	Subject	Enclosed Comments
133 Bowen St	Permit Unapproved	"... unsuitable due to a high water table (less than 12" of original surface, Rule 1942). The lot consists of 48" to 58" of dredged fill which is not naturally occurring soil conditions. The material which is below the fill is of a salt marsh origin and is considered unsuitable for septic tank systems"
304 & 305 N Shore Dr I	Construction Requirement	"Existing septic tank must be properly abandoned."
511 & 512 N Shore Dr I	Infrastructure Plan	"The system is under-sized due to severe site limitations and cannot be expected to function under heavy use. Practice extreme water conservation. If this system fails, these two mobile homes must be removed from the park or put on permanent pump and haul."

4. DISCUSSION

4.1 Surface Cover and Runoff

The amount of impervious land coverage is approaching 40% which classifies this area as an impacted-to-damaged landscape (Table 1.1; Schueler, 2000). During a precipitation event, impervious surface cover would result in higher runoff volumes and reduced deep and shallow infiltration respectively, inhibiting the amount of groundwater recharge (Schueler, 1995). Areas with impervious cover >30% results in 20% increase in runoff and 15% less ground infiltration compared to natural ground cover (Arnold and Gibbons, 1996).

Given that the narrow unsaturated zone and the sparse pervious land cover quickly becomes saturated during heavy rainfall, stormwater may not infiltrate the soil or be abated by vegetation. Thus, because impervious cover is roughly 2/5 of the land surface in the canal system, the majority of stormwater likely flows overland at a faster rate and at higher volumes than a natural, unurbanized landscape and advances over land as the soil and vegetation have a limited capacity to absorb or attenuate this flow (Burns et al., 2005). In addition, higher runoff loads associated with development can result in dramatic reductions in the richness of plants which is evident in the low NDVI values within the canal system and around the fringes of the marsh area to the left of the canal system (Taylor, 1993). Together, the sparse vegetation, amount of impervious land surface area (Table 1.1) relative to the small amount of storm drain coverage (Table 1.2), and the degree of slope elevation (Fig. 1.3) further suggest that the majority of stormwater is inadequately captured or abated, and flows into the canal waters.

4.2 OWTS and Water Quality

Due to time constraints on the part of the county in gathering the remaining septic tank records, the data may not be fully representative of the entire canal system. The available data do, however, provide information on 129 of the septic systems. Studies show the age of a septic system, also known as

onsite wastewater treatment systems (OWTS), can affect its efficacy (Withers et. al, 2014). Generally the average septic system can last 20-35 years, however the range is highly variable for each system because of differing levels of maintenance provided by homeowners (Sewers, 2000). Given the reported age ranges, the average septic tank system in the canal system is approaching the end of its life expectancy (Fig. 1.5). From the available records, their age suggests existing systems may be presently capable of effective treatment, however, whether or not the necessary maintenance (i.e., pump every 3-5 years) and other site-specific recommendations have been carried out is unknown. In addition, only the connection request dates were available for some of the septic systems, suggesting that some of the septic systems currently in use may have installation records that date back further than we were able to find in the documentation. For some houses, the town was unable to locate permit records, further indicating there may be unknown systems unaccounted for in our study.

Statements found within the available septic system records present qualitative information regarding construction area suitability and installment requirements. These excerpts convey professional recommendations from the licensed state inspectors and environmental health specialists regarding OWTS in the canal system. For example, the statement from 133 Bowen Street mentions that the area is unsuitable for septic systems based on soil characteristics, and the statement from 511-512 N Shore Dr I demonstrates that water conservation in shared systems is highly advisable (Table 1.3). The suggestion regarding water conservation demonstrates that there are risks associated with septic system failures and overflow (Table 1.3). This written statement also illustrates that the burden to exercise severe caution is placed on the users. These notes also acknowledge the presence of abandoned septic tanks not currently in use. In particular, there may be several abandoned septic tanks with unknown standing wastewater volumes throughout the canal system that could pose concerns in the future (Table 1.3). Currently, there is limited information, research, and regulations regarding the management of abandoned septic tanks, thus little can be concluded regarding their role in the canal system. Overall, these excerpts imply the soil is unfit for septic systems, the presence of old septic tanks not in use, and that water conservation is highly advisable.

4.3 Implications of Development Density

In Carteret County, 68% of people use OWTS, and septic problems are known to occur in low-lying, high density areas (Robertson et al., 1991). When many septic tank systems exist in a given area, the high density can reduce the effectiveness of soil filtration and render the treatment ineffective (Mallin, 2013). Residential development can result in high bacteria concentrations in soil and receiving waters when more than one septic drain field is present per seven acres (Duda & Cromartie, 1982). Therefore septic tank density is another important factor when evaluating wastewater treatment efficacy (Parker et. al, 2010; Robertson et al., 1991). Across the canal system, housing density was moderate, but property lots may not have the water-holding capacity to adequately accommodate sustained septic system usage (HCP, 2008). Areas in the Atlantic Beach canal system, such as the north entrance, are of particular interest because this area has the highest housing density and is in close proximity to Bogue Sound (Fig. 1.4). All potential septic system issues, including water quality patterns described and discussed in subsequent sections, could result in effluent material being carried out to the canal (HCP, 2008). These areas are directly exposed to the sound, meaning that if any effluent from septic systems entered the receiving waters, the sewerage constituents could be diluted effectively in the larger water body or could potentially impact the surrounding waterway. Although Atlantic Beach is not adjacent to any waters classified as Outstanding Resource Waters (ORW), it is bordered by high quality waters (HQW) and the shellfish harvesting waters of Bogue Sound (HCP, 2008). This emphasizes the necessity of conducting further study to determine the effects of high septic tank density on water quality in the area surrounding this system.

5. CONCLUSION

The goal of this study was to better understand the processes influencing water quality indicators in the canal system. We aimed to provide a visualization of these factors that could aid in assessing their interconnectivity. We hypothesized that the land area was largely characterized by impervious surface cover with an inadequate amount of stormwater capture and vegetative land cover. The bulk of the results seemingly support this hypothesis, highlighting the potential factors that pose a risk to the water quality of the canal system. TThe physical characteristics of the canal system could contribute to negative impacts on water quality, but it should be noted possible confounding factors not considered here require further research.

Water quality outcomes may differ during peak season. The shallow unsaturated zone, where the OWTS are located, should be taken into consideration for future studies as this zone can quickly become inundated during a precipitation event. Additionally, understanding how homeowners are managing and maintaining their septic systems may be helpful in order to more accurately assess the effectiveness of treatment, the potential for plumes, and the overall state of wastewater treatment in the canal system.

Similar areas in NC, namely Greensboro and Wilmington, facing analogous stormwater issues have installed bioretention basins or rain gardens that have been shown to promote infiltration and stormwater capture (Li et al., 2009). In other areas in the United States, urban forestry initiatives and various hydrology models have demonstrated that adding vegetation, such as trees, can reduce runoff volumes (Zolch et. al, 2017). Retrofitting green infrastructure into existing areas has been shown to significantly reduce the volume of stormwater runoff (Dietz & Clausen, 2005). In addition, tidal salt marshes in particular are efficient in capturing suspended solids that contribute to inputs of organic carbon, and other cities have taken to restoring these areas to assist with promoting water quality (Stumpf, 1983; Temmerman et al., 2013). These practical solutions could be applied to the existing development to improve the stormwater capture and attenuate runoff.

In sum, although the canal system evaluated here may not experience much increase in development, the findings demonstrated here may be of aid when considering the impacts of future infrastructure.

Chapter 2: Circulation and Flushing

1. INTRODUCTION

Understanding the processes that determine how water in a system renews itself is important in determining the potential for hazardous water quality conditions. A canal system with good flow continuously moves water throughout the system which ultimately disperses potentially hazardous materials. In comparison, water within a poorly flowing canal system would fail to fully circulate through the system, causing input concentrations to accumulate. Without proper circulation, a canal system can become vulnerable to impaired water quality due to the accumulation of contaminants from extraneous inputs, such as surface runoff. Assessing the flow conditions and the mechanisms that drive them are key aspects in analyzing the Atlantic Beach canal system.

Flushing of a canal system is driven by tides, surface runoff, wind, and their interactions with the geometry of the canals (Defne & Ganju, 2015). With every tidal cycle, water is brought in to the system as resident water is cycled out. Incoming water during a flood tide mixes with preexisting water in the system and subsequently ebbs out, creating a net water movement of zero. The tidal range in Bogue Sound, adjacent to the Atlantic Beach canal system, ranges from 0.6 m during neap tide to 1.1 m during spring tide. Post-storm surface runoff adds to baseline flow of groundwater and can contribute to an elevation gradient that causes water movement out of the canal system (Kirby-Smith, 1994).

Additionally, wind can cause surface velocities to increase or decrease depending on relative direction. The effect of wind on circulation within a system varies, and can be an important factor in areas where there is minimal circulation from tides. Similarly, water density can affect the movement of water in the canal system. The density difference between dense saline water that enters the system due to tides and fresher less dense water affected by surface and groundwater inputs can result in a circulation into the canal near the bottom and out of the canal near the surface. Lastly, the geometry of the canal can factor into the movement and circulation of water, with narrow and or shallow parts of the canal accelerating currents and potentially restricting water flow.

A number of different approaches have been proposed for estimating how well a semi-enclosed water body, like a canal, is flushed. The residence time of a water parcel in a system the time it takes for a parcel of water to move out of the canal from a given position (Monsen et al., 2002), and can be estimated by

$$T_R = x / \overline{u} \tag{2.1}$$

In this equation $\overline{u}$ refers to mean velocity and x refers to distance to the canal exit. Another way of quantifying flushing is through the flushing time, which is the ratio of the total canal volume to the volume of water that enters the canal with tides (Monsen et al., 2002).

$$T_f = \frac{VT}{(1-b)P} \tag{2.2}$$

T_f refers to the time-scale over which water in the system is renewed, assuming that the incoming water mixes entirely with the water already in the canal during every tidal cycle. V is the volume of the canal, T is the duration of a tidal cycle, and P is the volume of water that comes in during a tidal cycle. The return rate, b, represents the fraction of incoming water that was in the canal the previous tidal cycle. Because b is hard to quantify, the upper and lower bounds of T_f are usually calculated using a range of b values. These calculations regarding how long water stays and takes to leave can be complemented by drifter data that illustrate how water moves (Monsen et al., 2002).

We estimated the circulation and flushing of the Atlantic Beach canal system by measuring the components of flow mentioned above. This was done by deploying current profilers, releasing drifters, and taking bathymetry measurements to estimate canal volume. In order to observe the variability of the flow across the entire canal system, we sampled in two locations: a short canal near the top of the canal system and a long canal with a cul-de-sac further from the entrance of the canal system (Fig. 0.1). These

data will allow us to calculate residence time and the flushing time, as well as make assessments of the main drivers of flow in the canal system.

2. METHODS

We approximated circulation in the two canals through two main approaches: (1) releasing drifters in order to learn about the circulation of the surface of the canal, and (2) installing current profilers to learn about the circulation of water beneath the surface. Additionally, we collected bathymetry measurements in order to understand the shape and size of the canals. The creation of a bathymetric model for two of the canals allowed us to better understand the residence time and circulation of the canal system.

2.1 Bathymetry Measurements

We measured the bathymetries of the canals in order to better understand the general shape and depth of the canals and calculate the volume of water in the canal. Measurements were made while moving along the short and long canals in a shallow-bottomed 21ft boat. We collected data points every few meters. This resulted in around 130 and 250 data points in the short and long canals, respectively. At each location, Global Positioning System (GPS) coordinates, depth, and time were collected. A handheld GPS unit, measuring the latitude and longitude at various points, was used to obtain the location of a given depth measurement. GPS coordinates were recorded in Degree Decimal Minutes (DDM) and then converted into Universal Transverse Mercator (UTM). This allowed for a standard coordinate system between bathymetry and drifter coordinate measurements. Additionally, we used a depth sounder in order to record the water depth. Finally, time for each measurement was recorded in Eastern-Daylight-Time (EDT) and converted to Eastern-Standard-Time (EST) to match the time readings on the current profilers.

Using records from the NOAA Tide and Water Levels database at Atlantic Beach, we adjusted the data points for tide by subtracting the water level relative to mean tide at the time of the measurements (NOAA Tide and Water, 2018). After retrieving the current profilers, we compared the water levels in the canal to the NOAA tide predictions at the Atlantic Beach bridge in order to determine if there was any lag. Finally, we developed a bathymetric model to display the variations in depth in the short and long canals.

2.2 Drifter Releases

Grapefruit drifters were released in order to determine the surface movement of water in the short and long canal. In order to properly identify drifters when collected, we labeled them 1 through 24 with permanent marker prior to release. We conducted drifter releases on four separate days, twice at flood tide and twice at ebb tide, in order to better understand the impact of different tidal cycles in the canals (Johnson et al., 2003). At ebb tide, as the water moved from high to low tide, we expected that the drifters would move out of the canals. During flood tide, as the water moved from low to high tide, we expected that the drifters would move into the canal. If the drifters experienced little movement, it would suggest that the canals did not experience high amounts of movement from tidal or wind currents.

We released the drifters from 21 ft and 24 ft flat-bottomed boats at several locations in sequence from the end of the canal to the mouth to minimize boat disturbances. Drifters were released in groups of 4 and 5 from the stern of the boat. We released drifters in groups of 5 at three releasing sites in the short canal and in groups of 4 at six releasing sites in the long canal (Fig. 2.1a). The releasing sites were around 75 and 125 m apart in the short and long canals, respectively. The last set of drifters were released a couple of meters from the mouth of the canal. We recorded the drifter number, time, and GPS coordinates for each drifter during release. After approximately 30-60 minutes, we collected the drifters starting from the mouth of the canal and proceding to the end. Drifter collection at the mouth of the canals allowed for further minimization of disturbances created by the boat. During collection, drifter numbers, GPS coordinates, and times were re-recorded.

Figure 2.1*:* Short and long canal, with a) red circles indicating drifter release drop points in the canals and b) yellow stars indicating locations of current profilers.

GPS coordinates of the release and pick-up locations were collected in DDM and were converted into UTM in order to better calculate distance traveled. The velocity of each drifter was then calculated and averaged within release groups. Lastly, we calculated the standard deviation of velocities of each release group. This information was then plotted to convey the average velocity, direction, and dispersion determined from each drifter release group during various stages in the tidal cycle.

2.3 Aquadopp Profiler Measurements

We installed 2 HMz Aquadopp Profilers in both the short and long canal (Fig. 2.1b). A current profiler was placed halfway between the mouth and end of the short canal and halfway between the mouth and middle of the long canal. During deployment, we lowered each current profiler to the bottom of the canal and tied it to a piling with a weighted ground line. Both current profilers were programmed to take a measurement of the current profile for 60 seconds every 5 minutes. We measured water velocities every 20 cm throughout the entire water column. The current profilers collected measurements for approximately 16 days between 9-24 October 2018.

We plotted the current profiler data in MATLAB. Lower and upper bound estimates of residence time were calculated using the velocity of water at the surface, which was generally the fastest in the water column, and the depth-averaged velocity of water. The lower bound accounts for no mixing, while the upper bound accounts for total mixing of the water column.

To measure water quality parameters, we calculated residence times (Eq. 2.1) at each of the 5 sample sites in order to represent the average time it would take for a particle to exit the canal from each location. Additionally, the upper and lower bound estimates of total flushing time were calculated using pressure sensor data collected by the current profiler (Eq. 2.2). Variables V and P required an estimate of the volume of each canal. We estimated the length and width of each canal on Google Earth. Depth estimates were derived from means of the bathymetric measurements gathered in both canals at mean tide. Because depths around the end of the longer canal were noticeably deeper, its volume was separately calculated and added to the remainder of the long canal estimate. For the purpose of the calculation, the canals were treated as rectangles with no gradual slope to the top, and a flat bottom. Finally, we multiplied the average depths gathered from the bathymetry measurements by the length and width of each canal to get P. Lastly, a mean velocity was estimated at each height above the bottom that was consistently submerged throughout deployment. These mean velocities were used to calculate location specific ranges for residence time.

3. RESULTS

3.1 Bathymetry

The long canal is deeper on average than the short canal, with the end of the long canal being the deepest (Fig. 2.2). The sides of the short canal are very shallow, reaching nearly 0.5 m at various points. At its deepest, the short canal reaches around 2 m at the mouth of the canal. The long canal, on the other hand, ranges from approximately 1-4 m in depth.

Inspection of the data collected in the Aquadopp current profilers revealed there was no observable lag between the tides at the NOAA Tide and Water Levels database at Atlantic Beach and the canal systems at Atlantic Beach (NOAA Tide and Water, 2018).

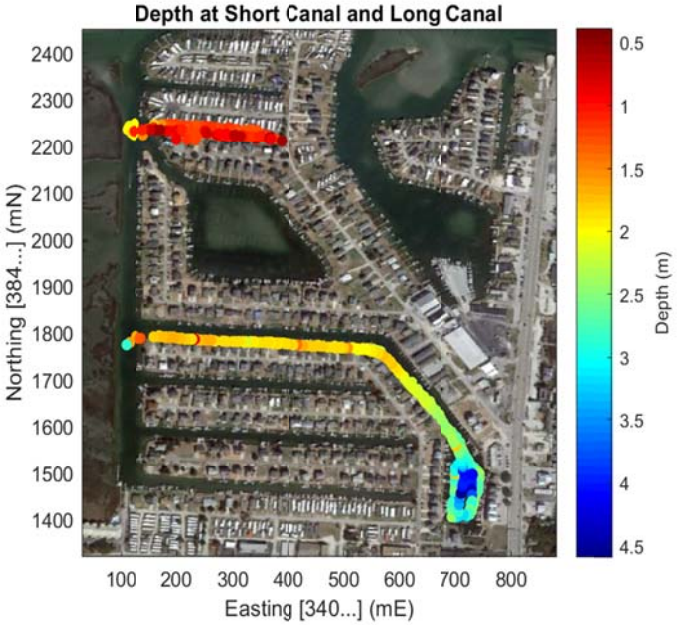

Figure 2.2. Bathymetry of the short and long canals, coordinates in UTM, zone 18 S, and depths are relative to mean tide. The primary vertical y-axis represents the Northing of a coordinate and the x-axis represents the Easting of a coordinate. A color bar is used on the secondary vertical y-axis to represent the depths of the water in a certain location in meters.

The depth of the canals is not uniform. In general, the short canal is around 1.5 m deep. The canal becomes more shallow around the end, reaching around 0.75 m in depth (Fig. 2.2). The short canal reaches its deepest points at the mouth of the canal. The long canal was deeper than the short canal, averaging around 2.0 m in depth. The mouth of the long canal averaged around 2 m in depth. In general, depth increased from the mouth to the end of the canal. In the bend of the long canal, the depth was around 2-2.5 m. The deepest points recorded were near the end of the long canal. It averaged around 3-3.25 m in depth around the canal edge and 4.0-4.5 m in depth in the center.

3.2 Drifter Measurements

The flood tide drifter release on 9 October 2018 experienced some of the largest overall velocities seen during the drifter release trials (Fig. 2.3). Nearly every drifter release group was pushed toward the mouth of the canal, contrary to what was expected to occur during flood tide. In the short canal, the drifter's velocity increased slightly from the end to the mouth of the canal. Additionally, the standard deviation increased from the end to the mouth of the canal, implying more dispersion at the mouth of the canals. In the long canal, the velocity was lowest at the end. The drifters experienced almost no

movement there and had a relatively small standard deviation. Overall, the velocity of the drifters generally increased from the middle to the front of the canal.

During the second flood tide release on 17 October 2018, nearly every drifter experienced a net movement from the end of the canal toward the mouth of the canal (Fig. 2.3). Similar to the drifter release on 8 October 2018, this contradicted what was expected to occur during flood tide. All of the drifters in the short canal experienced almost no movement. Similarly, the drifters released at the mouth and middle of the long canal experienced a negligible amount of movement. The only clear movement during this release was seen at the end of the long canal and was primarily directed westward, toward the mouth of the canal.

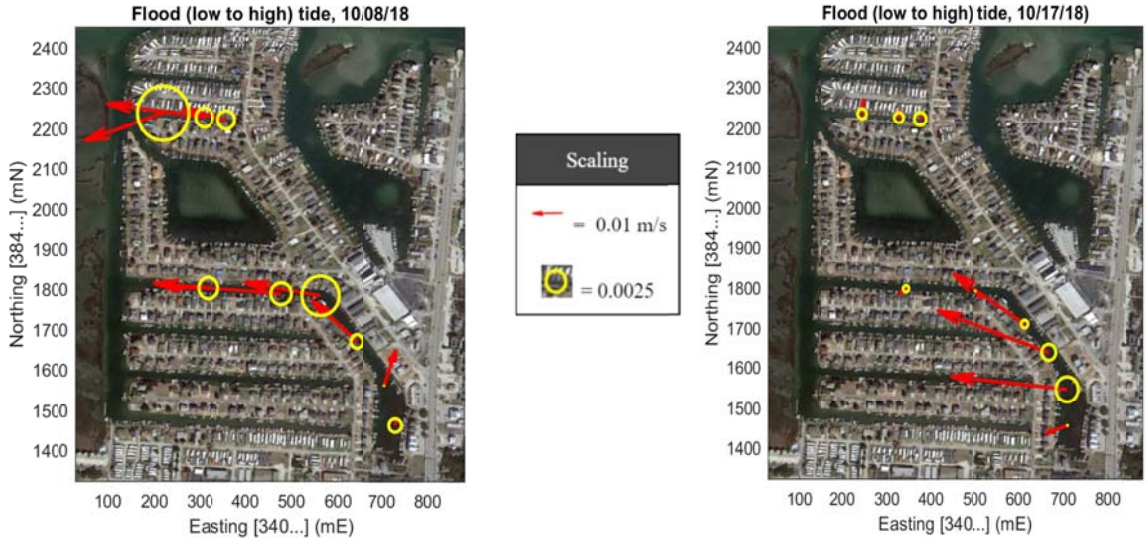

Figure 2.3. Velocity and direction from drifters released at flood tide. Each point represents the average values for drifters released at that point. Yellow circles represent the standard deviation of each drifter group.

Figure 2.4. Velocity and direction from drifters released at ebb tide. Each point represents the averaged values of the drifters released at that point. Yellow circles represent the standard deviation of each group of drifters.

The first ebb tide drifter release on 9 October 2018 demonstrated the highest velocities at the mouth of the canal. Velocities at all release locations were relatively high on this day compared to the other releases (Fig. 2.4). Every drifter group moved toward the mouth of the canals, following the predicted ebb tide motion. In general, the standard deviations were relatively large, implying a significant amount of dispersion amongst drifters released in the same group in comparison to the other release dates.

During the second ebb tide release on 24 October 2018, there was a large amount of directional variation between the different release points. For example, the short canal had a net movement in the east direction, with little movement in the back of the canal (Fig. 2.4). In comparison, the long canal experienced westward velocities near the mouth and southward velocities toward the end.

3.3. Aquadopp Profiler Measurements:

Velocities were faster in both the bottom and the surface in the long canal than in the short canal. Throughout the water column, velocities shifted toward the end of the canals during flood tide and away from the canal, in the direction of the mouth, at ebb tide. Velocities near the bottom reach 0.2 m/s while surface velocities are between 0 m/s and 0.5 m/s during flood tide (Fig. 2.5). The velocities near the bottom are mostly positive, representing water entering the canal. During ebb tide, velocities near the bottom are near 0 m/s and reach -0.2 m/s at the surface. Near the surface of both canals, velocities are slightly negative, indicating water moving toward the mouth, out of the canals. Overall, the longer canal experienced slightly higher velocities, indicated with the red, orange, and blue colors (Fig. 2.5)

The gradient of velocities with depth are accentuated during the spring tide, as seen from 8-11 October 2018 in the long canal. The tidal range is similar between the two. The occurrence of Tropical Storm Michael can be seen on 11-12 October 2018, where water levels dipped and high tide did not occur.

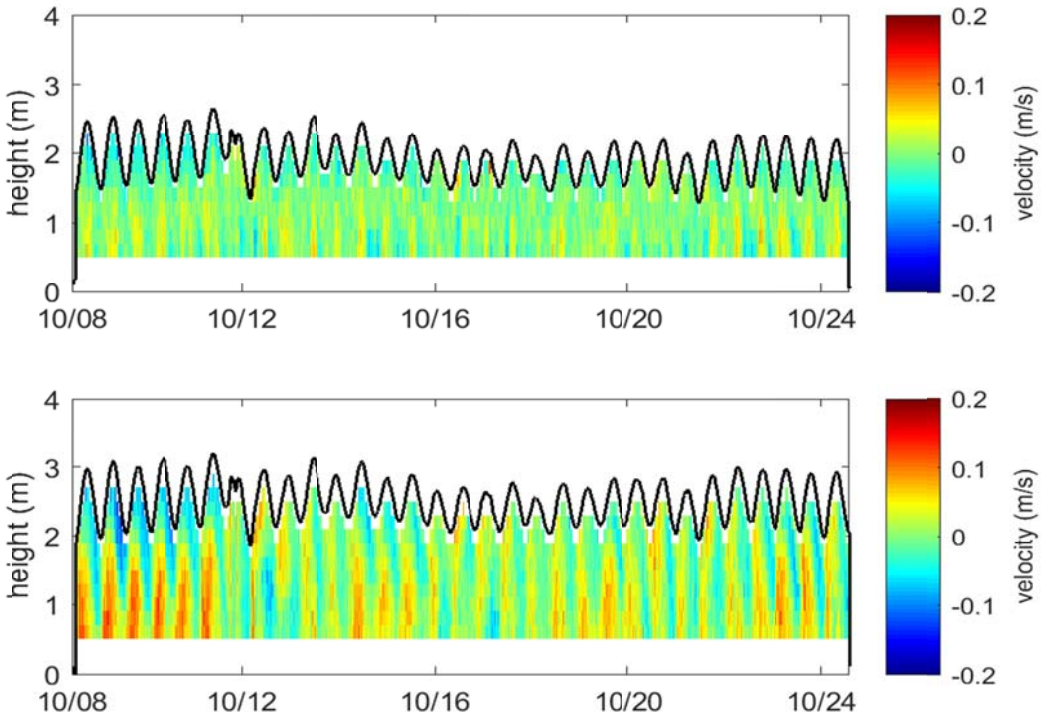

Figure 2.5. Measured along-channel component of velocity of water with height above bottom in the short canal (*top*) and long canal (*bottom*). Negative values (cool colors**)** represent water leaving the canal, while positive values (warm colors) represent water coming into the canal. The dotted black line represents the height of the water surface above the bottom.

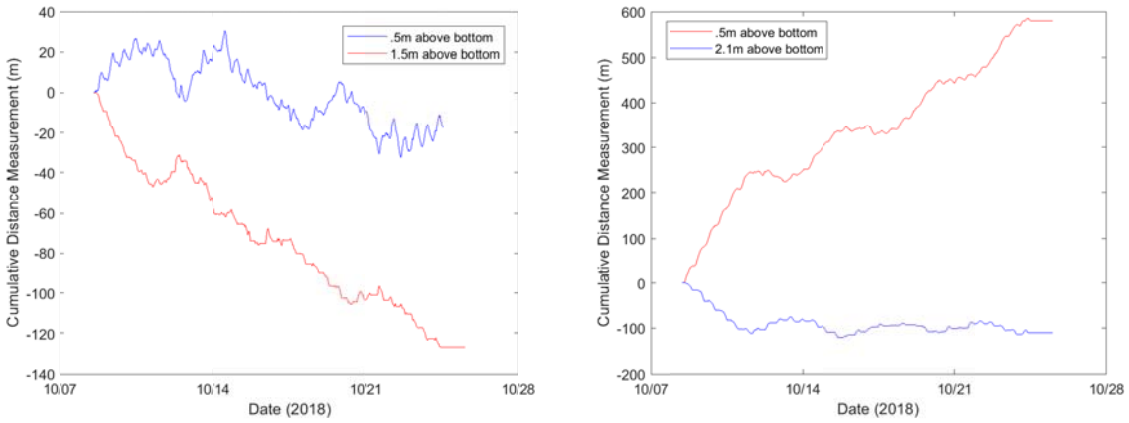

Figure 2.6. *(Left)* The cumulative distance that water travels near bottom and near the top depths at the short canal. Water at .5 meters above the bottom moves slightly out of the canal, while water at 1.5 meters above the bottom leaves the canal at a faster rate. *(Right)* Cumulative distance that water travels at near top and near bottom depths at the long canal. Water at 0.5 meters above the bottom moves into the canal, while water at 2.1 meters above the bottom leaves the canal.

At 0.5 m above the bottom in the short canal, the cumulative distance travelled over the span of the current profiler deployment was less than 20 m toward the mouth of the canal. At 1.5 m from the bottom (near the surface) the water travelled approximately 125 m out of the canal over time (Fig. 2.6). The highest velocities in the short canal, therefore, occurred near the top of the water column. In comparison, the long canal experienced the highest cumulative distances traveled lower in the water column over the deployment of the current profilers. In the long canal, water 0.5 m above the bottom traveled nearly 600 m toward the back of the canal. At 2.1 m above the bottom of the canal, near the surface, water travelled approximately 110 m in the direction of the mouth of the canal over the time of deployment.

Both systems experienced a gradual movement of water into the canal with increasing depth from the surface. Time averaged surface velocities in the short canal were moving near 0.04 meters per second out of the canal, while bottom time averaged velocities were near zero (Fig. 2.7). The time averaged velocity for the short canal changed directions at about 1 meter above the bottom and shifted directions again at 0.5 meters above the bottom. Time averaged surface velocities in the long canal were near 0.08 meters per second out of the canal, while bottom time averaged velocities were greater than 0.02 meters per second moving into the canal. The time averaged velocity for the long canal changed directions at about 1.7 meters above the bottom, and gradually moved faster into the canal with depth.

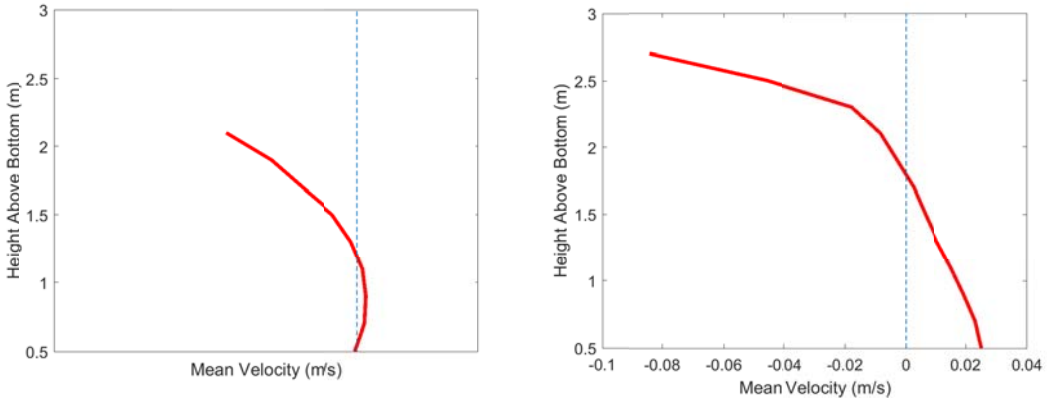

Figure 2.7. *(Left)* Time averaged velocity of water with depth at the short canal. *(Right)* Time averaged velocity of water with depth at the long canal. Negative x-values represent water moving out of the canal, while positive x-values represent water moving into the canal.

The estimated time to completely flush the short canal is between 0.428 and 0.857 days (Table 2.1). In comparison, it would take between 1.836 and 3.672 days to completely flush the long canal. The difference in flushing times between the two canals can be explained by the tidal range in relation to the volume of water that each canal is estimated to hold. Assuming that each canal has a rectangular shape, the short canal holds an approximate volume of 7,141.5 m^3, while the long canal holds around 73,354 m^3. The ratio between volume that fluxes in and out with tides and the estimated volume that the canal holds at mean tide is larger in the short canal than the long canal.

Table 2.1. Flushing times of each canal represented in days. This is the amount of time that it would take for the estimated volume of water in the canal to be replaced by tidal water. The volumetric flow rate is variable to the amount of incoming water that leaves the system in the same tidal cycle. A higher return rate of incoming water means a longer flushing time in the canal.

Short Canal			Long Canal
% Return rate	Flushing Time (days)	% Return rate	Flushing Time (days)
0.00	*0.42842*	*0.00*	*1.8359*
0.10	*0.47602*	*0.10*	*2.0399*
0.20	*0.53552*	*0.20*	*2.2949*
0.30	*0.61202*	*0.30*	*2.6227*
0.40	*0.71403*	*0.40*	*3.0599*
0.50	*0.85683*	*.50*	*3.6718*
0.60	*1.071*	*0.60*	*4.5898*
0.70	*1.4281*	*0.70*	*6.1197*
0.80	*2.1421*	*0.80*	*9.1796*
0.90	*4.2842*	*0.90*	*18.359*
1.00	*infinite*	*1.00*	*Infinite*

Estimated residence times are longer at the end of each canal. The end of the short canal had an estimated residence times of 8.68-28.11 hours and the end of the long canal had an average residence time of ≥ 29.13 hours (Table 2.2). Residence times near the mouth of the canals were 1.34-4.33 hours and ≥ 1.59 hours respectively. Additionally, residence times were estimated to be higher in the long canal. Since the time and depth averaged velocity of the longer canal was going into the canal, only lower bound estimates were conclusive.

Table 2.2. Estimated residence times of a water parcel at the surface at each of the sampling locations. Upper and lower bound values were estimated at each location. (*1A*) Mouth of the short canal, (*1B*) End of the short canal, (*2A*) Mouth of the long canal (*2C*) End of the long canal.

Location	Estimated Residence Time (R_t) (hours)
1A	1.34-4.33
1B	8.68-28.11
2A	≥ 1.59
2B	≥ 15.81
2C	≥ 29.13

4. DISCUSSION

4.1 Bathymetry

The variation in depth along both canals provides important information regarding transport of sediment in the canal system. Because the canals are manmade, it can be assumed that there was some uniformity in the way canals were originally constructed and excavated. Over time, sediments entering and exiting the canal were transported with the tide and currents, causing the bottom of the canal system to change. For example, in the short canal, the edges are much more shallow than the middle section. Over time, the edges of the canal system have been influenced by incoming currents and sediments, causing them to fill in slightly. Generally, areas with slower currents are able to settle the sediment at a quicker rate than areas subjected to stronger currents. As seen in the data collected from the current profilers, both canals experienced a relatively low current flow, allowing for an accumulation of sediment within the canal system.

4.2 Drifters

In general, the drifter releases did not follow the expected patterns for ebb and flood tide. Pairing the drifter releases with wind data collected from a NOAA meteorological sensor at Duke Marine Lab during the time of release provided a possible explanation for the discrepancies in the releases.

During the first drifter flood tide release on 8 October 2018, for example, there were strong easterly winds (Fig. 2.8a). This could explain the net movement of drifters to the west. During the following drifter release on 9 October 2018, during ebb tide, the drifters experienced their strongest net velocities as a system in both canals. Similar to the previous drifter release, there was a strong easterly wind during the time of release (Fig. 2.8b). The strong wind in addition to the ebb tide explain the strong velocities pushing the drifter out of the system.

On 24 October 2018, the drifters displayed their largest variation regarding the direction of their movement (Fig 2.4). Pairing the drifter movement with their corresponding wind data explained some of the movement during the release, however, it does not explain why three of the release groups drifted northward. During the time of release, there were moderate northerly winds, which could have possibly created a slight southward movement in the canals (Fig. 2.8d). This explains why five of the six drifter

release groups were pushed toward the bottom southern side of the canals. It remains unclear, however, why the drifters in the short canal moved toward the northeast, as this contradicted both the movement from the tide and the wind. It is possible that the drifters were redirected by a nearby boat, or that buildings around that section of the canal redirected the wind flow.

During the drifter release on 17 October 2018, the long canal experienced its largest velocities at the end of the canal (Fig. 2.4). In the middle and mouth of the canal, there was nearly no movement. During the time of release, it was flood tide and there were light westerly winds (Fig. 2.8c). If the canals are heavily influenced by wind, it is possible that winds were able to drive some of the movement of the drifters, causing the minimal movement displayed in the majority of the release areas. Although we are not sure why the drifters in the short canal moved in counteracting directions from the wind and tide, a possible explanation could be movement from a boat near the drifters, causing them to move further than the wind and tide would have pushed them without interference. The overall displacements of the drifters were relatively minimal and generally moved around 0.025 m/s or less.

4.3. Current Profiler

Based on the volumes calculated for short (7,141.5m^3) and long (73,354 m^3) canals it is reasonable that short canal peak velocities remained closer to 0 than those in the longer canal, assuming no significant water elevation differences between canals. The long canal is much larger, and requires more influx of water during a tidal cycle. However, higher velocities of water moving in and out of the canal did not result in faster estimated flushing times in the long canal, as the ratio between the flux of volume with tides and the total volume of water was much smaller. While the average velocity in the short canal was 0.0025 m/s moving out of the canal, the average velocity in the long canal was 0.0096 m/s moving into the canal. This may be due to error, as there are no other means of dispelling the water in the canal besides through the mouth. There may have been variations in the flow across the canal cross-sections that were not captured in our current meter measurements. The average velocities computed from the measurements are very small relative to the instantaneous velocities observed, and it is likely that the average velocity for both canals was approximately to zero.

The canal system is strongly influenced by tides. We can see the velocities moving into the canal with a flood tide and moving out with an ebb tide (Fig. 2.6). However, there is a definite gradient of velocities with depth. Surface velocities were more consistently moving outward, while bottom velocities were more consistently moving inward. We hypothesize that this is a result of the salinity gradient, and corresponding density gradient, along the canals, especially in the long canal.. The wind also appears to have a strong influence on circulation in the system. This hypothesis is supported by the NOAA wind data collected at the Duke Marine Lab station (Fig. 2.8). At the point where there is the biggest discrepancy in velocities with depth for the long canal, from 8-11 October 2018, there are strong easterly winds. On 12 October 2018, when the canal system was being affected by Tropical Storm Michael, winds increased in intensity and blew from the west, and this extreme weather event likely caused mixing. We can see this effect after 12 October 2018 in the velocity profile, where there is less discrepancy in velocities with depth. After the storm, top versus bottom velocities slowly started to return back to their original state before the storm. This could be further substantiated by measuring salinity profiles along the length of the canals. Residence times we calculated provide an estimate of how long water takes to leave the system. Measurements taken midway along each canal are not indicative of all areas within the canal. For example, at the closed ends of the canals, the velocities must go to zero. Therefore, even the upper bound estimate of the flushing time may be an underestimate of the actual time it takes for water to be flushed near the closed ends of the canals. The probability of underestimating the residence time is especially high in the back of the long canal because larger depths could hold in waters for a long time.

Figure 2.8. NOAA wind data collected on Piver's Island. The blue arrows indicate direction and the red line indicates intensity of wind in knots (*a*) Data collected on 8 October 2019 from midnight to 4 pm. Releases occurred from 2:24pm-4:06pm (*b*) Data collected on 9 October 2018 from midnight to 2pm. Releases occurred between 9:37am-11:22am. (*c*) Data collected on 17 October 2018 from midnight to 2pm. Releases occurred between 8:57am-10:45am. *(d)* Data collected on 24 October 2018 from midnight to 2pm. Releases occurred between 9:51am-11:41am. (NOAA Wind, 2018).

5. CONCLUSION

To better understand the Atlantic Beach canal system several methodologies were used, including placing current profilers, releasing drifters, and using bathymetry measurements to identify the shape of the canal and calculate canal volume. Using these data, the flushing time, residence time, and time averaged velocity profile were calculated. Drifters measurements revealed details of the overall circulation.

In general, the mouths of the canals appeared to have a fair amount of flow. Both the short and long canals were estimated to be able to flush in a few hours and the drifter data generally supported the idea of strong movement at the mouth. Based on the data, however, it is possible that the end of the long canal is infrequently fully flushed. Deeper water depths at the end of the long canal could cause it to have poor flushing and be vulnerable to stagnation. Drifter releases near the closed ends of the canals revealed little movement. The data also suggest that drifter movement may be primarily wind driven. Further, data from the drifter releases and current profilers indicate that a baroclinic pressure gradient is important for driving circulation in the system.

Future studies with additional current profiler measurements taken throughout more of the canal system would better describe the water movement. Reliable salinity data down the water column could help explain the system's stratification and quantify the along-channel salinity gradient. These findings will assist in understanding the mechanisms that drive flow and control flushing, thereby affecting water quality in the Atlantic Beach canal system.

Chapter 3: Nutrients

1. INTRODUCTION

Nutrients are substances that promote energetic biological processes required for maintaining life. Nitrogen and phosphorus are two macronutrients that are vital to the existence of primary producers and bacteria in estuarine systems. Both nitrogen and phosphorus are necessary to sustain life at the base of the food chain, and each nutrient can be limiting at different times according to seasonal changes, human influence, or environment type (Paerl et al., 2009). Organisms can only be as productive as is allowed by the nutrient that is least abundant in the system, which is referred to as the law of minimum. Sufficient supplies of these nutrients in tandem allow microorganisms to proliferate, and established ratios of carbon, nitrogen, and phosphorus are commonly found in phytoplankton biomass and ocean waters (Redfield et al., 1963; Zweifel et al., 1993).

Both nitrogen and phosphorus are delivered to coastal zones and are taken up and regenerated through nutrient cycling. Microorganisms like phytoplankton and bacteria are major drivers of nutrient transformations in coastal systems, and nutrient cycling processes are often complex (Arrigo, 2005). Nitrogen is fixed from the atmosphere or discharged from terrestrial sources into coastal zones. This nitrogen is assimilated into microorganisms as organic matter and accumulates in higher trophic levels. Bacterial decomposers break down this organic matter and release nitrogen back into the water column to be recycled by other organisms or released into the atmosphere. Some nitrogen is eventually buried in sediments and removed from the system (Herbert, 1999). Phosphorus enters coastal systems through erosion of mineralized material, and is also incorporated into microorganisms as organic matter and eventually undergoes sediment burial (Yang et al., 2016).

When nutrients are added to a system in excess through anthropogenic inputs (e.g. runoff from agricultural processes, wastewater), higher concentrations can enhance phytoplankton and bacterial growth rates. The addition of excess nutrients to a system through anthropogenic inputs can result in harmful algal blooms, low oxygen events, and fish kills (Herbert, 1999). A higher abundance of microorganisms is detrimental to water clarity, safety for swimming and fishing, and the overall health of the ecosystem. Healthy nutrient levels make an ecosystem optimal to provide services to humans, which means that poor ecosystem health impacts human health (Myers et al., 2013). Currently, there are no overarching standards regulating nutrient levels in all North Carolina water bodies, but there are rules in place throughout the state monitoring nutrient loading in some bodies of water; however, the Atlantic Beach, NC canal system is not one of those water bodies (Schiavinato and O'Hara, 2016). There is no current regulation or monitoring of nutrient levels in the canal system, and so the extent to which nutrients may be influencing this system is relatively unknown. Thus, in this chapter, we (1) measure nutrient concentrations at multiple sites in the Atlantic Beach, NC canal system, and (2) determine the nitrogen flux characteristics in the sediments at these sites. We chose to do these analyses because both raw nutrient concentrations and flux dynamics are important to predict how the system cycles nutrients over time.

2. METHODS

2.1 Sample sites

IWe used five study sites and a reference point. Sites 1A and 1B are located along the second most northern canal, Sites 2A, 2B, and 2C are located along the longest, curved canal, and the reference site (Reference 1) is located in the open waterway of Bogue Sound. Site 1A is located at the mouth of the short canal and Site 1B is located at the end of the short canal. Site 2A is located at the mouth of the long canal, Site 2B is located in the middle of the long canal, and Site 2C is located at the end of the long canal (Fig. 0.1).

2.2 Water column nutrient concentration analysis

We measured nutrient concentrations from water samples taken at the water surface and near the sediment surface in each of the canals. We collected these water samples during four ebb tide and three flood tide events from 3-24 October 2018. We collected the water samples using a Van Dorn water sample. The samples were held in 250 mL containers on ice until being returned to the lab. We filtered the water samples to remove particulate material using glass microfiber filters with a 0.7 µm nominal pore size. 100 mL of water were filtered, and approximately 40 mL of water were left in 50 mL containers to be stored at -20°C until time of processing. Frozen nutrient samples were quick-thawed and ammonium (NH_4^+), total dissolved nitrogen, combined nitrate (NO_3^-) and nitrite (NO_2^-), denoted NO_x, and phosphate (PO_4^{3-}) concentrations were determined using a Lachat QuikChem 8000 auto-analyzer (Lachat, Milwaukee, WI, USA; Lachat QuikChem methods 31-107-04-1-C, 31-107-06-1-B, and 31-115- 01-3-C, respectively). Detection limits for NO_x, NH_4^+, total dissolved nitrogen, and PO_4^{3-} were 0.88 µg/L, 1.05 µg/L, 1.80 µg/L, and 7.30 µg/L, respectively.

2.3 Sediment nitrogen flux analysis

Nitrogen flux analysis was based on a flux experiment that involved coring sediment at a site of interest and transporting that sediment to the lab for *ex situ* experiments. Sediment cores were obtained during ebb tide on 9 October 2018. Cores were taken at the mouths and ends of the canals (Sites 1A, 1B, 2A, and 2C). Three replicates were obtained for each site. The cores were readied for experiments in an incubator with a continuous flow system by removing excess sediment, pressure-capping each cylinder, and attaching the cores to two tubes: one to constantly supply an inflow of water and the other to release.

At different time points, the water that exited from the cores and the water feeding into the cores were analyzed using the membrane inlet mass spectrometer (MIMS). This device accurately measures N_2 gas concentrations in water samples using a high pressure pump and gas-permeable tube. The change in concentrations of N_2 gas over time with respect to an inert gas reveals if the core is performing net denitrification or nitrogen fixation. Nitrogen flux was calculated using the equation presented below:

$$flux = \frac{(outflownitrogenconcentration - inflownitrogenconcentration)(flowrate)}{surfaceareaofcoresediments} \quad (3.1)$$

In addition, following the completion of the flux experiment, sediment subsamples from each of the cores were dried in ovens at temperatures of 350°C for 4 hours and then 550°C for 4 additional hours. This was to determine dry weights and 2 combustion weights which represented the labile and refractory organic matter (or the organic matter more easily and less easily utilized by microbes) in the sediment. These data were incorporated into the nitrogen flux analysis as well.

2.4 Statistical analysis

The statistical software JMP was used to gather statistical information about the concentration and flux data. The nitrogen concentration data were analyzed using a one-way analysis of variance (ANOVA), and differences between sites, between ebb and flood tide sampling times, between the long and short canals, and between surface and bottom water concentrations were examined for each of the nutrient parameters. The nitrogen flux data were analyzed using the Tukey-Kramer HSD test in conjunction with an ANOVA to detect means that are significantly different from each other.

3. RESULTS

3.1 Water column nutrient concentrations

Concentrations of nitrate and nitrite, ammonium, total dissolved nitrogen, and phosphate were examined in relation to multiple variables including canal, sample site, tide level, and location within the water column. Tide level did not have a significant impact on concentration for any of the nutrient parameters, which justified integrating the data by canal and by sample site. The date of sampling did not significantly impact nutrient levels except that nitrate and nitrite levels were significantly higher on 17 October 2018 than on other dates (Fig. 3.1). When grouped by canal, nutrient concentrations were not significantly different, but the long, curved channel had consistently higher concentrations for all of the nutrient parameters. When grouped by site, the end of the longest canal (Site 2C), had consistently higher concentrations for all of the nutrient parameters than the other sites, and this difference was significant for ammonium, total dissolved nitrogen, and phosphate levels ($p<0.05$, Fig. 3.2). There were no statistical differences between any of the other sites besides the end of the long canal (Site 2C), including the reference site. Nitrate and nitrite concentrations were also high in the middle of the long canal (Site 2B) in comparison to other sites regardless of date or tidal cycle. Differences between surface and bottom waters were not statistically significant, but only nitrate and nitrite values were higher in the surface waters with all other nutrient parameters higher in the bottom waters (Fig. 3.3).

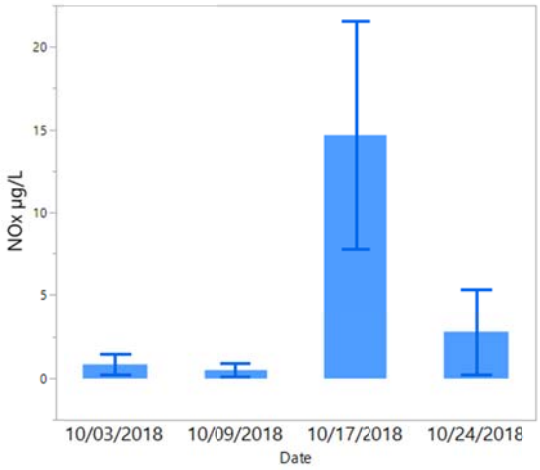

Figure 3.1. Mean nitrate and nitrite concentrations by date of sampling. Mean values are plotted with error bars representing 95% confidence intervals.

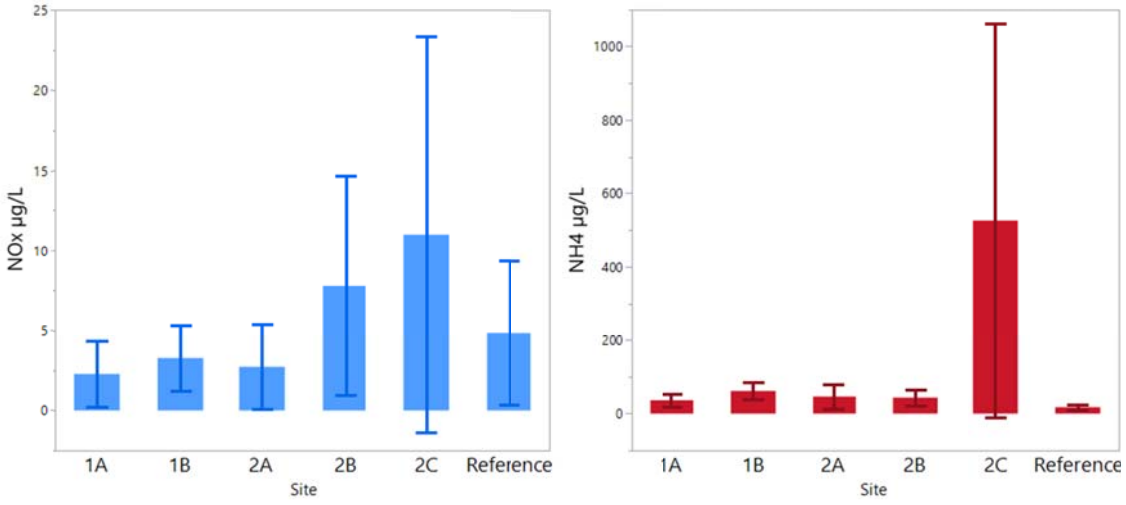

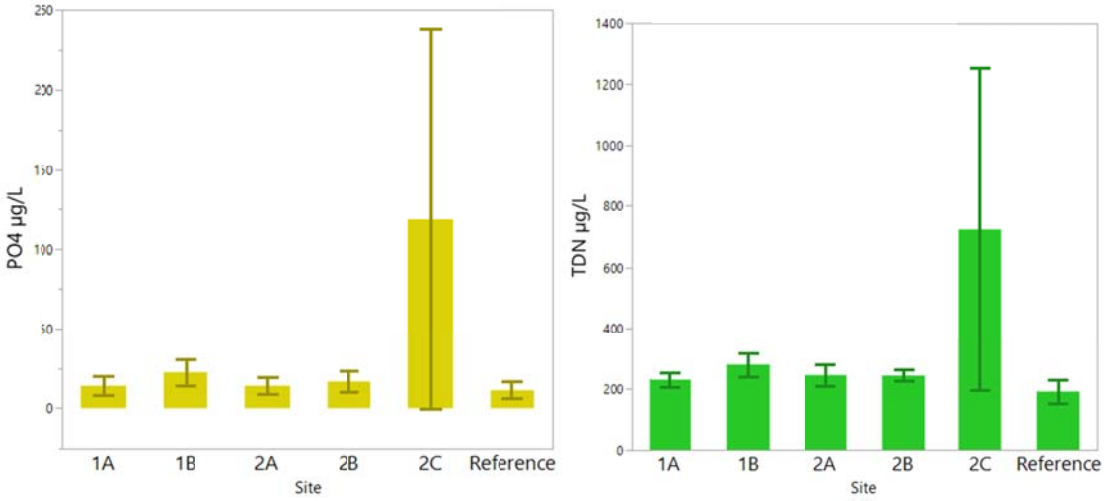

Figure 3.2. Average (*top left*) nitrate and nitrite, (*top right*) ammonium, (*bottom left*) phosphate, and (*bottom right*) total dissolved nitrogen concentrations in each of the sample sites. Mean values are plotted with error bars representing 95% confidence intervals.

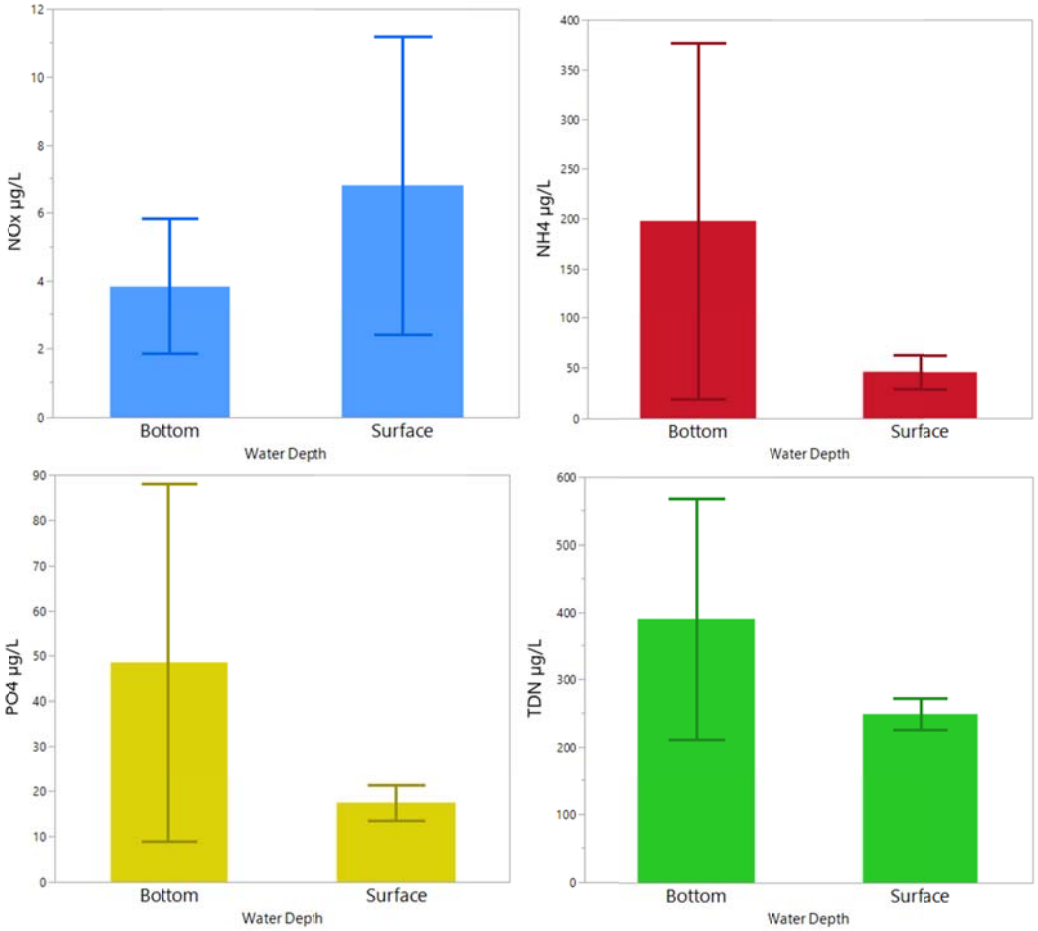

Figure 3.3. Average (*top left*) nitrate and nitrite, (*top right*) ammonium, (*bottom left*) phosphate, and (*bottom right*) total dissolved nitrogen concentrations for surface and bottom waters. Mean values are plotted with error bars representing 95% confidence intervals.

3.2 Sediment nitrogen flux

All of the sites measured had positive rates for nitrogen flux, which is indicative of denitrification in the sediments. The end of the short canal (Site 1B) had a significantly higher rate of denitrification than the other three sites tested; the other sites were not significantly different from each other ($p<0.05$, Fig. 3.4).

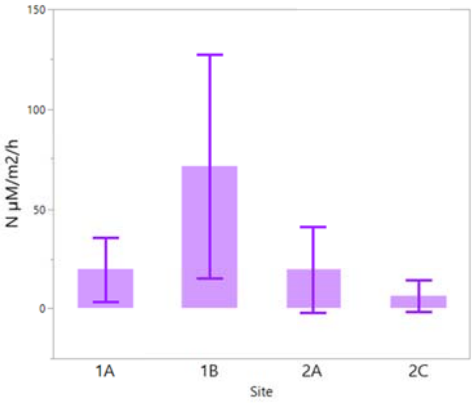

Figure 3.4. Levels of nitrogen flux at four of the sampling sites in the canal system. Mean values are plotted with error bars representing 95% confidence intervals.

4. DISCUSSION

4.1 Water column nutrient concentrations

Nitrate and nitrite concentrations were significantly higher on 17 October 2018 than on other dates, including at the reference site. We hypothesize that high freshwater input from Tropical Storm Michael, which traveled through North Carolina from 10-12 October 2018, may have deposited nitrogen into the canals from the nearby Atlantic Beach land area as well as into the open waterway. Excess nitrate and nitrite are often sourced from activities related to human presence, which is why these nutrients may have been more abundant on 17 October 2018 when other nutrients were not different across the other dates of sampling. Hurricane Florence, a high impact hurricane in North Carolina, would also impact nitrate and nitrite concentrations in this way, but Hurricane Florence had vacated North Carolina at least two weeks before this study began, which is why these same effects are not evident on the first day of sampling. When comparing surface and bottom nutrient levels across all dates, nitrate and nitrite concentration was the only nutrient parameter that was more concentrated at the surface, which is also indicative of human sourced effluent entering this system and changing nutrient dynamics.

In grouping data by canal, consistently higher concentrations of all of the nutrient parameters were observed in the longer canal (Canal 2). This canal is bordered by a greater length of land area than the shorter canal, and greater exposure to impervious surface may explain the larger deposition of nutrients in this canal. In addition, the site located at the end of the longer canal (Site 2C) had significantly higher levels of all of the nutrient parameters tested except for nitrate and nitrite, which is consistent with the notion that Canal 2 is more heavily impacted by anthropogenic inputs to the system. The other canal sites in the study were not significantly different to the reference site for any of the nutrient parameters, suggesting that low flushing in the longer canal contributes to the high concentration of nutrients at Site 2C and reduces nutrients from being expelled from the canal and diluted in the open waterway (Chapter 2: Circulation and Flushing: Sections 3.1 & 4.4). The flushing times in the longer canal are longer than in the short canal, and the depth at the end of the longer canal is greater than the depth at the mouth or middle of that canal. This bathymetry creates a pressure gradient that resists flushing and makes water at the site prone to stagnation.

4.2 Sediment nitrogen flux

The raw nutrient concentration data reflect that anthropogenic inputs of nutrients are likely impacting the canal system, but the flux characteristics are also important in determining how the system will adapt to stressors like excess nutrients. The positive flux rates indicate that each of these sites is performing net denitrification and removing some of the bioavailable nitrogen present in the system.

Denitrification is the process of taking bioavailable species of nitrogen and converting them into inert nitrogen gas, which is not biologically available to most organisms. This removal of bioavailable nitrogen can mitigate some of the effects of anthropogenic nutrient loading and contributes to the bottom-up control of phytoplankton and bacterial communities in the system.

Site 1B, located at the end of the short canal, had a significantly higher rate of net denitrification than the other test sites, which is consistent with field observations of the state of that site. The end of the short canal, (Site 1B) was fully vegetated by salt marsh plants and oysters and this more unperturbed and "natural" state may have supported a more extensive denitrifying community in the sediment. In contrast, the mouths of the canals (Sites 1A and 2A) and the end of the long canal (Site 2C) were located adjacent to hardened shorelines and no vegetation was observed at these sites. Hardened shorelines like bulkheads and seawalls are installed to prevent erosion and protect property, but can have detrimental impacts on the ecosystem services performed in the adjacent intertidal area (Gittman et al., 2015). One strategy to achieve both property protection and still support the natural coastal ecosystem is to utilize living shorelines, which contain both hardened and natural components. Living shorelines with salt marshes and fringing oyster reefs have been shown to support higher rates of denitrification when compared to hardened shorelines, and therefore the presence of these organisms can aid in the mitigation of excess nutrient deposition in coastal systems like the Atlantic Beach, NC canal system (Onorevole et al., 2018).

5. CONCLUSION

Nutrient characteristics of the Atlantic Beach, NC canal system are important indicators of ecosystem health because they reflect anthropogenic inputs of nonpoint source water pollution, which influences microorganisms. The most important parameter that influenced nutrient concentrations and flux dynamics in this system was the location within the canals. Site 2C, located at the end of the long canal, had significantly higher levels of nutrient concentrations than other sites, and this is likely due to the low flushing and high exposure to the surrounding community of water in this canal. The highest rates of denitrification were observed at Site 1B, located at the end of the short canal, because this site was adjacent to a shoreline with living components like salt marsh grasses and oysters.

Elevated nutrient levels are linked to increased turbidity, lower dissolved oxygen levels, and can stimulate harmful algal blooms. They negatively impact food resources and marine habitat, and can make water bodies unsafe for fishing and swimming. North Carolina has a growing population of over 10 million residents; additional development and urbanization to accommodate growth is likely to result in increased nutrient runoff, and this poses a challenge for effective management of nutrient impairments (Schiavinato and O'Hara, 2016). However, it is promising that denitrification is occurring throughout the Atlantic Beach, NC canal system because this nitrogen removal process serves as a natural source alleviating the pressures excess nutrients can create.

Chapter 4: Primary Production

1. INTRODUCTION

Phytoplankton primary production and community composition are influenced by a variety of factors, including physical water properties such as flow rate and residence time, as well as light and nutrient availability (Cloern, 2001). Autotrophic organisms provide one of the main sources of organic carbon to higher trophic levels in estuarine systems, making them integral to aquatic environments (Chen & Borges, 2009). A rapid expansion or bloom of algae can be a natural and critical process for food webs of marine and freshwater systems. However, when these blooms grow out of control and inhibit natural processes, or shift to harmful, toxin-producing species, it can be an indication of an increase in nutrient loading from sewage effluent, agriculture, or animal operations (Gilbert, 2016). Algal blooms and eutrophication can have significant deleterious effects on ecosystems, and are known to cause hypoxic dead zones, significant shifts in trophic dynamics, and loss of essential habitat (Gilbert, 2016).

It is evident that primary producers play a vital role in aquatic systems and can be an indicator of overall environmental health. Further, an imbalance of phytoplankton due to anthropogenic influences can have detrimental effects on the health of ecosystems. We conducted a detailed analysis of the primary producers in the canal system in Atlantic Beach, NC to better understand the water quality in terms of the phytoplankton community. The canals are subject to influence by human activities due to their proximity to many residential homes, which could affect the primary producer community in the system via increased nutrient inputs, potentially leading to eutrophication. Our goal was to determine the phytoplankton biomass, species abundance and composition, and productivity rates relative to environmental conditions in the canal system. The data we collected can help to demonstrate the anthropogenic factors influencing the water quality of the system and whether the conditions of the canal should be improved through appropriate management strategies.

2. METHODS

In order to analyze the primary productivity, phytoplankton growth rate, and community composition of the Atlantic Beach canal system, we collected water samples at six selected sites on four dates: 3 October 2018, 9 October 2018, 17 October 2018, and 24 October 2018. Five of these sites were located within 2 Atlantic Beach canals, and the sixth was a reference site located in Bogue Sound outside of the canal system (Fig. 0.1). Samples were taken during ebb tide, with neap tides on 3 October 2018 and 17 October 2018 and spring tides on 9 October 2018 and 24 October 2018 (NOAA Tide and Water, 2018). These samples were analyzed for phytoplankton biomass, growth rate, and species composition.

2.1 Field Measurements

At each of the six sites, we collected samples at the surface and at depth in 250mL opaque bottles after 2 sample rinses. We took surface samples manually by holding the mouth of the bottle just under the surface, while samples at depth were taken immediately above the sediment surface using a Van Dorn Sampler. In addition to taking two water samples at each site, we recorded the GPS coordinates of the site and measured surface temperature, salinity, light levels, and total water depth. We measured temperature at the surface using a thermometer and salinity of each of the samples using a refractometer in the lab. We evaluated light levels with the use of a Secchi disk on all four sampling days, as well as with a Li-Cor 2π PAR sensor on a YSI 6600 Sonde on the third and fourth sampling days. These two methods were compared to see how the less precise method (Secchi disk) compared to the more precise method (YSI Sonde). Light attenuation can be found based on the light extinction coefficient per meter (K) calculated from the Secchi disk or YSI Sonde data collected in the field, using one of the following equations for the Secchi or Sonde data, respectively (Smith, 1990):

(1) $K = 1.7/(Secchi\ depth)$ (4.1)

(2) $K = ln(Id/I0)/-d$ (4.2)

In equation 2, *Id* represents light flux to depth *d*, *I0* is light flux at depth 0 (immediately below the surface), and *d* is depth below the surface in meters. Total depth was approximated by extending the Secchi disk to the sediment using the markings on the Secchi disk rope, which indicated depth in 0.25 meter increments. Latitudinal and longitudinal coordinates for each sampling location were recorded using a handheld GPS on the first sampling day, and a smartphone on the remaining three sampling days.

We performed three different laboratory analyses: chlorophyll-a content via fluorometry as an indicator of phytoplankton biomass, growth rate and photosynthetic efficiency via radioactive carbon tagging, and the characterization of phytoplankton community species composition via microscopy.

2.2 Chlorophyll-a Analysis

To perform the chlorophyll-a analysis, we vacuum filtered 50 mL of each water sample onto separate glass microfiber filters. We prepared three replicate filters of each sample in order to increase our procedural validity. We then folded the filters in half using forceps, wrapped them in labeled foils, and froze the samples at -20°C for at least 24 hours. To quantify the chlorophyll-a pigment present, we placed the filters in vials of 10mL acetone, sonicated the samples, and froze them for 12-24 hours. Afterwards, we centrifuged the vials, refiltered the acetone using a syringe to remove filter fragments, and then measured the fluorescence using a Turner Trilogy benchtop fluorometer. The fluorometer was calibrated using two standards: a blank and a solid standard with a known reading (31.38 µg/L). The concentrations given by the fluorometer were adjusted for the dilution in acetone and the value given by the blank standard. The equation used to calculate the final chlorophyll-a concentration in µg/L is:

$$chlaconcentration\left(\frac{\mu g}{L}\right) = \left(fluorometerconcentration\left(\frac{\mu g}{L}\right)\right) - \left(blankstandardconcentration\left(\frac{\mu g}{L}\right)\right)\left(\frac{volextracted(L)}{volfiltered(L)}\right)(dilutionfactor) \quad (4.3)$$

These concentrations are used as an indicator of biomass and photosynthetic productivity.

To examine potential relationships between nutrients and phytoplankton, two linear regressions were conducted: the first was between chlorophyll-a concentration (a proxy for phytoplankton presence), and dissolved inorganic nitrogen (the sum of nitrate, nitrite, and ammonium concentrations), and the second was between chlorophyll-a and phosphate concentrations. These nutrient types represent much of what is bioavailable to microorganisms, and therefore are the best parameters to examine in relation to phytoplankton abundances.

2.3 Growth Rate and Photosynthetic Efficiency

We analyzed four of the six sampling sites for growth rate of the phytoplankton at the surface; these samples were from the end of the short canal (1B), the mouth of the long canal (2A), the end of the long canal (2C), and the reference site. This procedure determines the growth rate of the phytoplankton in each sample in terms of carbon uptake after exposure to a range of light levels. We tagged 100 mL of each water sample with 400 µL of a 14 mCi/L, ^{14}C radioactive bicarbonate solution. We then dispensed 2 mL aliquots into twenty-four vials. Twenty-one of the tagged subsamples were placed into the Photosynthetron, a controlled environment algal culturing system which exposes the subsamples to a measurably attenuating light source ranging from 0.183 µE/m^2/s to 531.561 µE/m^2/s for approximately 30 minutes at *in situ* water temperatures specific to each sampling day (Lewis and Smith, 1983). Three subsamples served as controls and were not exposed to light. After incubation, we acidified the samples and controls with 500 µL of HCl and left them under the fume hood for approximately 24 hours before

neutralizing with 500 µL of NaOH and finally adding 10 mL of scintillation cocktail. After waiting approximately 24 hours, we placed the samples in the LS 6000 Liquid Scintillation Counter, which measured the uptake of radioactive ^{14}C into each sample during its exposure to light in the Photosynthetron in terms of degradations per minute (DPM). The equation used to convert DPM to productivity in µgC/µgChla/hour is:

$$IncorporatedC12 = SampleDissolvedInorganicCarbon\left(\frac{mg}{L}\right)(1.06)\left(\frac{DPMmeasured-backgroundDPM}{totalDPMadded}\right) \quad (4.4)$$

$$Productivity\left(\frac{\mu gC}{\mu gChla(h)}\right) = \left(\frac{incorporatedC12}{Chla\left(\frac{\mu g}{L}\right)*incubationtime(h)}\right) \quad (4.5)$$

We used these data to compare light exposure to photosynthetic activity and to model the biomass growth rate as indicated by carbon uptake. This allowed for the determination of a photosynthesis vs. irradiance relationship fitting the following equation, where P is photosynthetic productivity measured in µgC/µgChl-a/h, Pmax represents the maximum carbon fixation due to light saturation, α represents the slope of the photosynthetic curve at unsaturated light levels, and PAR is photosynthetically activated radiation measured in µE/m^2/s (Jassby and Platt, 1976):

$$P = (Pmax)tanh\left(\frac{\alpha*PAR}{Pmax}\right) \quad (4.6)$$

We used this relationship to illustrate the potential productivity of the phytoplankton in the analyzed sites. We used incident irradiance data recorded at the Duke University Marine Lab and light attenuation data collected in the field to determine the actual irradiance levels and subsequent biomass-adjusted productivity rates through the water column and over the course of the day at the selected sampling dates and locations. We derived growth rates from the calculated productivity values using chlorophyll-a concentration and the conversion to biomass based on an assumed ratio of 50g C • g Chl-a^{-1} (Lefèvre et al., 2003). This allowed us to characterize the productivity and growth rates of the phytoplankton in the selected sites throughout the canal system given the true natural light and environmental conditions, species-specific tendencies, the canal flushing rate, and other abiotic factors.

2.4 Species Identification Via Microscopy

We carried out microscopic species identification by first preserving 50mL subsamples in Lugol's iodine solution. We then placed these samples into 15 mL settling cylinders to prepare slides, and then viewed the samples at 400x using a Leica DMIRB inverted microscope (Wetzlar, Germany). We identified phytoplankton species, relative abundances, and made generalizations about the patterns in frequently observed species. This analysis was completed for surface samples from four sites (the end of the short canal (1B), the mouth of the long canal (2A), the end of the long canal (2C), and the reference sample) on one sampling day (24 October 2018). We analyzed diversity by listing species and genera present throughout the slides we examined (listed in Table 4.3). Cryptophyta and euglena densities were also analyzed by counting the number of each within the grid cells in the middle of the slides. Organisms partially in the grid were considered to be "within" the grid and were counted towards the total number of units counted. This was completed for 8 slides for each of the 4 sites. The densities were standardized using the following equation:

$$\frac{cells}{mL} = (2.84)(unitscounted) \quad (4.7)$$

3. RESULTS

3.1 Field Measurements

The depth of each site (Fig. 0.1) varied slightly among sampling dates, but the end of the long canal (site 2C) was consistently deepest, and the end of the short canal (1B) consistently shallowest (Table 4.1). Surface water temperature and salinity measurements are shown. Overall temperature and salinity of the surface water declined slightly over time.

Table 4.1. Depth of water column, surface temperature, and surface salinity measurements.

Date	Site	Depth (m)	Temp (°C)	Salinity (psu)
10/3	1A	1.5	25.4	32
10/3	1B	0.75	25.1	30
10/3	2A	1.7	25.4	26
10/3	2B	2	25	29
10/3	2C	3	25	30
10/3	Ref.	N/A	25.9	30
10/9	1A	1.7	27	31
10/9	1B	1	26.8	28
10/9	2A	2	27.6	32
10/9	2B	2.3	27.4	31
10/9	2C	3.2	27.4	30
10/9	Ref.	4.2	27.1	30
10/17	1A	1.5	24	27
10/17	1B	1	24	26
10/17	2A	1.1	24.4	26
10/17	2B	1.5	24.1	27
10/17	2C	2.75	23.7	27
10/17	Ref.	4.2	24	27
10/24	1A	1.25	18.4	27
10/24	1B	1	18.7	28
10/24	2A	1.6	18	27
10/24	2B	1.1	19	27
10/24	2C	3.5	18.1	27
10/24	Ref.	N/A	19	29

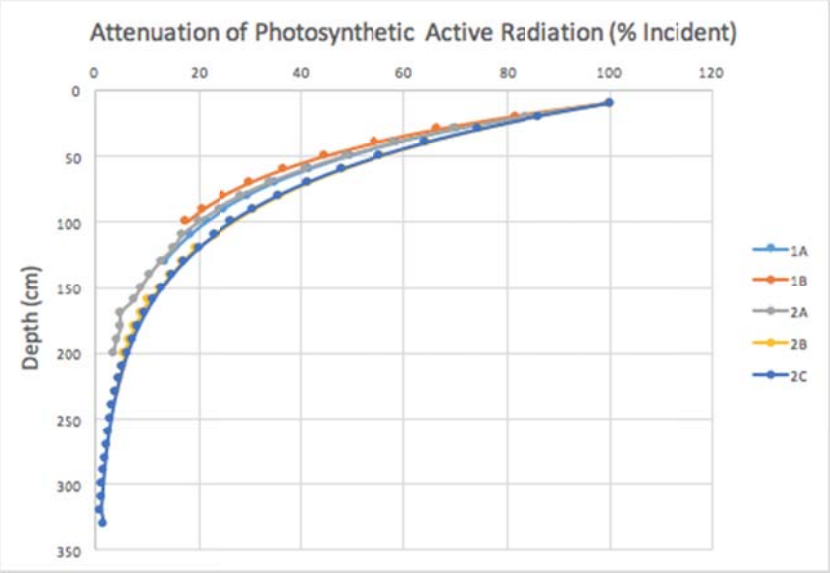

The time-averaged light attenuation levels of all six sites, expressed in units of photosynthetically active radiation (PAR), differed slightly, with the most rapid attenuation over depth occurring at the middle and end of the long canal (sites 2B and 2C, respectively; Fig. 4.1). The light attenuation of the reference site could not be reliably calculated due to strong water currents preventing the Secchi disk or Sonde to be lowered vertically in the water column.

Figure 4.1. Percent PAR attenuation of each site over all sampling dates.

3.2 *Chlorophyll-a Analysis*

Each site was assessed for its concentration of chlorophyll-a. Chlorophyll-a is used for photosynthesis by all autotrophic organisms; thus, its concentration is an indicator of total phytoplankton and primary producer biomass. There was a significant difference in chlorophyll-a concentration over time in the surface samples ($p=0.005$). Changes in concentration over time did not vary monotonically, nor based on spring tide (9 October 2018, 24 October 2018) or neap tide (3 October 2018, 17 October 2018; Fig. 4.2). However, on 17 October 2018, following Tropical Storm Michael, chlorophyll-a concentrations at all sites were lowest, possibly due to the associated rainfall and flushing of the system.

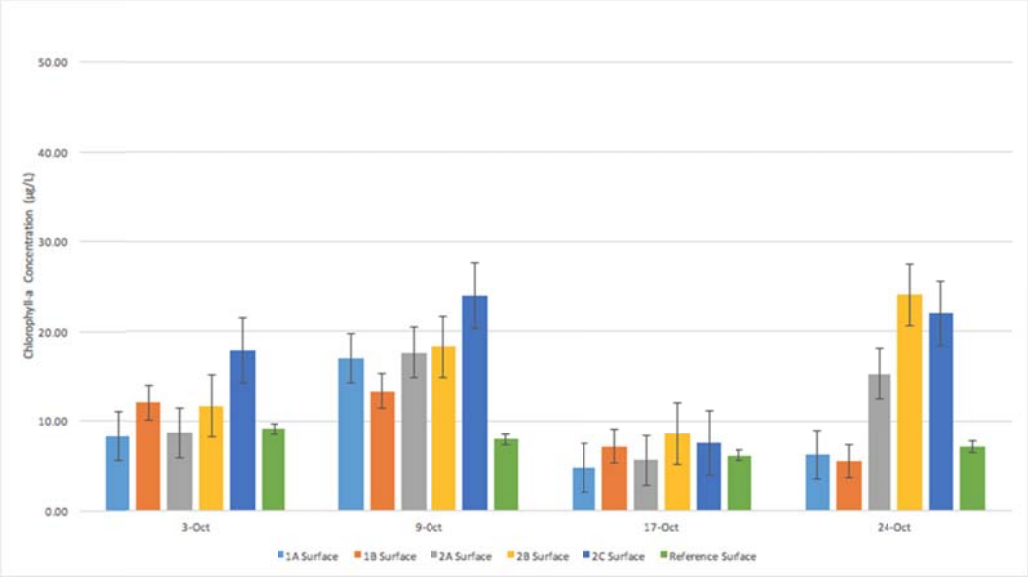

Figure 4.2. Surface chlorophyll-a concentration at each site across all four sampling dates.

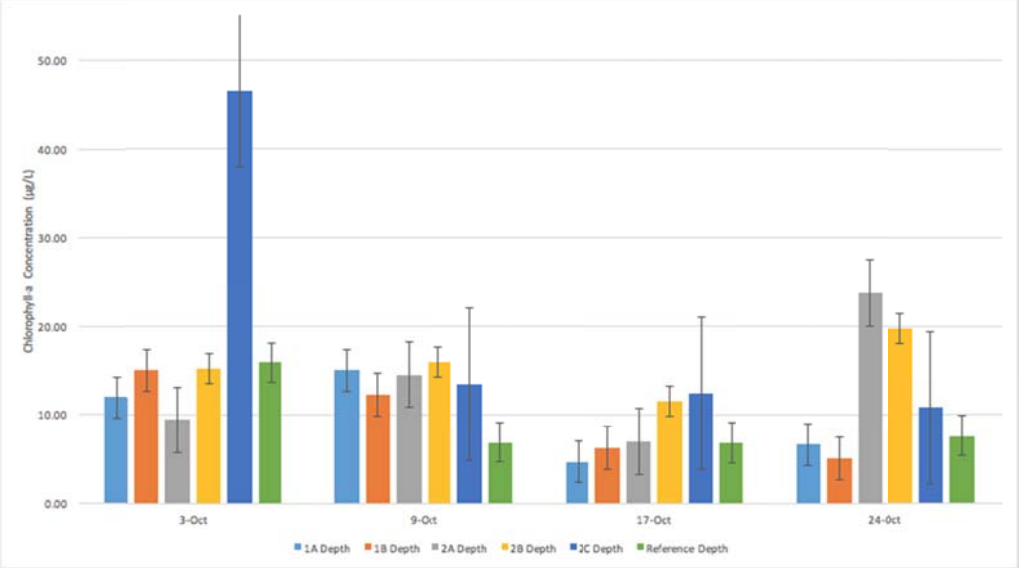

Figure 4.3. Chlorophyll-a concentration at depth at each site across all four sampling dates.

Due to outliers and high standard deviation in depth samples, conclusions could not be made regarding time trends in chlorophyll-a concentrations (Fig. 4.3). There was no significant difference in concentration between samples taken at depth over all sampling dates ($p=0.16$).

The median chlorophyll concentrations over time in each sample were compared to characterize the relative productivity and abundance at each site (Fig. 4.4 and 4.5). In the long canal, the surface waters had slightly higher chlorophyll-a concentrations, and the concentrations at the long canal increased slightly from mouth (2A) to end (2C). There was a significant difference among all sites ($p=0.014$).

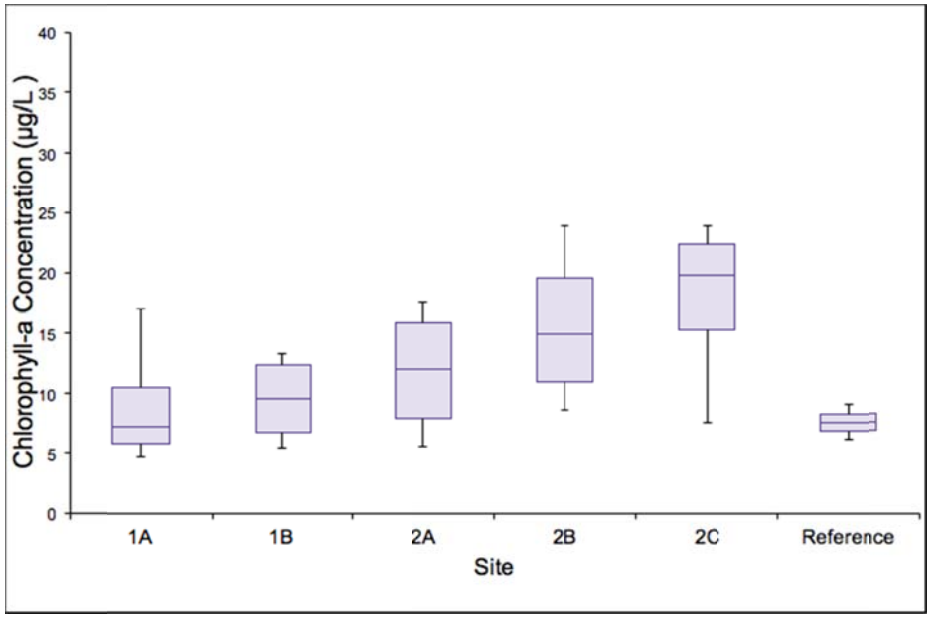

Figure 4.4. Median chlorophyll-a concentrations (µg/L) for surface samples at all six sites

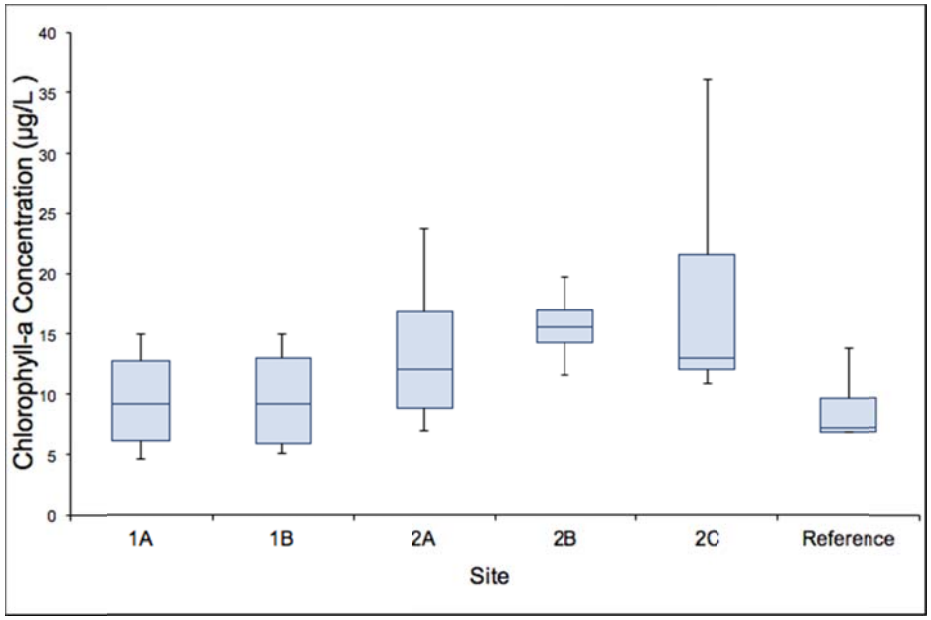

Figure 4.5. Median chlorophyll-a concentrations (µg/L) for depth samples at all six sites

Overall median chlorophyll-a concentrations were similar between surface and depth (Fig. 4.4 and 4.5). The deeper samples within the longer canal had marginally higher median chlorophyll-a concentrations than the other samples taken at depth. The chlorophyll-a concentration at the middle of the long canal (2B) slightly exceeded that of the end of the long canal (2C), different than the pattern seen among the surface samples of canal 2. However, there was no significant difference between median concentration at depth at any of the sites ($p=0.28$).

There was no significant difference between median chlorophyll-a concentrations at the surface and at depth ($p=0.056$). This implies that productivity is relatively constant through the water column, possibly indicating that the water column is relatively well mixed; in other words, the time required for the water column to mix is shorter than the growth timescale of the phytoplankton. Furthermore, the PAR

attenuation curve (Fig. 4.1) indicates that in general, light is available throughout most of the column, supporting phytoplankton productivity at depth.

Dissolved inorganic nitrogen was significantly higher at the end of the longest canal (Site 2C) than at the other sites ($p<0.05$). When analyzed across all sites, chlorophyll-a is negatively correlated with dissolved inorganic nitrogen and phosphate concentrations (Figs. 4.6 & 4.7). Approximately 23% of the variability in chlorophyll-a can be explained by dissolved inorganic nitrogen concentrations, and approximately 18% of the variability in chlorophyll-a can be explained by phosphate concentrations. There are significant relationships between chlorophyll-a and dissolved inorganic nitrogen ($p = 0.0180$) and between chlorophyll-a and phosphate ($p = 0.0409$).

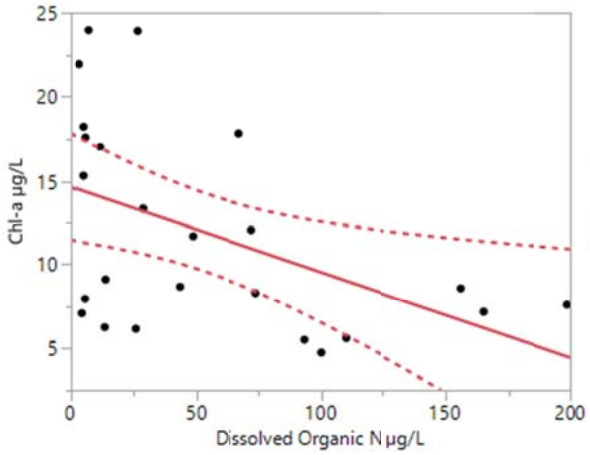

Figure 4.6. Linear regression of chlorophyll-a and dissolved inorganic nitrogen concentrations across all sites ($r^2 = 0.229$, $p = 0.0180$).

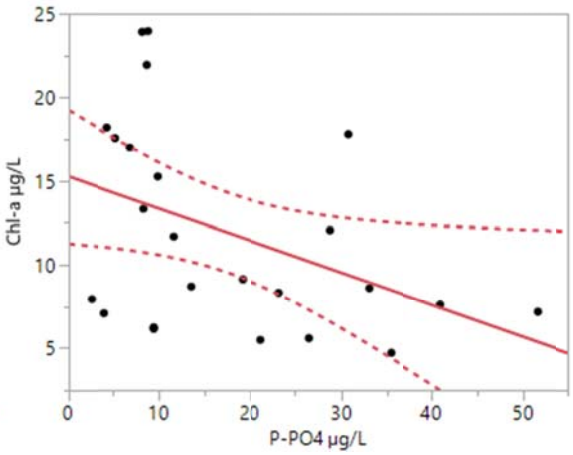

Figure 4.7. Linear regression of chlorophyll-a and phosphate concentrations across all sites ($r^2 = 0.177$, $p = 0.0409$).

3.3 Growth Rate and Photosynthetic Efficiency

Using the biomass-adjusted productivity of each surface sample relative to the irradiance exposure, we modeled the photosynthesis vs. irradiance. The models are shown below with raw data overlaid for each of the 4 selected sites and all four sampling dates (Fig. 4.8). This curve can be represented by two parameters: the initial slope (α), which represents the photosynthetic efficiency under lower light levels, and the asymptote of the curve (Pmax), which is the daily photosynthetic rate per unit of biomass at light saturation (Bouman et al., 2017). These data indicate the different productivity levels at different sites due to physiological characteristics of the phytoplankton communities. The lowest range of Pmax values over all sampling dates is seen at the end of the long canal (2C), and the highest is seen at the end of the short canal (1B).

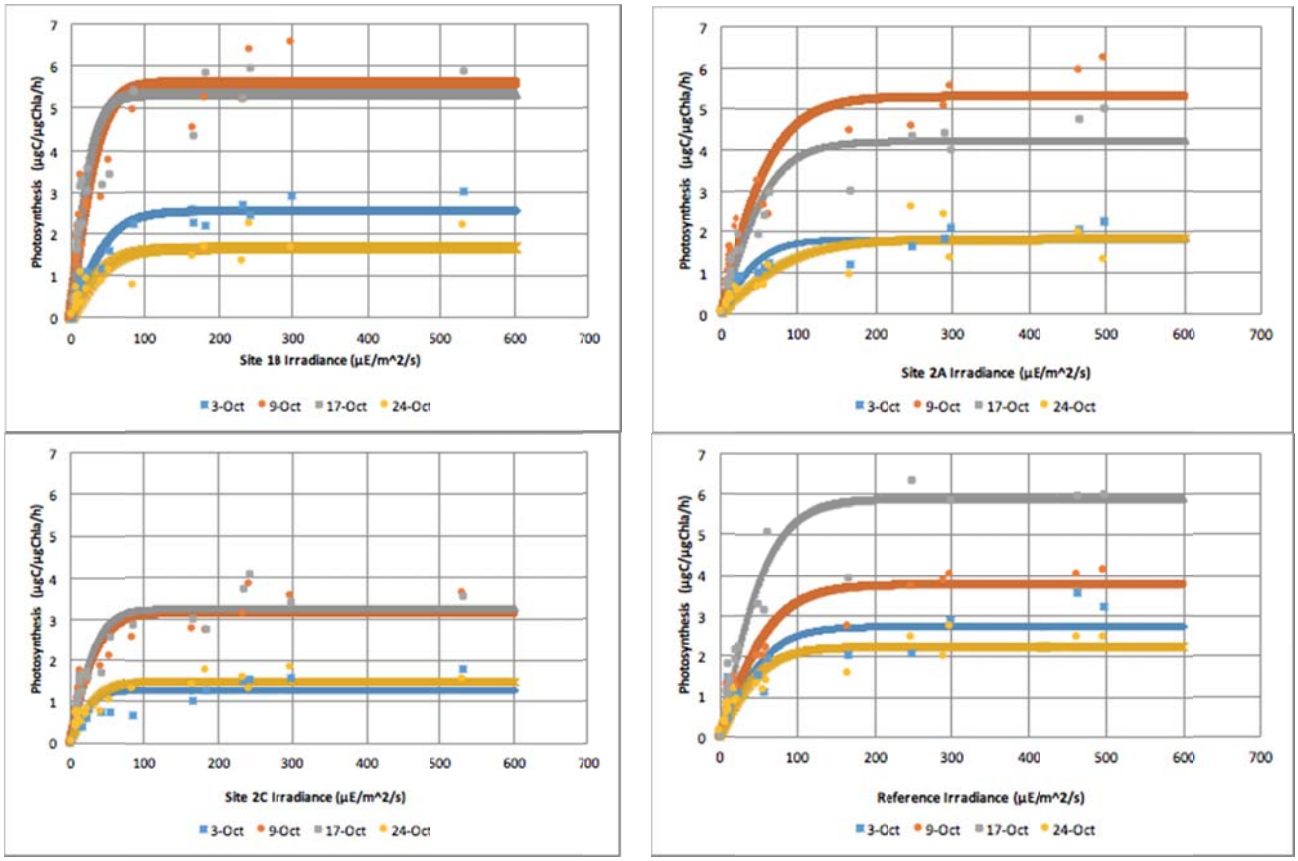

Figure 4.8. Photosynthesis vs. Irradiance at site 1B, 2A, 2C, and reference.

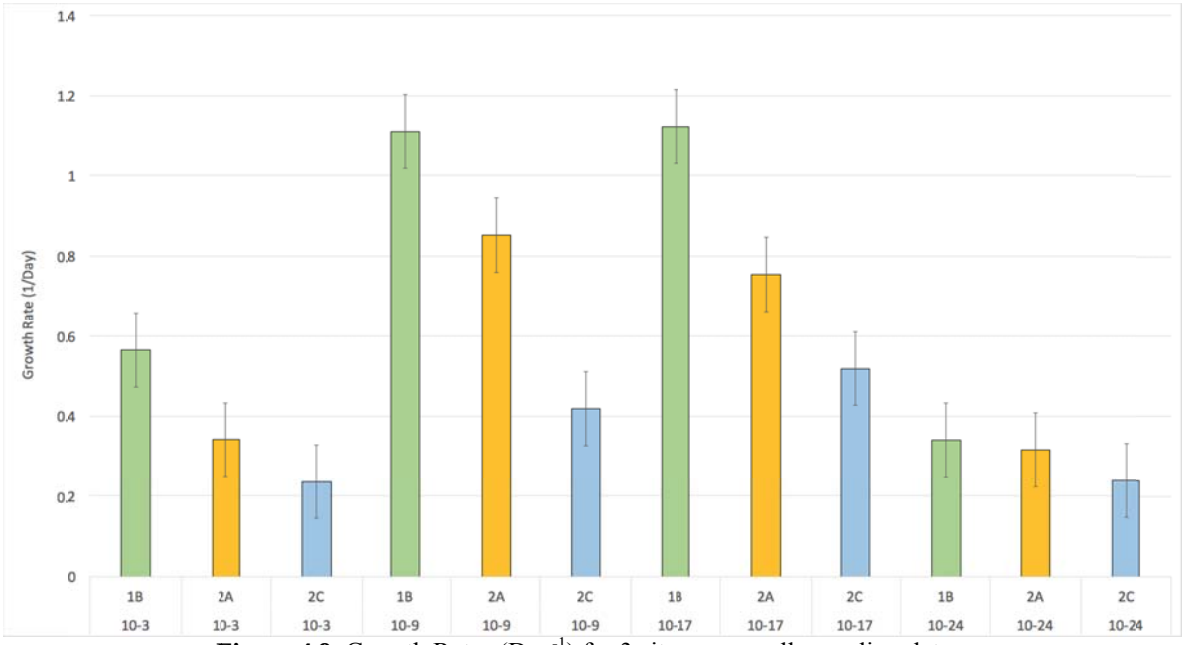

Figure 4.9. Growth Rates (Day^{-1}) for 3 sites across all sampling dates.

Biomass-adjusted productivity according to irradiance level at each date and site was averaged through the water column and summed over each 24-hour period to produce daily productivity values for the end of the short canal (1B), the mouth of the long canal (2A), and the end of the long canal (2C). This allowed for the calculation of population growth rates in each site (Fig. 4.9). The end of the short canal (1B) consistently had the highest growth rate, followed by the mouth of the long canal (2A), and finally the end of the long canal (2C). This represents the rate of population expansion in each of the sites. These results may be a reflection of the physiological characteristics of these phytoplankton and indicative of differences in phytoplankton photosynthetic rates in different areas of the canal system.

Actual primary productivity was determined by comparing biomass-adjusted productivity to actual biomass concentrations over depth at the three analyzed sites (Fig. 4.10). The relative primary productivity rates correlated with the chlorophyll concentrations determined at each site. Despite the lower photosynthetic efficiency of the phytoplankton at the end of the long canal (2C), the daily primary productivity measured in terms of grams of carbon uptake per square meter was higher at 2C on all sampling dates. Primary productivity was similar between the end of the short canal and the mouth of the long canal (1B and 2C) over all dates.

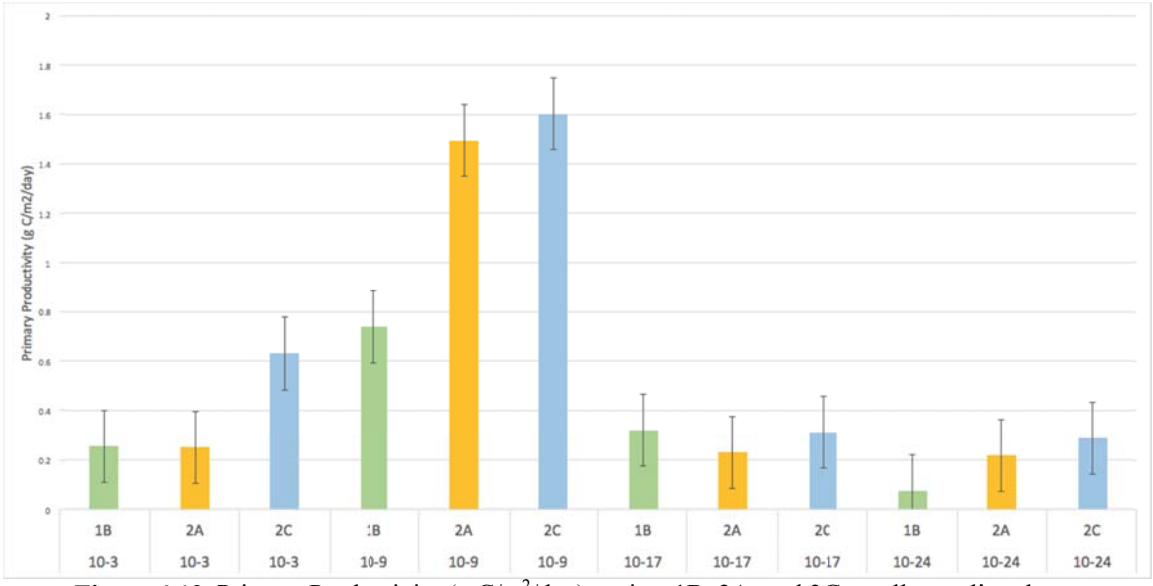

Figure 4.10. Primary Productivity (g C/m^2/day) at sites 1B, 2A, and 2C on all sampling dates.

The average primary productivity at each site over all dates was modeled over the course of a 24-hour period. These values were compared to one another in order to characterize the relative productivity differences in the different locations within the canal and demonstrated that the end of the short canal (1B) had the lowest mean productivity during peak hours, while the end of the long canal (2C) had the highest peak productivity (Fig. 4.11). This indicates that most growth in terms of biomass occurred at the end of the longest canal (2C), the site with the lowest photosynthetic efficiency. Site 1B, at the end of the short canal, appears the most consistently light-saturated over the peak light hours of the day, despite having the highest growth rate, and its low productivity may be a result of biomass limitation at this site as indicated by its relatively low chlorophyll-a concentration.

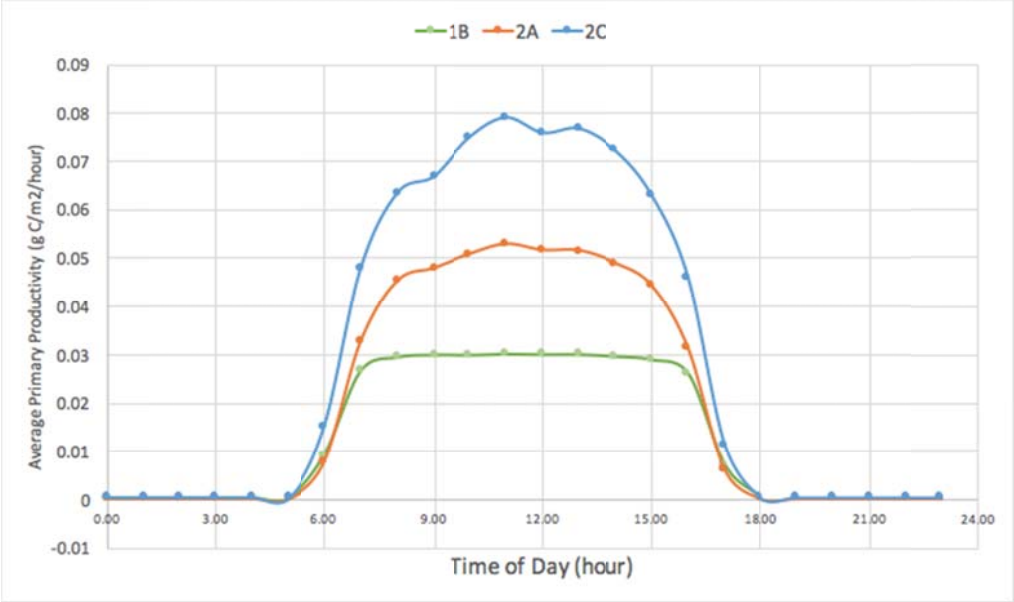

Figure 4.11. Average daily productivity values for sites 1B, 2A, and 2C over the course of one day.

Residence time (measured in days) is the amount of time it takes for a water parcel to leave the canal from each of the sampling sites. Estimations for residence time can be compared to the intrinsic growth rates due to cell division (measured in 1/day). The following equation can be used to estimate net growth rate, where r is intrinsic growth rate due to cell division, d is dilution, g is grazing, s is sinking, and C is net growth rate:

$$C = r - d - g - s \tag{4.8}$$

Residence time was estimated to be between 8.68 to 28.11 hours for the end of the short canal (1B), ≥1.59 hours for the mouth of the long canal (2A) and ≥ 29.13 hours for the end of the long canal (2C) (Chapter 2: Circulation and Flushing). These values were converted to days, and the inverse of each (d) was subtracted from phytoplankton growth rate (r) to estimate the overall net growth rate (C) (Table 4.2).

Table 4.2. Net growth rates for 3 sites averaged across all sampling dates.

Site	**Average growth rate (day^{-1})=r**	**Dilution factor (day^{-1})=d**	**Net growth rate (C=r-d)**
1B	0.785	2.77-.854	-1.98 - 1.91
2A	0.566	≥15.1	≥ - 14.5
2C	0.353	≥0.824	≥ - 0.471

If biomass in the canals is unchanging over time (at a steady state), then C=0, as the combination of losses must account for growth rate. All but one of the resulting net growth rates are negative, which is evidence that for the most part, the canals are flushing out faster than the phytoplankton populations present are growing. The end of the short canal (site 1B) is the only site where the minimum dilution factor was less than the average intrinsic growth rate due to cell division, resulting in a positive net growth rate.

3.4 Species Identification Via Microscopy

Representative microscopy slides for four sites on 24 October 2018 are shown below, in which the cell densities between each site can be visually compared (Fig. 4.12). The end of the short canal (1B) contained 8 of the 11 taxonomic groups analyzed, and had the highest diversity of organisms, as compared to the reference site, in which we identified 3 of the 11 groups (Table 4.3). We observed a higher overall density and abundance of cryptophyta and euglena at the mouth and end of the long canal (2A and 2C, respectively; Table 4.4).

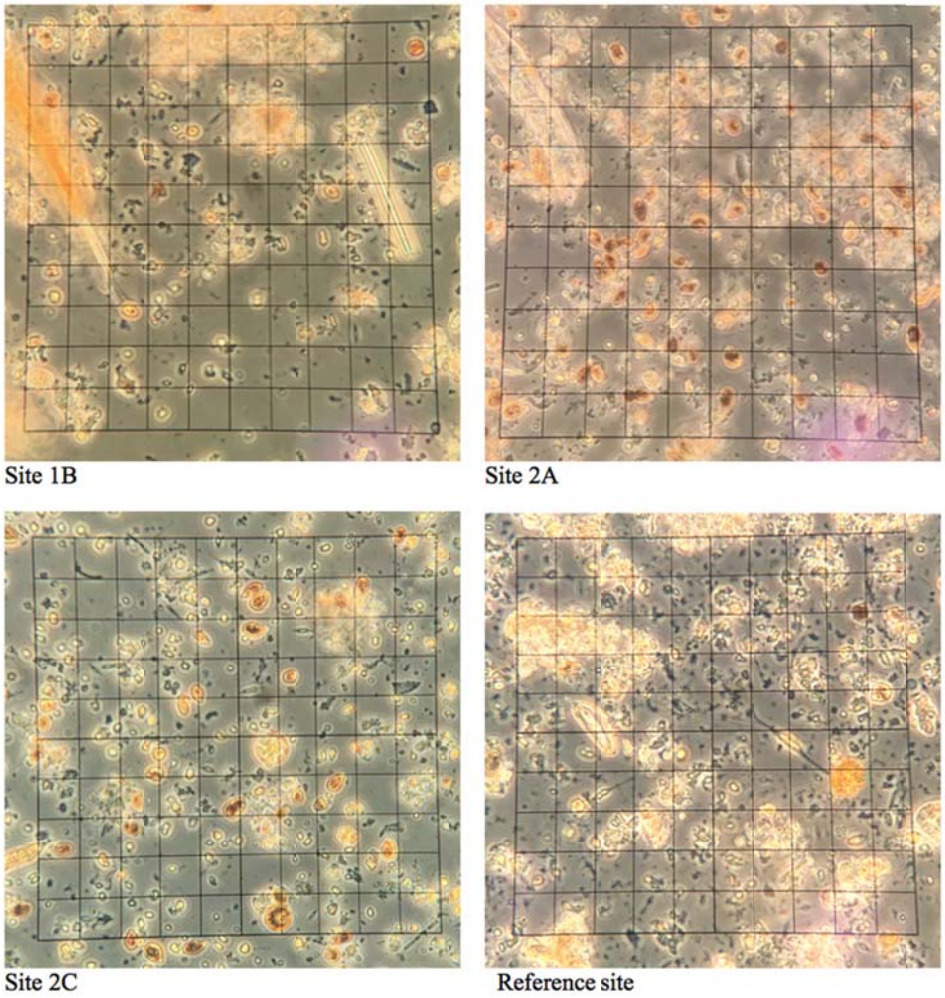

Figure 4.12. Site 1B, 2A, 2C, and reference microscopy slides.

Table 4.3. Phytoplankton present at each of the four sites analyzed.

Taxonomic Group	Sites of Observation
Cryptophyta	1B, 2A, 2C
Euglena	1B, 2A, 2C
Gyrosigma/pleurosigma (diatom)	1B, reference
Prorocentrum (dinoflagellate)	1B
Pennate diatom	1B, 2C, reference
Ciliate	1B, 2A, 2C

Skeletonema (diatom)	2A, 2C
Raphidophyta (genus Chattonella)	1B, 2C
Ditylum (diatom)	reference
Lithodesmium (diatom)	1B
Asterionellopsis glacialis (diatom)	2C

Table 4.4. Cell counts (cells/mL) of cryptophyta and euglena in 4 surface samples collected on 10/24.

Site	**Taxonomic group**	**Cell counts (cells/mL)**
1B Surface	Cryptophyta	346
2A Surface	Cryptophyta	8950
2C Surface	Cryptophyta	7452
Ref Surface	Cryptophyta	158
1B Surface	*Euglena*	0
2A Surface	*Euglena*	276
2C Surface	*Euglena*	749
Reference Surface	*Euglena*	0

4. DISCUSSION

4.1 Field Measurements

Field measurements were taken to see how salinity, temperature, and depth would affect the primary producers in the canals. Because we sampled before low tide each time, the depths did not vary greatly between sampling dates. The depths are reflected in Figure 4.1, in which the Photosynthetically Active Radiation (PAR) values at the end of the short canal (1B) did not attenuate to the same extent as the other sites, because the water depth was shallow and the light was able to penetrate the entire depth. PAR designates the spectral range of solar radiation from 400-700 nanometers that photosynthetic organisms are able to use in the process of photosynthesis, which attenuates with depth as light is absorbed and scattered through the water column (Mõttus et al., 2011). This attenuation, and the overall depth of the canal, affect productivity of photosynthetic organisms. Overall, all of the sites had very similar PAR vs depth curves, with the main difference between them being the length of the asymptote (determined by the depth of the site).

In terms of the other abiotic parameters measured, the salinity was typical of an estuarine system in close proximity to tidal influence and did not vary among sites. Additionally, no correlation between salinity and chlorophyll-a was found after conducting a linear regression comparing the two parameters (R^2=.108). Likewise, no correlation was found between temperature and chlorophyll-a (R^2=.004).

4.2 Chlorophyll-a Analysis

Due to its presence in all photosynthetic organisms, chlorophyll-a is commonly used as a measurement of water quality and as an indicator of phytoplankton abundance and primary productivity in aquatic systems. Chlorophyll-a biomass reflects the influence of both growth and loss processes, and is considered a consistently reliable indicator of primary production. Chlorophyll-a concentrations fluctuate naturally, and are often highest after rain events, which flush nutrients from land into adjacent water systems (Boyer et al., 2009). This is potentially relevant in our study due to the influence of Tropical Storm Michael in North Carolina occurring between the second and third sampling days, as well as

Hurricane Florence occurring shortly before the start of the sampling study, because each event brought high amounts of rainfall to eastern North Carolina. These events may have led to results that do not reflect the normal seasonal conditions of the canals, including in regards to the biomass of phytoplankton, by either increasing their biomass with the addition of nutrients to the system or decreasing their biomass by flushing out the system.

The North Carolina standard for chlorophyll-a in lakes, reservoirs, and other waters subject to growths of microscopic vegetation is a maximum of 40 µg/L, as designated by the NC Department of Environment and Natural Resources (Surface Waters and Wetland Standards, 2007). At all sites, the median chlorophyll-a concentrations were less than half of this standard. The highest observed median concentration was 19.87µg/L at the end of the long canal (2C).

In both of the two Atlantic Beach canals selected for quality assessment, chlorophyll-a concentration was marginally higher than that of the reference location in Bogue Sound. In general, productivity is highest nearer to the surface, where light still penetrates the water column (Fig. 4.1). However, the chlorophyll-a concentrations within the canal system did not exhibit significant difference between surface and depth samples based on a t-test of paired means. This provides the basis for our assumption that productivity is fairly consistent through the column and is determined primarily by light with little influence of density- or salinity-driven stratification, which is an assumption used in the determination of productivity through the water column. The water column is fairly shallow and well-lit, with a relatively small tidal range in the estuarine system driving the tidal currents of the area; these factors may also contribute to the lack of significant difference between surface and depth samples.

Trends in chlorophyll-a concentration between sampling locations and over time were statistically significant in the surface samples. However, this is not true in the samples at depth; statistically significant changes in concentration were not found between locations or over time. Throughout our sampling dates, chlorophyll-a concentration changed non-monotonically, with particularly low values on 17 October 2018 in both surface and depth samples. This is likely a result of Tropical Storm Michael, a hydrologic event which may have flushed out the existing phytoplankton community preceding 17 October 2018. On 24 October 2018, one week after the sampling date immediately following Tropical Storm Michael, chlorophyll-a concentrations in all sites were similar to that in the two sampling dates prior to Tropical Storm Michael, indicating that the system had returned to a normal range of productivity levels. Other than this event, there was little variation among dates, neither as a function of temperature decreasing with the season, nor with the changing tidal magnitudes from spring to neap tide.

Differences in median concentrations between sampling locations were statistically significant at the surface, but not at depth. The long canal consistently had higher chlorophyll-a and thus more phytoplankton biomass. In the surface samples, this level increased from the mouth to the end of the canal. Possible explanations for this include the housing density at the longer canal (canal 2) – higher housing density is an indicator of bioavailable nutrients (Chapter 1: Spatial Analysis: Section 3.3, Figure 1.4; Hobbie et al., 2017). Additionally, canal 2 was the longest canal and thus had a lower flushing rate with increasing distance away from the mouth, allowing for the greatest phytoplankton population expansion (Chapter 2: Circulation and Flushing).

Both dissolved inorganic nitrogen and phosphate concentrations were significantly negatively correlated with chlorophyll-a. This indicates that higher abundances of phytoplankton are associated with lower nutrient levels in the system. Nutrient concentrations are negatively correlated with increased presence of phytoplankton because the community present in the water column is absorbing those nutrients and using them for growth. This trend is consistent with investigations of daily variation in nutrients in relation to chlorophyll-a (Li et al., 2012). This connection between nutrients and phytoplankton could be concerning in the face of cultural eutrophication because as nutrient levels increase over time, the resources available to phytoplankton for growth increase. High phytoplankton density causes high turbidity and lower light penetration, and cyanobacteria grow best under these conditions, which can result in harmful algal proliferation (Chorus and Bartram, 1999). When growth like this occurs, the effects of the toxic algal blooms and shifts in primary producer abundance could be felt more severely by the system.

4.3 Growth Rate and Photosynthetic Efficiency

The relationship between photosynthesis and incident irradiance is fundamental to the study of phytoplankton ecology. This relationship is not fixed; rather, the photosynthetic response will adjust according to fluctuations in ambient environmental conditions (Lewis and Smith, 1983). The Photosynthesis vs. Irradiance models (Fig. 4.8) show photosynthetic productivity in each of the samples at a full range of irradiance exposure and how the analyzed samples fit these models based on the irradiance exposure during analysis. The sampling dates of 9 October 2018 and 17 October 2018 demonstrated the highest biomass-adjusted growth rates at light saturation, while the first and final sampling dates (3 October 2018 and 24 October 2018) exhibited the lowest growth rates at all sites. The differences in growth rate (indicating photosynthetic efficiency) both within each site over time and between the four analyzed sites were statistically significant.

Over the course of a day, the end of the short canal (1B) consistently exhibited the highest average photosynthetic efficiency based on its daily growth rate, while the end of the long canal (2C) exhibited the lowest on average (Fig. 4.9). This reflects the lower overall maximum photosynthetic rate at light saturation at the end of the long canal (2C; Fig. 4.7). However, productivity was highest in site 2C and lowest in site 1B (Fig. 4.10). As with site 2C, the mouth of the long canal (2A) exhibited a lower average daily growth rate than the end of the short canal (1B), yet 2A had a similar rate of productivity as well as a higher average chlorophyll-a concentration, when compared to site 1B. The primary productivity rates at the three analyzed sites ranged from 0.075 to 1.6 g C $\bullet m^{-2} \bullet d^{-1}$. These are typical of productivity values in nearby North Carolina estuaries; in the Neuse, productivity has been found to be around 0.78 g C $\bullet m^{-2} \bullet d^{-1}$ (Fisher et al., 1982) or 1.24 g C $\bullet m^{-2} \bullet d^{-1}$ (Boyer et al., 1993). In the Newport River, productivity was found to be around 0.3 g C $\bullet m^{-2} \bullet d^{-1}$ (Fisher et al., 1982). It is important to note that the end of the long canal (2C) was the deepest site and the end of the short canal (1B) was the shallowest (Chapter 2: Circulation and Flushing: Section 3.1, Figure 2.3). Light attenuated most rapidly at site 2C and much of overall productivity in aquatic ecosystems occurs in well-lit surface waters. Factors such as these may create preferable conditions in site 2C for a larger population, albeit one with lower photosynthetic efficiency, such that 2C was the location of the greatest rate of primary productivity. Additional reasons for these results may include increased nutrient input to site 2C based on proximity to sewage systems and residential areas (Chapter 3: Nutrients: Section 3.1, Figure 3.2), as well as low flushing rates in 2C (Chapter 2: Circulation and Flushing: Section 3.3, Table 2.2). The calculated photosynthesis and growth rates showed intrinsic growth rate and the differences therein throughout the canal system based on possible physiological characteristics of the phytoplankton communities; however, other factors contributing to cell loss, such as grazing and sinking, may also have an impact on the measured population sizes at different sites. Although we did not account for the loss parameters, the net growth rate calculated from the intrinsic rate due to cell division and the dilution factor allows the determination of the impact of these two factors on the total biomass present in the canal systems. The results also suggest a potential difference in phytoplankton species composition throughout the canal system, as both of the analyzed sites in the long canal had lower photosynthetic efficiencies than the sites in the short canal. To determine the ability of the phytoplankton population to grow within the context of hydrologic dynamics of the canal system, it is necessary to compare these daily growth rate values with the flushing rates of the canals. These comparisons suggested that growth is not likely in any of the canals due to high flushing rates (Table 4.2). In all sites, the flushing of the canals apparently outpaced the potential for growth.

4.4 Species Identification Via Microscopy

Euglena is a genus of more than 1,000 single-celled flagellated species featuring both plant and animal characteristics. Studies have shown that they are often prevalent in waters receiving high organic matter inputs (Caldwell, 1946). Of the four surface samples analyzed, the abundance of *Euglena* was highest at the end of the long canal (2C), and occurred at a density of 749 cells/mL. The mouth of the long canal (2A) was the only other site where *Euglena* were found, which were at a lower density than the

end of the long canal (2C) (276 cells/mL). *Euglena* were not identified at the end of the short canal (1B) or the reference site. They could be present at these sites, but were not observed on the slides for the single sampling day analyzed. More analysis would be needed to make conclusions about the presence or absence of species at all of the sites. The higher density of *Euglena* at the end of the long canal (2C) could be indicative of higher organic matter inputs, due to the proximity to higher densities of homes with septic tanks (Chapter 1: Spatial Analysis: Section: 3.3, Figure 1.5) influencing water quality or the longer residence time at this site (Chapter 2: Circulation and Flushing: Section: 3.3, Table: 2.2).

Cryptophyta, unicellular algae known to thrive over a range of aqueous habitats from marine to freshwater, were one of the most abundant taxonomic groups present in the four samples analyzed. Cryptophyta were present at all sites, and were found in the highest densities at the mouth of the long canal (2A) and end of the long canal (2C) with 8950 and 7452 cells/mL, respectively. The sites in the long canal (canal 2) had the highest density of both cryptophyta and *Euglena*. It is likely that the higher nutrient levels in this canal support a higher abundance of phytoplankton. More specifically, the end of the long canal (2C) had the highest levels of all of the nutrient parameters tested except for nitrate and nitrite, further supporting that this canal is more heavily impacted by anthropogenic nutrient inputs which may support higher phytoplankton counts. The reference site had the lowest densities of cells of both taxonomic groups. This could be indicative of the higher flushing rate at this site outpacing the growth rate of phytoplankton, leading to a lower abundance of species presence at this site. However, further microscopic analysis across more dates and at more locations is required to accurately assess the diversity of phytoplankton in the canal system.

The highest cell counts of cryptophytes and euglenids were found at the mouth and end of the long canal (sites 2A and 2C), the two sites with the lowest growth rates yet the highest phytoplankton biomass. This could be explained by the known slower growth rates of flagellates (such as euglenids and cryptophytes). Smayda (1997) cites that flagellates are generally slower growers than diatoms, and points to their lower maximum photosynthetic rates as the driver (Smayda, 1997). This is supported by our data; the longest canal had the highest flagellate cell counts (Table 4.4), the lowest growth rates (Fig. 4.9), and the lowest maximum photosynthetic rates at mouth and end (2A and 2C) for nearly all sampling dates (Fig. 4.8).

5. CONCLUSION

The assessment of phytoplankton community throughout the canal system shows higher biomass presence within the canals relative to the reference site, likely due to factors such as low flushing and anthropogenic nutrient additions. Biomass in the long canal was higher than in the short canal ; however, the average growth rate over the depth of the column was higher in the short canal than in the long canal. This may in part be due to the physical attributes of the short canal, in which the well-lit, shallower water column facilitates productivity throughout; it also may indicate different physiological characteristics of the phytoplankton in the different canals, as the maximum chlorophyll-normalized productivity at light saturation was lower in the long canal based on our analysis, indicating a larger but generally less productive population of phytoplankton. Species composition was different within the canals than in the surrounding area in Bogue Sound, with much higher observed densities of euglenids and cryptophytes, supported by higher nutrient availability. In general, the phytoplankton community is not a threat to the water quality within the season and time interval of this study, as concentrations of total phytoplankton biomass in chlorophyll-a are below state standards. However, the canals are more conducive to phytoplankton growth and residence than the deeper, nutrient-deplete, unconfined, regularly-flushed areas of the waterway. Further urban development contributing to eutrophication or confinement of water in the canal systems may increase phytoplankton presence to potentially hazardous concentrations.

Chapter 5: Filtration

1. INTRODUCTION

The uptake of phytoplankton, contaminants, and detritus by filtration is an integral process to the improvement of water quality. Excess nutrients, such as nitrogen and phosphorus, can be introduced from runoff sources. In a poor flushing environment, these nutrients may fail to leave the system. Filtration can be accomplished in estuaries by naturally present organisms such as oysters, which act as biological aides to water quality. Oysters are filter feeders and consume suspended solids and particles, excreting the waste as biodeposits, or pseudofeces. Adult oysters have the ability to filter 50 gal day (Newell, 1988), which can clear the water column of excess particles, phytoplankton, and suspended solids such as sediment (Dame 1993). While oysters can filter out materials like these in the water column, bacteria are too small for the oysters to filter. Bacteria, however, can be taken up by oysters when attached to larger particles that are filtered and retained by oysters, thus decreasing bacterial contamination in the water column.

2. METHODS

2.1 Pilings and Bulkheads

From boat surveys, we gathered bulkhead information along the length of each canal. Compositional changes in bulkhead type were recorded, as well as marking the transition point marked in UTM using a Garmin GPSmap76 handheld GPS. We used Google Earth to count the number of docks, determine the length of each type of bulkhead using the distance tool, and stored GPS coordinates. We counted the number of pilings on five of the docks during the field survey, and estimated the total pilings throughout the canals by multiplying the average number of pilings counted on each dock by the number of docks in each canal.

In this study, we found six different types of bulkheads in addition to natural shorelines (NAT) in the two canals selected for analysis. These included the following types of bulkhead compositional materials: asbestos (ABS), an asbestos/cement mixture (ASB/CEM), polyvinyl chloride (PVC), cinderblock (CDRB), concrete (CON), and pressure treated wood (PTW). We estimated filtration capacity of oysters in each canal based on the oyster densities on each bulkhead type as well as on pilings.

2.2 Oyster Density

Nichols (2012) studied the relationship between bulkhead types and oyster density and size. We combined the estimates from this study with several direct measurements of the intertidal surfaces supporting oysters in the Atlantic Beach canals to calculate oyster densities on pilings and bulkheads. We determined the circumferences of 10 pilings in each canal, 20 in total, using a measuring tape. We found the vertical oyster range on each of the measured pilings using a meter stick. The vertical range started in the water the furthest down that an oyster could be seen to the highest part of the piling where oysters were found. The averages of the circumference and the oyster height range were multiplied to find the total area of oysters on pilings. To find oyster density on the pilings, known oyster densities on pressure treated wood, from Nichols (2012), were applied to the pilings, as they are made of the same material. Because we could not access the bulkheads during the boat survey, we used the same vertical range for piling and bulkheads.

Again, oyster density estimates from Nichols (2012) were applied to the bulkheads in both canals. Nichols (2012) covered all but two of the bulkhead types found in the canal system: asbestos/ cement mixes and cinder block. Oyster densities on asbestos and concrete bulkheads were averaged together and applied to the asbestos/cement mixes. Cinderblock bulkheads were left without densities attributed to them (Fig. 5.1). While oysters can grow on cinder blocks (Theuerkauf, 2015), direct observations from the bulkheads within the canals showed no oyster growth (Fig. 5.2). Although the canals contained rip rap in front of the cinderblock bulkheads that may have contained oyster growth, they were not considered part of the bulkhead because canal depth did not allow for bulkhead sampling.

Figure 5.1. Cinderblock bulkhead found in the short canal.

3. RESULTS

In the short canal, asbestos-cement mix bulkheads comprised 49.2% of the bulkhead coverage and constituted a majority (Fig. 5.2, *left*). In the long canal, PVC constituted 54.3% of its bulkheads (Fig. 5.2, *right*). Overall, the most common type of bulkhead was PVC with 38% coverage in both canals.

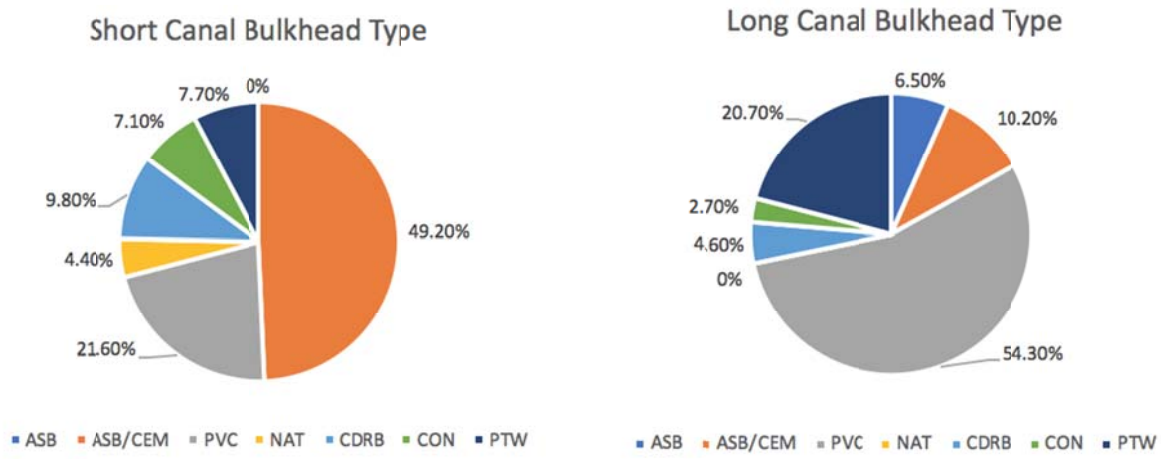

Figure 5.2: The percentages of bulkhead types in the short (*left*) and long (*right*) canals.

The short canal had 33 docks composed of approximately 700 pilings. The long canal had 126 docks composed of approximately 2671 pilings.

Using the density and filtration rates of oysters, found in Nichols (2012) on different types of bulkheads, estimates of the filtration capacity of the oysters present in both canals were made by multiplying the density of oysters by the area of oysters and the individual oyster filtering capacity. The piling oysters of the short canal are capable of filtering 240.8 m^3 of water every day. The oysters on the bulkheads in the short canal can filter 595 m^3 (Fig. 5.3, *left*) of water per day. This totals to 835.8 m^3 of water per day for the short canal. The long canal can filter a total of 2361.4 m^3 per day by the pilings and bulkheads, making up 1017.8 m^3 and 1343.6 m^3 respectively (Fig 5.3, *right*). At mean tidal range the short canal can hold 7141.5 m^3 while the long canal can hold 73,354 m^3.

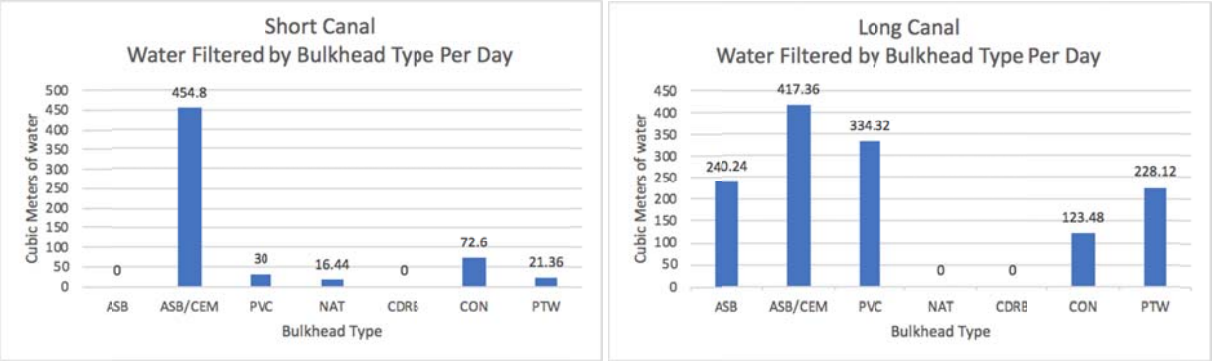

Figure 5.3: The volume of water filtered by the oysters in the short (*left*) and long (*right*) canal broken down by bulkhead type.

To find the time it takes for the oysters to filter the complete volume of water at mean tide level in each canal, the resident water volume was divided by the total filtration capacity over a 12 hr period (on average the oysters, which are intertidal, are exposed in the air for half the day). Consequently, oysters in the short canal would completely filter the water in 8.5 days and would need 31 days to filter the water in the long canal.

4. DISCUSSION

Oysters can positively affect water quality due to their filter feeding, which allows them to remove suspended solids from the water column. Oysters can also reduce the amount of phytoplankton in the area, which is important when trying to control harmful algal blooms.

The predominant bulkhead type that was found in the short canal was the asbestos/cement mixture while PVC was the most commonly found in the long canal (Fig. 5.2). This increase in the implementation of PVC bulkheads within the longer canal may be due to the newer development towards the rear of the long canal. Despite the longer canal being made up over half by PVC, the asbestos/cement mix bulkheads had the highest amount of filtration capacity in that canal due to the higher density of oysters that prefer to settle on the asbestos/cement mix bulkheads.

Given the total filtration rates paired with the total volume of each canal it would take the long canal about four times longer to be completely filtered than the short canal. This is due to the sheer size difference between the two canals as well as the short canal having a greater percentage of bulkhead surfaces that support a greater abundances of oysters. Future studies could integrate oyster filtering capacity and water circulation to gain a better understanding of the role that oysters play in influencing water quality.

5. CONCLUSION

Without any other filtration or flushing influences, it would take 8.5 days for the oysters in the short canal and 31 days in the long canal to filter the entire body of water in each canal. Since blooms could occur in this area in as little as 1-2 days (Chapter 4: Primary Production: Section: 3.3, Figure 4.9), the oysters on the pilings and bulkheads alone are not enough to control a bloom if one were to occur. More precise bathymetry data covering a greater range of the canal would be needed to estimate the amount of water the canal can hold. Additionally, measurements could be improved by gathering oyster densities directly from the bulkheads themselves.

Chapter 6: Bacteria

1. INTRODUCTION

Harmful strains of bacteria are a primary concern when assessing water quality because they pose a significant threat to human health. Not only can bacterial pathogenic strains jeopardize water quality and impact the surrounding community, they can also compromise a variety of important ecosystem services. Filter feeders harvested from the ecosystem, such as oysters, concentrate pathogenic bacterial strains, particularly *Vibrio spp.,* at concentrations 10 times higher in their bodily tissues than the surrounding water (Froelich et al., 2017). Although oysters are not impacted by *Vibrio spp.* they accumulate, consumption of an infected oyster can cause negative impacts to human health such as gastroenteritis or septicemia. Bacterial communities such as fecal indicator bacteria (FIB) can be introduced into the system through a variety of sources such as sewage runoff, leaky septic systems, wildlife, and sewage overflows (Ohrel & Register, 2006). Large storm events, like Hurricane Florence or Tropical Storm Michael, can increase sewage runoff into water systems in close proximity to human development, creating massive outbreaks of bacterial infections (McMichael, 2015). Analyzing the bacterial pathogenic communities present in the Atlantic Beach canal system would provide insight into the water quality as it varies spatially and temporally in the canals used for this study that may have management implications.

1.1 Fecal Indicator Bacteria and Thresholds

To address the concern of water quality in the Atlantic Beach canal system, four key bacterial groups were identified: *Enterococcus,* total coliforms, *Escherichia coli (E. coli),* and *Vibrio spp.* These specific bacteria were prioritized because they are representative of other dangerous bacterial communities (Ohrel & Register, 2006). Although total coliforms and *Enterococcus* are generally not pathogenic, they serve as proxies for other notable strains like *Norovirus,* hepatitis, and typhoid fever, whose presence is a human health concern. *E. coli* is a type of fecal indicator bacteria (FIB) present in the intestines of warm-bodied animals and freshwater systems that could make an individual extremely sick upon consumption (Jin, 2004). The state of North Carolina, among many other municipalities, uses concentrations of *Enterococcus* to assess coastal recreational water quality due to the cost effective nature and relative simplicity to estimate (USEPA, 1986). Bacteria counts are quantified by colony forming units (CFU) or by a most probable number (MPN), which are synonymous. Recreational waters are considered to be unsafe at *Enterococcus* concentrations above 104 colony forming units (2.01 log MPN) per 100 mL of seawater. Threshold values for *E. coli* as outlined by the Environmental Protection Agency (EPA), are 320 CFU (2.51 log MPN) per 100 mL of sampled water (USEPA, 1986). Water that contains values above these thresholds is deemed unsafe for recreational use, but lesser values still pose a risk to human health and should not be ignored.

1.2 Vibrio spp.

Vibrio species are autochthonous, meaning they are naturally found in aquatic environments, but their abundance is influenced by a variety of anthropogenic activities. Past research provides evidence that the abundance of *Vibrio spp.* bacteria can be increased by excess nutrients, copepods, and suspended solids on which *Vibrio spp.* aggregate (Carli, 1993). Their abundance provides information on the risk of bacterial infection of open wounds from contact with canal water (Egidius, 1987). *Vibrio vulnificus* and *Vibrio parahaemolyticus* are both pathogens that contaminate shellfish and the humans that consume them (Froelich et al., 2017). *Vibrio vulnificus* infects open wounds that may result in amputation of the infected limb or death (Egidius, 1987).

2. METHODS

2.1 Field Methods

To assess the aforementioned native and FIB communities present in the Atlantic Beach canal system, we took 1-L water samples from designated sample sites. These sample sites were the mouth and end of the short canal (1A, 1B), the mouth and end of the long canal (2A, 2B), a historical reference site that contained previous *Enterococcus* data from NC Department of Environmental Quality (Historical Reference), and a reference site in Bogue Sound (Reference) (Fig. 0.1). Sampling took place during ebb tide on 3 October 2018 and 9 October 2018, and during both ebb and flood tide on 17 October 2018 and 24 October 2018. Ebb tide samples were prioritized because they are indicative of bacteria originating from land sources rather than being diluted with incoming sea water, and are therefore expected to be the samples with the poorest water quality. Flood tide samples would provide insight on whether tidal influence is enough to displace or dilute the bacterial communities present in the canal.

We obtained the water samples by using an extended one-meter PVC handle to avoid contact with the water. This device held the 1-L sample bottle at the end of a meter-long handle and was secured with a bungee cord. After rinsing the 1-L bottle three times with water taken from the designated site, the sample was then kept, the cap to the bottle was secured, and the bottle was kept on ice in an insulated cooler. Surface temperature and salinity were measured in situ using a hand-held thermometer and refractometer, respectively.

2.2 Lab Methods

Water samples were analyzed within six hours of collection for total coliforms, *E. coli, Enterococcus,* and *Vibrio spp.* Total suspended solids was determined from the water samples as well.

2.2.1 Enterococcus

We determined *Enterococcus* abundance by membrane filtration following methodology outlined by the EPA (USEPA, 2002). For each site, three different volumes (3 mL, 20 mL, and 50 mL) of the thoroughly mixed 1-L water sample were filtered on to a 47mm wide 0.45-micron membrane filter and carefully placed on mEI agar. After the samples were plated, they were incubated face down at 41□C for 24 hours before being counted. The samples were incubated face down to prevent condensation influencing developing colonies. After the incubation time had elapsed, colonies were counted and later multiplied to provide the number of CFU per 100 mL of sampled water.

2.2.2 Total Coliforms and E. coli

We enumerated both total coliforms and *E. coli* by following the EPA's guidelines for assessing recreational water quality (USEPA, 1986). Total coliforms and *E. coli* concentrations were estimated using IDEXX Quanti® -Tray methods, Colilert-18® media packets, and 1:10 mL dilutions of sample to deionized water. Each water sample was replicated twice to detect processing errors. Solutions were mixed by inverting the total sample twice, then Colilert-18® media packets were added to the solution and inverted until mixed for 2 minutes. We then drained the solutions into IDEXX Quanti® -Tray 2000 trays and sealed them using a Quanti® -Tray Sealer Plus and placed them into a 35□C incubator. Each IDEXX Quanti® -Tray 2000 consists of 49 large and 48 small wells. After incubating for 18 hours, each IDEXX tray was examined for the presence of yellow large and yellow small wells because they are positive indicators of total coliform bacteria. Large and small wells on the IDEXX Quanti®-Tray that were yellow in color and also fluoresced under a blacklight were considered positive for *E. coli* and were counted in the same manner as total coliform bacteria. From the number of yellow large and small wells, the most probable number was calculated using the IDEXX calculator to determine the number of bacteria that were present in the diluted sample. Due to the 1:10 mL dilution of sample to deionized water, the most probable number was multiplied by 10 to give the number of CFU per 100 mL of sampled water.

2.2.3 *Vibrio spp.*

We determined the abundance of *Vibrio spp.* using membrane filtration methods on CHROMagar that followed previously established guidelines (Kaysner & DePaolo, 2004). For each site, three different dilutions were made with phosphate buffered saline (PBS) and the water sample depending on in situ salinity. All of the collected water samples were consistently above 24.1 PSU, so the same PBS and water sample dilutions were used throughout the whole study (Table 6.1). These dilutions were made because salinity limits the habitable range of different *Vibrio spp.* (Blackwell & Oliver, 2008). After the solutions of PBS and sample were thoroughly mixed through repeated inverting, 5 mL of the mixed homogeneous solution was filtered using a 47 mm wide 0.45-micron membrane filter and plated on CHROMagar. After the samples were plated, they were incubated face down at 35□C for 24 hours before being counted. Once the incubation period passed, we counted the plates for white, purple, and blue colonies that were referenced using the proprietary guidelines (CHROMagar, 2018). White colonies indicate the presence of *Vibrio alginolyticus,* purple colonies are indicative of *Vibrio parahaemolyticus,* and blue colonies represent *Vibrio vulnificus.* After counting the colonies, each plate count was multiplied appropriately given the salinity to give the number of CFU per 100mL of water sample.

Table 6.1. *Vibrio spp*. dilutions for salinity greater than 24.1 PSU.

Dilution A	Dilution B	Dilution C
Sample: 3 mL *PBS*: 30 mL	*Sample*: 5 mL *PBS*: 28 mL	*Sample*: 10 mL *PBS*: 23 mL

2.2.4 Total Suspended Solids (TSS)

Past research suggests bacteria that aggregate on suspended sediments have longer residence times in a sample area (Fries et al., 2008). To determine TSS, 25 mm wide 0.8 mm glass microfiber filters dried at 55□C at least a week before use were initially massed to an accuracy of 0.001 grams. After massing, 100 mL of sample were filtered. Two replicates were done for each canal. The filters were dried at 55 □C for 7 days. After 7 days, the filters were re-massed, and their differences were recorded. The difference between the weight of the filter was averaged between the two replicates and multiplied by 10 to determine TSS in grams per liter in the sample.

2.3 Analysis

To normalize the data, the raw bacteria data were log transformed after being converted to CFU/100 mL to better determine smaller changes in bacterial abundance. The average bacterial abundance for each site was graphed to assess spatial differences between sites, and also by day to determine temporal changes in bacterial abundance of the canal system. Historical *Enterococcus* abundance for the historical reference site was obtained from North Carolina Department of Environmental Quality (NCDEQ) site 47A, which included data from 1998-2018.

Bacterial communities were analyzed by comparing the abundance of each strain to antecedent rainfall that fell within 24 hours before sampling time. This relationship was investigated because large amounts of rainfall would cause more land-based runoff to infiltrate the system, which could increase the abundance of bacterial strains originating from anthropogenic sources (Ackerman & Weisberg, 2003). These data were gathered from the weather underground website, using site KNCATLAN1, which is at the opening of the Atlantic Beach canal system.

In addition to analyzing R^2 values, an ANOVA test was also used to determine the statistical significance of relationships from regression analysis. These tests were determining significant relationships between average bacterial abundance at each canal and site-specific salinity, temperature, and TSS.

2.4 Enterococcus Mapping Methods

In collaboration with the spatial analysis group, we compiled *Enterococcus* data to provide visual reference of samples and to evaluate the spatial relationship between them. Bacteria data were mapped using a point vector layer to represent *Enterococcus*. This parameter was chosen because it is less likely to yield false positives, and it is used as an impaired water quality indicator for issuing an advisory (NCDEQ, 2018). A point vector layer was created that represented *Enterococcus* levels as rhombi categorized by color to display the concentrations that were observed during ebb tide for each sampling day.

3. RESULTS

3.1 Enterococcus

Concentrations of *Enterococcus* ranged from below detection limit (0 log CFU per 100 mL), to a maximum of 3.01 log CFU per 100 mL. Concentrations of *Enterococcus* above the State of North Carolina threshold for recreational waters of 104 CFU (2.01 log MPN) per 100 mL of sample water were only present at the end of the longest canal (Site 2C) on 3 October 2018. This date was the most immediate sampling event after Hurricane Florence.

These data were graphed to display how *Enterococcus* abundance changed within the canal sampling sites and between the sampling dates. This sequence of figures demonstrates that *Enterococcus* was higher on the 17 October 2018 than on any other sample date, and how the ends of the canals generally contained higher concentrations of *Enterococcus* (Fig. 6.1).

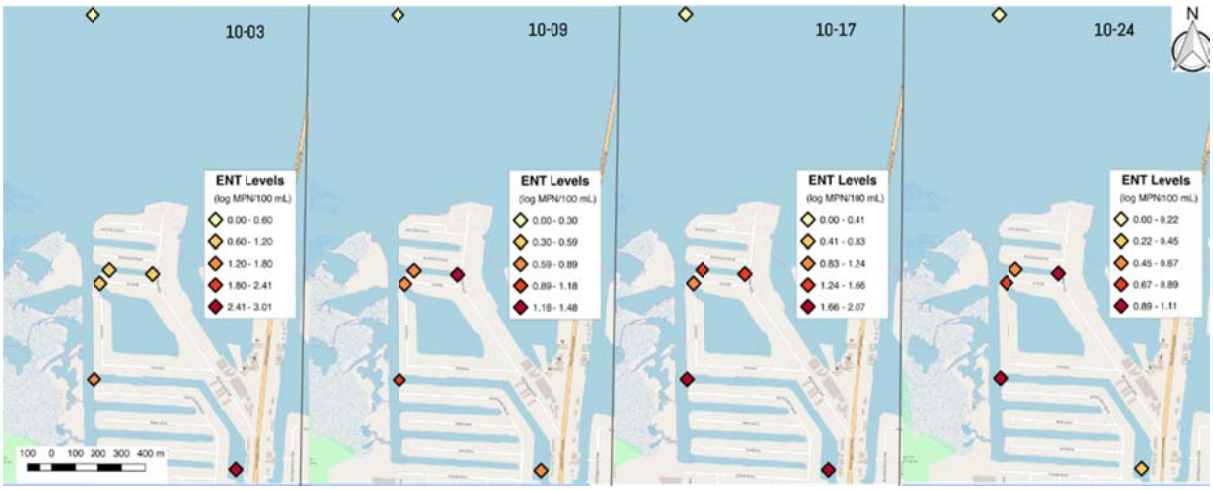

Figure 6.1. Changes in *Enterococcus* abundance throughout the sampling dates. Dark red indicates sampling areas that consisted of of higher concentrations of *Enterococcus* and yellow indicates sampling areas of lower concentrations.

Spatially, *Enterococcus* abundance was highest at the closed ends of the canals and tended to increase with distance from the mouth of the system (Fig. 6.2, *left*). Out of all of the sample sites, the end of the long canal (Site 2C) contained the highest concentrations of *Enterococcus.* The reference site in Bogue Sound did not contain detectable amounts of *Enterococcus* throughout all sample dates and tidal cycles (Fig. 6.2, *left*). In order to observe changes in bacterial abundance in the canal system temporally, *Enterococcus* abundance was averaged throughout the sample sites by day. *Enterococcus* concentration was highest on 17 October 2018 during ebb tide, and was lower during flood tide (Fig. 6.2, *right*). This was the first sampling event following Tropical Storm Michael. The lowest concentrations of *Enterococcus* were found on the 24 October 2018 and showed minimal difference in abundance between flood and ebb tide.

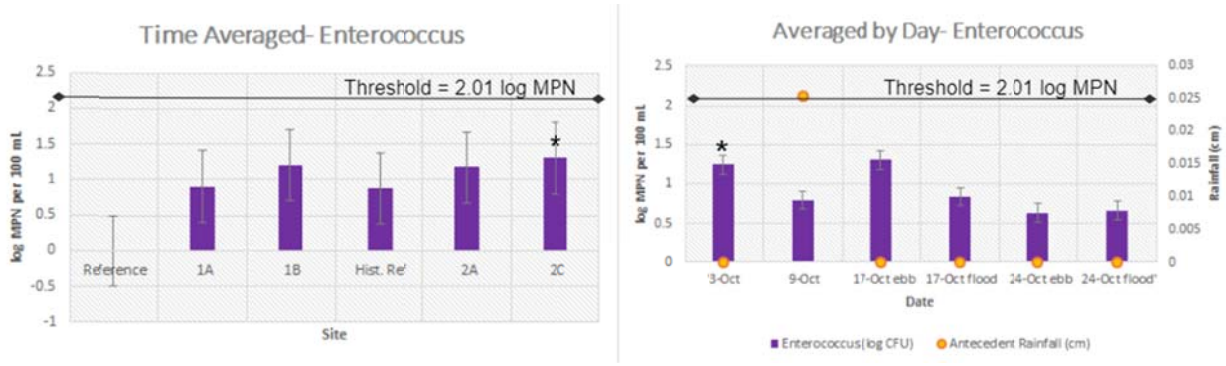

Figure 6.2. *Enterococcus* abundance with standard error bars in log MPN per 100 mL between the different sampling sites (*left*) and days of sampling (*right*). Asterisks indicate that a site or date contained values above the threshold.

Enterococcus concentrations exhibited a moderate negative correlation with both temperature and salinity with R^2 values of 0.705 and 0.623 respectively (Fig. 6.3). The relationship between temperature and *Enterococcus* abundance was statistically significant (ANOVA p=0.05), but salinity was not. The relationship between *Enterococcus* concentrations and TSS was weak and not statistically significant.

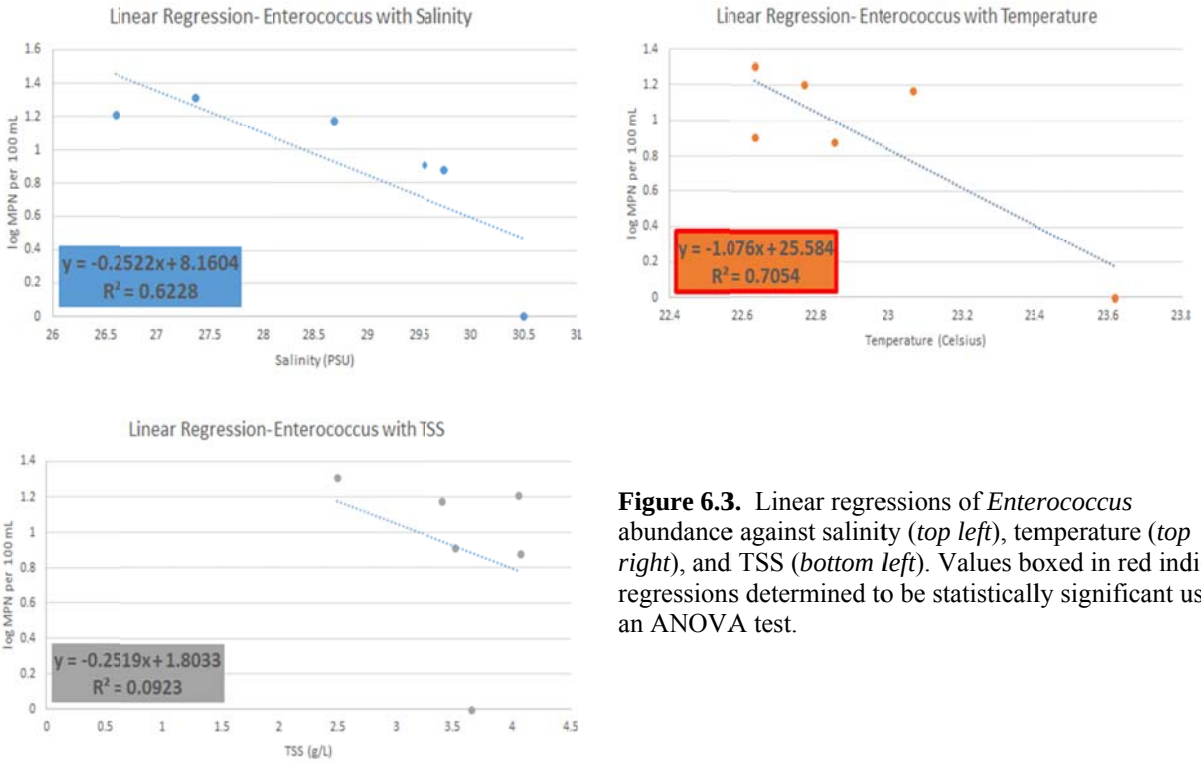

Figure 6.3. Linear regressions of *Enterococcus* abundance against salinity (*top left*), temperature (*top right*), and TSS (*bottom left*). Values boxed in red indicate regressions determined to be statistically significant using an ANOVA test.

3.2 Total Coliforms and E. coli

Concentrations of total coliforms ranged from 2.14 log MPN per 100 mL to 4.17 log MPN per 100 mL. Concentrations of *E. coli* ranged from below detection limit (0 log MPN per 100 mL), to 2.82 log MPN per 100 mL. *E. coli* colony forming units were above the threshold of 2.51 log CFU on the 17 October 2018 during both tidal cycles at the end of the longest canal (2C; Fig. 6.4). *E. coli* abundance was relatively high, but below the threshold, for sites at the closed end of the shorter canal and at the opening of the longest canal (1B and 2A; Fig. 6.4).

When comparing individual canal sites, concentrations of total coliforms and *E. coli* tended to

increase with distance into the canal system. The highest concentrations of total coliforms and *E. coli* were present at the mouth and closed end the longest canal (2A and 2C; Fig. 6.4, *left*). The reference site in Bogue Sound had the smallest concentrations of both total coliforms and *E. coli.* Total coliforms and *E. coli* abundance were analyzed by sample date to look for a temporal relationship with bacterial concentration. Total coliform and *E. coli* abundances were the highest on 17 October 2018 during ebb tide, which was the first sampling event following Tropical Storm Michael. Abundances of total coliforms and *E. coli* trended towards higher values during ebb tide and lower values during flood tide, with the exception of total coliforms on 24 October 2018 (Fig. 6.4, *right*).

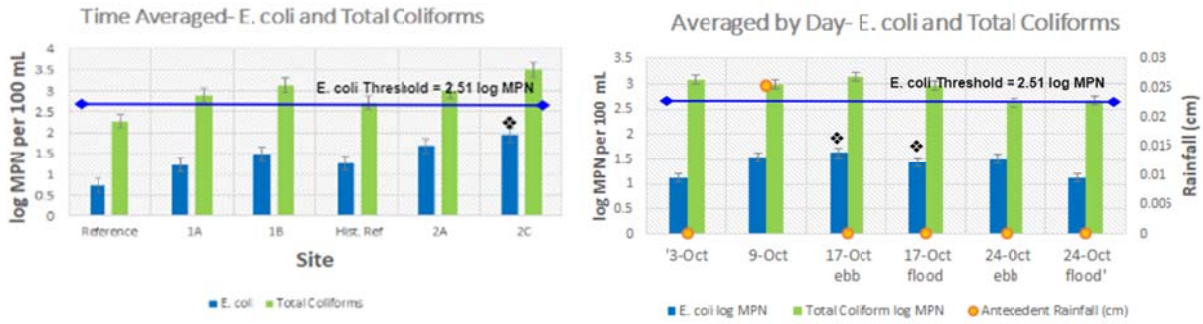

Figure 6.4. Total coliforms and *E. coli* abundance by site (*left*) and by sample date (*right*) with standard error bars. Asterisks indicate sites or dates that had E. coli values greater than the threshold.

There was a strong (R^2 =0.717) correlation between salinity and total coliforms abundance, and a moderate correlation (R^2 = 0.639) with temperature (Fig. 6.5). There was a weak correlation with TSS (R^2 = 0.333). Total coliforms abundance was found to be significantly correlated with changes in salinity (ANOVA p=0.033), but not significantly correlated with temperature or TSS.

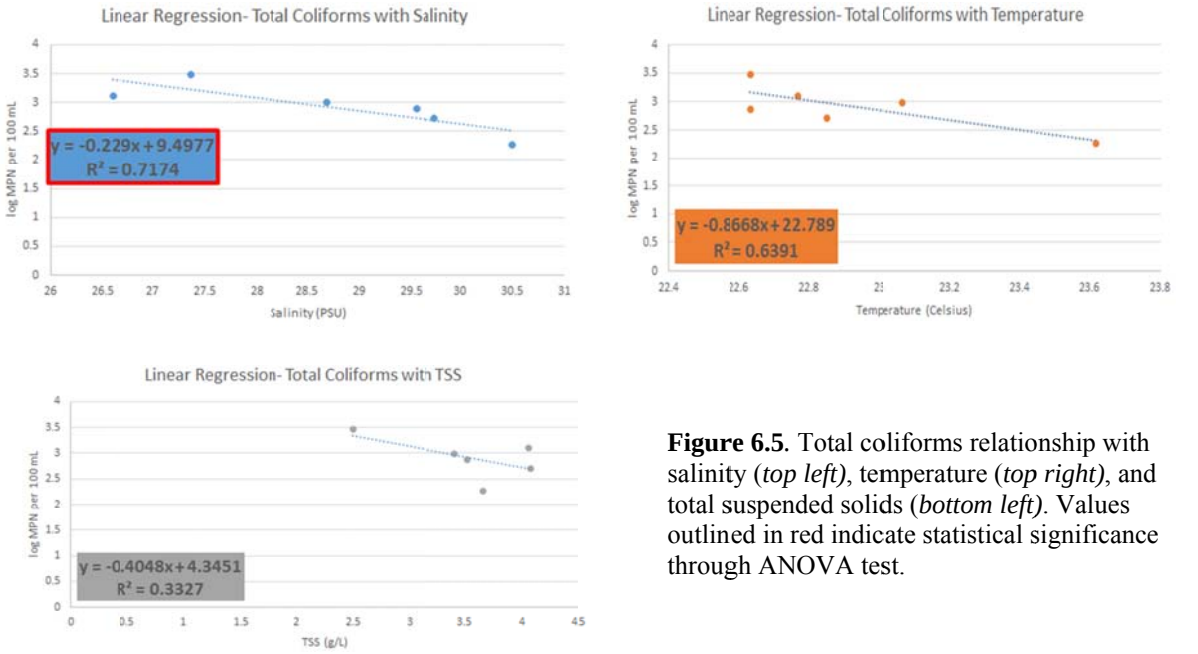

Figure 6.5. Total coliforms relationship with salinity (*top left)*, temperature (*top right)*, and total suspended solids (*bottom left)*. Values outlined in red indicate statistical significance through ANOVA test.

E. coli abundance similarly exhibited a moderate (R^2 = 0.571) and non-significant relationship with salinity, and a weak relationship with temperature (R^2 = 0.4581) and TSS (R^2 = 0.3361) (Fig. 6.6). Both TSS and temperature were not significantly related to *E. coli* concentration.

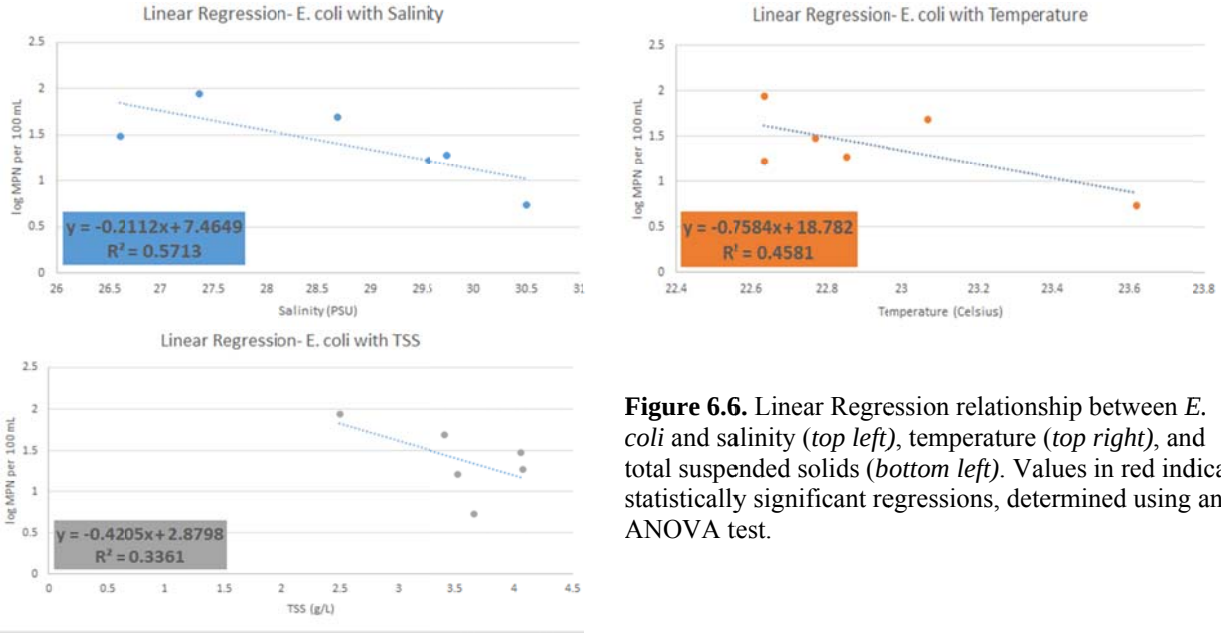

Figure 6.6. Linear Regression relationship between *E. coli* and salinity (*top left)*, temperature (*top right)*, and total suspended solids (*bottom left)*. Values in red indicate statistically significant regressions, determined using an ANOVA test.

3.3 Vibrio Species

Vibrio alginolyticus concentrations ranged between 1 to 3.65 log CFU per 100 mL. *Vibrio parahaemolyticus* concentrations ranged from below detection limit (0.95 log CFU per 100 mL) to 3.01 log CFU per 100 mL, and *Vibrio vulnificus* concentrations ranged from the detection limit (0.95 log CFU per 100 mL) to 2.76 log CFU per 100 mL. Across all sites, *Vibrio alginolyticus* was more abundant than both *Vibrio parahaemolyticus* and *Vibrio vulnificus. Vibrio spp.* abundances were highest at the site present at the end of the longest canal for *V. alginolyticus* and *V. vulnificus* (2C; Fig. 6.7). *V. parahaemolyticus* was most abundant at the end of the shorter canal (1B; Fig. 6.7). The concentrations of all *Vibrio spp.* were lowest at the reference site that was located at the channel marker in Bogue Sound. Salinity values were higher at the mouth than the closed end for both the short and long canals (Fig. 6.7).

Temporally, *Vibrio spp.* concentrations changed with variations in salinity between sample dates in the Atlantic Beach canal system. Concentrations across all *Vibrio spp.* were at their highest on 9 October 2018, and lowest on 24 October 2018 (Fig. 6.8). When comparing tidal influence, *Vibrio spp.* concentrations were higher during ebb tide than flood tide sampling on the same day, with the exception of *Vibrio alginolyticus* and *Vibrio parahaemolyticus* on 17 October 2018.

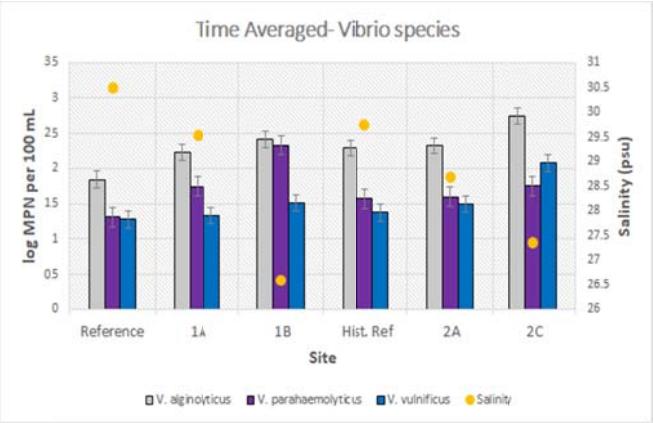
Time Averaged- Vibrio species
log MPN per 100 mL
Salinity (psu)
Reference
1A
1B
Hist. Ref
2A
2C
Site
V. alginolyticus
V. parahaemolyticus
V. vulnificus
Salinity

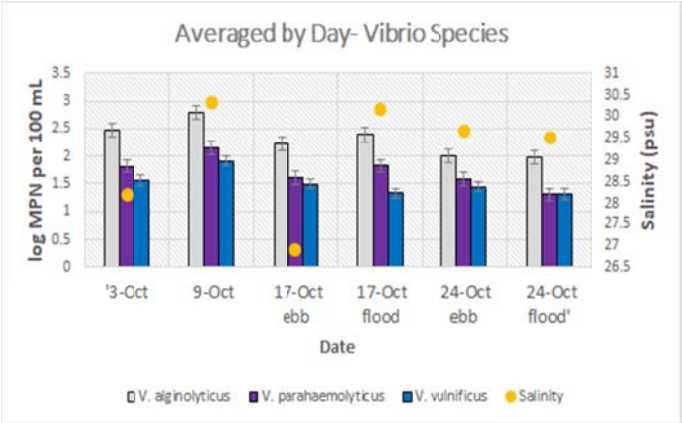
Averaged by Day- Vibrio Species
log MPN per 100 mL
Salinity (psu)
'3-Oct
9-Oct
17-Oct ebb
17-Oct flood
24-Oct ebb
24-Oct flood'
Date
V. alginolyticus
V. parahaemolyticus
V. vulnificus
Salinity

Figure 6.7. Concentrations of *Vibrio spp.* and salinities across the different sampling sites, averaged over sampling dates with standard error bars.

Figure 6.8. Changes in *Vibrio spp.* abundance averaged by date across all sample sites with standard error bars, which trended more strongly with measured salinity

Linear regression and ANOVA statistical analyses were also used to determine correlations between *Vibrio spp.* and salinity, temperature, and TSS. With the exception of the relationship of TSS and *V. parahaemolyticus,* all observed relationships were found to be negative. *Vibrio parahaemolyticus* was found to be significantly negatively correlated with salinity (ANOVA p=0.030), which also exhibited a high R^2 value of 0.7350 (Table 6.2). *Vibrio vulnificus* showed a significant and strong negative correlation with TSS (R^2 =0.6613, ANOVA p=0.049).

Table 6.2. *Vibrio spp.* linear regressions with salinity, temperature, and TSS with significance indicated through ANOVA tests.

		Salinity (PSU)	**Temp (Celsius)**	**TSS (g/L)**
V. alginolyticus	Regression Equation	y = -4.0402x + 38.064	y = -1.0229x + 25.288	y = -1.0822x + 6.0306
	R^2 value	0.6279	0.6471	0.3034
	ANOVA p-value	0.060	0.054	0.66
V. parahaemolyticus	Regression Equation	y = -3.7951x + 35.255	y = -0.6973x + 24.124	y = 0.301x + 3.0171
	R^2 value	0.7350	0.3989	0.0311
	ANOVA p-value	**0.030**	0.18	0.74
V. vulnificus	Regression Equation	y = -3.4488x + 33.951	y = -0.6267x + 23.874	y = -1.613x + 5.97
	R^2 value	0.4488	0.2383	0.6613
	ANOVA p-value	0.145	0.33	**0.049**

3.4 Total Suspended Solids

Values for total suspended solids were found to be the highest at the historical reference site and the site at the end of the short canal (1B; Fig. 6.9, *left*). Opposite of what was expected, values for TSS tended to decrease with distance into the canal system. When comparing the dates and tidal cycles that were sampled, TSS were highest on 17 October 2018 during flood tide, closely followed by 9 October 2018 (Fig. 6.9, *right*). Values of TSS were lower during ebb tides than flood tides on 17 October 2018 and 24 October 2018.

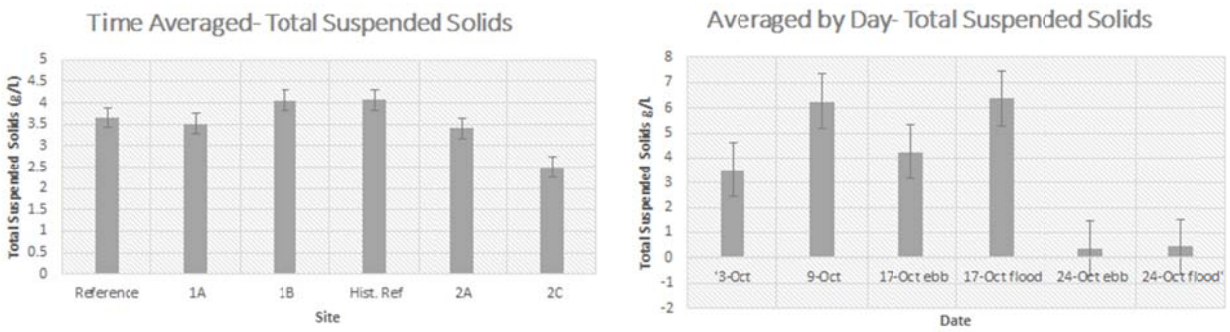

Figure 6.9. Total suspended solids as they changed spatially (*left*) and temporally (*right*) with standard error bars.

4. DISCUSSION

4.1 Spatial Patterns in Enterococcus, Total Coliforms, E. coli and Vibrio spp.

The sample sites furthest into the canal system, notably the end of the short canal and the mouth and end of the longer canal, contained the highest concentrations of total coliforms, *E. coli, Enterococcus,* and *Vibrio spp.* (1B, 2A, 2C; Figs. 6.2, 6.4, 6.7). Sites that contained the highest bacterial concentrations were located farthest away from the canal system's entrance to Bogue Sound, which allowed for high residence times resulting from the lower levels (the shorter canal had a residence time of 8.67-28.11 hours, and the longer canal had a longer residence time likely greater than 29.13 hours (Chapter 2: Circulation and Flushing: Section: 3.3, Table 2.2). The velocity of water moving through the longer canal was found to be slower than the water moving in the shorter canal, which allowed bacterial communities to proliferate due to warm and stratified waters (Chapter 2: Circulation and Flushing: Section: 3.3, Figure 2.4). When time averaged, the observed *Vibrio spp.* concentrations in the longer canal were almost four times higher at the end of the canal than the mouth of the canal. The shorter canal, closest to Bogue Sound, had only 60% higher *Vibrio spp.* concentration at its end. This is likely due to the lower flushing time and higher velocity of water moving in this shorter canal (Chapter 2: Circulation and Flushing: Section: 3.3, Figure 2.4). These data further the claim that adequate circulation has a large impact on *Vibrio spp.* in the canal (Fig. 6.7). CHROMagar has the possibility of producing false positive *Vibrio spp.* colonies, meaning *Vibrio spp.* concentrations could be an overestimate of the actual species concentrations. Additionally, since not all *Vibrio spp.* possess the genes for virulence, these data do not represent the concentration of *Vibrio spp.* that are pathogenic. These limitations could be corrected by isolating each colony and performing a polymerase chain reaction (PCR), which time and funds did not allow for. Further research of this canal system should take this information into consideration.

4.2 Temporal Patterns in Enterococcus, Total Coliforms, E. coli and Vibrio spp.

Tidal influence impacted the bacterial concentrations present in the canal system. The fecal indicator bacteria, *E. coli,* was present at higher concentrations during ebb tide than flood tide for all sites, excluding the reference site and the site present at the end of the long canal (Fig. 6.4). This trend was also seen with *Vibrio vulnificus* (Fig. 6.8). During ebb tide, the sampled water had been in the canal for the longest time, and it therefore may have been exposed to animal and human fecal material for a longer duration than water sampled during flood tide. Furthermore, the shallow water table present at the coast may have been higher than the water level in the canal during mid to low tide, and hence groundwater, possibly containing material from septic systems, may have entered the canal during ebb tide. Tidal cycles are also known to influence salinity within canal systems in estuarine environments (Savenije, 2006). Linear regression and ANOVA analysis found salinity to be significantly correlated with total coliforms and *Vibrio parahaemolyticus* (Figs. 6.4, 6.6, and 6.7). Both of these linear relationships were negative, meaning increasing bacterial community concentrations were found in areas of lower salinity. This is expected with *E. coli,* which likely comes from land sources and has a low salinity tolerance.

Enterococcus and *Vibrio spp.* are usually found in higher concentrations in relatively saltier systems, so this unexpected pattern may have been influenced by the small sample size in this study. In order to determine a distinct relationship between bacterial concentration, tidal influence, and salinity, more research should be done across tidal cycles in the future.

Tropical Storm Michael and remnant effects resulting from Hurricane Florence affected the bacterial concentrations present in the canal system. Total coliforms, *E. coli,* and *Enterococcus* abundance were highest on 17 October 2018, the first sampling day following Tropical Storm Michael, which made landfall on 11 October 2018 (Figs. 6.2 and 6.4). *Vibrio spp.* declined, but this could have been due to storm surge generated by wind which may have introduced more freshwater into the system (Fig. 6.8). Throughout the sample dates in the study, very little rain fell 24 hours before each sampling time, so its impact on the native bacterial strains present in the canal system was negligible in our study.

Over the past two decades, *Enterococcus* data gathered from NCDEQ have shown spikes in abundance during the mid-winter months (NCDEQ, 2018). There is no upward trend in *Enterococcus* abundance in response to increased human development in the canal system over that interval. *Enterococcus* concentrations from the same historical reference site in this study ranged from detection limit to 3 log MPN per 100 mL, and were consistent with concentrations observed in the past two decades (Fig. 6.10). These historical sampling events could have been disrupted by large storms where sampling by NCDEQ was impossible. This provided a very narrow frame of reference for how previous storms could impact the concentration of bacterial communities in the system.

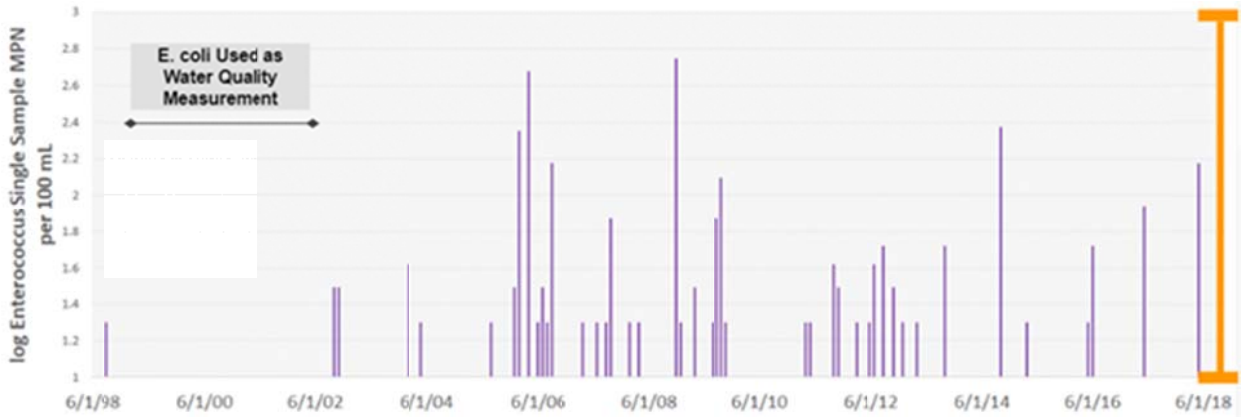

Figure 6.10. Trends in historical *Enterococcus* abundance from NCDEQ at historical reference site. *E. coli* was used for water quality measurements between 1999 and 2002. The orange bar on the right of this figure indicates the ranges that were found in this study.

The *Enterococcus,* total coliforms, and *E. coli* concentrations found in the samples from the Atlantic Beach canal system were generally lower than the 2012 same bacterial concentrations sampled in the Pine Knoll Shores canal system. The Pine Knoll Shores study had maximum *E. coli* concentrations of 3.3 log MPN per 100 mL and contained concentrations that were frequently above the threshold. This study only had one instance where the *E. coli* concentrations were above the threshold and had a lower maximum of 2.82 log MPN per 100 mL. However, *Vibrio parahaemolyticus* and *Vibrio vulnificus* concentrations found in our analysis appeared to be higher than the Pine Knoll Shores canal system. The 2012 study found maximums of 2.60 log CFU per 100 mL for both *Vibrio parahaemolyticus* and *Vibrio vulnificus*, where this study found maximums of 3.01 and 2.76 log CFU per 100 mL for those *Vibrio spp.* respectively. Further research would be needed in order to explore the relatively higher concentrations of *Vibrio spp.* found in this study in comparison to the 2012 Pine Knoll Shores study.

4.3 Evaluation of Total Suspended Solids

Total suspended solids were found to be a small determinant in bacterial concentrations. Spatially across the canal system, total suspended solids values were greater at locations closer to the exit of the canal system to Bogue Sound (Fig. 6.2). High bacterial abundance in tandem with low TSS values were found at the end of the longest canal, site 2C. The low amount of flushing, stagnant water, stratification, and larger water depth in this part of the system may have impacted the resuspension of solids and therefore bacteria residing in benthic sediments. Water passing over benthic sediments at a low velocity offers little frictional energy to elicit the resuspension of sediments in comparison to the larger frictional energy transferred by water moving at a higher velocity. Furthermore, bacterial concentrations at the reference site were consistently lower than all canal sites, but contained the 3rd highest values for TSS. This may be a result of high velocity current at the reference site, which retained sediments in suspension but actively flushed bacterial communities. This was supported by the low R^2 value and high ANOVA p-value produced from most linear regression analyses, with the exception of *V. vulnificus,* with TSS and bacterial abundance (Figs. 6.3, 6.5, and 6.6). Combining all of these patterns, there is evidence to suggest that parameters other than TSS play a larger role in determining bacterial abundance in the Atlantic Beach canal system. Past research provides abundant evidence that temperature and TSS consistently impact bacterial community concentrations, so the lack of relationship depicted is likely due to the narrow scope and sample size allowed for this study (Fries et al., 2008).

5. CONCLUSION

There are several factors that influence the abundance of bacterial communities that pose a threat to water quality in the dynamic Atlantic Beach canal system. The geometry of the canal system is a large determinant in the abundance of observed bacterial communities. Sites that were located at the end of a canal and further inland had higher bacterial concentrations, likely resulting from low flushing and slower moving water. Sites that were closer to the canal entrance had lower concentrations of the observed bacterial communities, but higher values for TSS (Fig. 6.9).

Tidal influence can alter the bacterial concentrations found in the Atlantic Beach canal system. Ebb tide can bring harmful bacterial communities into the canal system from groundwater (Shergill et al. 2004). Flood tide can aid in the flushing of harmful strains that entered the system during ebb tide, which was observed in *E. coli* and *V. vulnificus* concentrations (Figs. 6.3 and 6.7). Large storm events could alter normal tidal cycles and characteristics of the canal system through storm surge, turbulent mixing due to strong winds, and large influxes of fresh water through precipitation runoff. These combined effects on the bacterial community can persist through time in areas of low flushing. *Enterococcus,* total coliforms, and the fecal indicator bacteria *E. coli* all increased in abundance after Tropical Storm Michael (Figs. 6.2 and 6.4). *Vibrio spp.* in particular, undergo range shifts as a result of the large influxes of fresh water due to a large storm event (Blackwell & Oliver, 2008). Shifts in *Vibrio spp.* distribution has the potential to cause the more dangerous strains, *V. parahaemolyticus* and *V. vulnificus*, to reside in higher concentrations, which can increase the risk of infection. Overall, the interplay of tidal influence and large storm events play a large, and opposite, roles in the abundance of notable strains of bacteria present in the Atlantic Beach canal system. Even though concentrations of indicator bacteria resulting from this analysis resided below threshold values for water quality standards, their concentrations still pose a concern for human health and should be closely monitored.

Chapter 7: Synthesis

In order to assess water quality within the Atlantic Beach canal system, we sought to spatially analyze the impacts of development in the canal system, as well as characterize water circulation, nutrient concentrations, primary production, filtering capacity, and bacterial concentrations as they varied within the selected canals. From the compilation of our data analysis, characteristics associated with higher water quality were found in areas of high flushing and tidal influence in which flood tide displaced the contaminants that entered the system during ebb tide. Additionally, canals that contained saltmarsh, notably the end of the shorter canal 1B, had higher rates of denitrification, which aid in the expulsion of excess nutrients from the system. The end of the longest canal, site 2C, consistently contained the highest nutrient, phytoplankton, and bacterial concentrations. This pattern can likely be explained by the low flushing rates determined in this study; however, even with the low degree of flushing at the end of the long canal, FIB concentrations rarely surpassed the threshold established by the USEPA and were consistent with trends seen in the last decade.

Groundwater discharge is positively correlated with low-tide elevation, and thus may be an explanation for the high nutrient, phytoplankton, and *Enterococcus* levels observed during ebb tide on 17 October 2018. During ebb tide, water drains out of the canals and into the surrounding water body, changing the water pressure within the sediment pores and effectively draining the sediments (Riedel et al., 2010). This would result in nutrients and *Enterococcus* that effectively moved through the subsurface and entered the canal through groundwater after the rain event. This excess nutrient input from groundwater could result in phytoplankton blooms that can disturb the water quality within the canal system. Further research into the role of groundwater in this system would help describe the interplay between excess human inputs of nutrients, bacteria and their interactions with tidal cycles.

The long residence time at the ends of the long canals may also lead to the persistence of pollutant-containing runoff, which is exacerbated by impervious surface cover and can result in increased nutrient loading of nitrogen and phosphorus into receiving water bodies (Glasoe and Christy, 2004). Under certain conditions, septic tank systems can introduce concentrations of nitrogen enriched runoff as well as bacteria, such as *Enterococcus*, into both surface and groundwater (Parker et al., 2010; Mallin, 2013). The shallow unsaturated zone is characterized by a high water table and porous soils that provide little attenuation and absorption of pollutants (Withers et al., 2014). The distribution and role of impervious surfaces and OWTS are important to analyzing over-land water movement and inputs into the receiving waters of the canals. Stormwater runoff management provides a way to support environmental water quality, and further research can establish canal-specific measures. No immediate risk of harmful algal bloom formation or immensely concerning bacterial concentrations were detected in this study; however, nutrient loading and bacteria levels in the canal system require additional research in greater depth and across a broader temporal scale, as water quality and associated hazards could fluctuate seasonally. The ability of septic systems to keep up with the high traffic associated with warmer seasons should be tested. If problems are identified, impacts can be directly addressed and mitigated.

Consistent monitoring of water quality throughout the year would broaden the understanding of processes influencing the system. This knowledge will aid in designing improvements and adaptable solutions to promote and maintain water quality throughout the canal system.

Acknowledgements

Special thanks should be given to those who made this study possible. We would like to thank our capstone research mentors Dr. Stephen Fegley and Dr. Johanna Rosman for their patience and guidance during the semester. A special thanks to Captain Joe Purifoy for his time transporting us to and from our sampling sites. We would like to extend our thanks to the officials of the town of Atlantic Beach, in particular Mayor Pro-Tem Richard Porter for reaching out regarding this study, and Mary Hall, Amy Guthrie, and Christine Nitt for tirelessly providing the data and septic tank records that were a large component of the Spatial Analysis chapter. We thank the Rosman Lab for providing resources and guidance for the Circulation chapter. We would like to thank the Noble Lab for their guidance and providing us with the resources needed to complete the Bacteria chapter of this study: Dr. Rachel Noble, Denene Blackwood, Tom Kiffney, Rachel Canty, Matt Price, Dr. Kelsey Jesser. Thank you to the Piehler Lab for providing us with the lab materials and guidance needed to construct the Nutrient chapter of this report: Mollie Yacano, Leslie Arroyo, Suzanne Thompson. Further, we would like to thank the Paerl Lab for providing us with their lab space and resources, and for their guidance in the analyses necessary to the Primary Production chapter of this study: Dr. Hans Paerl, Dr. Nathan Hall, Jeremy Braddy, Karen Rossignol, Randy Sloup, Betsy Abare. Thank you to the Fegley lab for assistance with the Filtration chapter. We are immensely grateful for all of your support and contributions.

References

Abarca et al. (2012)

Ackerman, D. & Weisberg, S. B. (2003). "Relationship between rainfall and beach bacterial concentrations on Santa Monica Bay beaches." *Journal of water and health* 1(2), 85-89.

Andrew, J. & Cooper, G. (2005) Microtidal Coasts. In: Schwartz M.L. (eds) Encyclopedia of Coastal Science. Encyclopedia of Earth Science Series. Springer, Dordrecht

Arnold Jr, C. L., & Gibbons, C. J. (1996). Impervious surface coverage: the emergence of a key environmental indicator. *Journal of the American planning Association* 62(2), 243-258.

Arrigo, K.R. (2005). Marine microorganisms and global nutrient cycles. *Nature 437,* 349-55.

Blackwell, K. D. & Oliver, J.D. (2008). "The ecology of *Vibrio vulnificus*, *Vibrio cholerae*, and *Vibrio parahaemolyticus* in North Carolina estuaries." *The Journal of Microbiology* 46(2), 146-153.

Bouman, H. A., Platt, T., Doblin, M., Figueiras, F. G., Gudmudsson, K., Gudfinnsson, H. G., & Sathyendranath, S. (2017). Photosynthesis-irradiance parameters of marine phytoplankton: Synthesis of a global data set. *Earth System Science Data Discussions* 1-32. doi:10.5194/essd-2017-40

Boyer, J. N., Christian, R., & Stanley, D. (1993). Patterns of phytoplankton primary productivity in the Neuse River estuary, North Carolina, USA. *Marine Ecology Progress Series* 97, 287-297. doi:10.3354/meps097287

Boyer, J. N., Kelble, C. R., Ortner, P. B., & Rudnick, D. T. (2009). Phytoplankton bloom status: Chlorophyll a biomass as an indicator of water quality condition in the southern estuaries of Florida, USA. *Ecological Indicators, 9*(6). doi:10.1016/j.ecolind.2008.11.013

Burns, D., Vitvar, T., McDonnell, J., Hassett, J., Duncan, J., & Kendall, C. (2005). Effects of suburban development on runoff generation in the Croton River basin, New York, USA. *Journal of Hydrology* 311(1-4), 266-281.

Caldwell, D. H. (1946). Sewage Oxidation Ponds: Performance, Operation and Design. *Sewage Works Journal* 18(3). Retrieved November 7, 2018.

Carli, A., et al. (1993) "Occurrence of Vibrio alginolyticus in Ligurian coast rock pools (Tyrrhenian Sea, Italy) and its association with the copepod *Tigriopus fulvus* (Fisher 1860)." *Applied and environmental microbiology* 59(6), 1960-1962.

Chen, C. A., & Borges, A. V. (2009). Reconciling opposing views on carbon cycling in the coastal ocean: Continental shelves as sinks and near-shore ecosystems as sources of atmospheric CO2. *Deep Sea Research Part II: Topical Studies in Oceanography,* 56(8-10), 578-590. doi:10.1016/j.dsr2.2009.01.001

Chorus I. & Bartram J., eds. (1999). *Toxic cyanobacteria in water: a guide to their public health consequences, monitoring and management.* London, United Kingdom: E. and F.N. Spon.

CHROMagar. (2018). *CHROMagar Vibrio*, American Type Culture Collection.

Cloern, J. E. (2001). Our evolving conceptual model of the coastal eutrophication problem. *Marine Ecology Progress Series* 210, 223-253. doi:10.3354/meps2102

Dame, R. F. (1993). The role of bivalve filter feeder material fluxes in estuarine ecosystems. In *Bivalve filter feeders* (pp. 245-269). Springer, Berlin, Heidelberg.

Defne, Z. and Ganju, N. (2015). Quantifying the Residence Time and Flushing Characteristics of a Shallow, Back-Barrier Estuary: Application of Hydrodynamic and Particle Tracking Models. *Estuaries and Coasts* 38(5), https://doi.org/10.1007/s12237-014-9885-3.

Dietz, M. E. & Clausen, J. C. (2005). A field evaluation of garden flow and pollutant treatment. *Water, Air, and Soil Pollution* 167(1-4), 123-138.

Duda, A.M. & K.D. Cromartie. (1982). Coastal Pollution from Septic Tank Drainfields. . 108(6),1265-1279.

Egidius, E. (1987). Vibriosis: pathogenicity and pathology. A review. *Aquaculture* 67(1-2), 15-28.

Fisher, T. R., Carlson, P. R., & Barber, R. T. (1982). Carbon and nitrogen primary productivity in three North Carolina estuaries. *Estuarine, Coastal and Shelf Science* 15(6), 621-644. doi:10.1016/0272-7714(82)90076-2

Fisher, T.R., Harding, L.W., Stanley, D.W., & Ward, L.G. (1988). Phytoplankton, nutrients, and turbidity in the Chesapeake, Delaware, and Hudson River Estuaries. *Est Coastal Shelf Sci* 27, 61-93.

Flood, J. F. & Cahoon, L. B. (2011). Risks to coastal wastewater collection systems from sea-level rise and climate change. *Coastal Education & Research Foundation* 27(4), 652-660.

Fries, J. S., Characklis, G. W., & Noble, R. T.. (2008). "Sediment–water exchange of *Vibrio* spp. and fecal indicator bacteria: implications for persistence and transport in the Neuse River Estuary, North Carolina, USA." *Water Research* 42(4-5), 941-950.

Froelich, B. A., et al. (2017). "Differences in abundances of total *Vibrio* spp., *V. vulnificus*, and *V. parahaemolyticus* in clams and oysters in North Carolina." *Applied and environmental microbiology* 83.2e02265-16.

Gilbert P.M. (2016) Algal Blooms. In: Kennish M.J. (ed) Encyclopedia of Estuaries. Encyclopedia of Earth Sciences Series. Springer, Dordrecht.

Gittman, R.K., Fodrie, F.J., Popowich, A.M., Keller, D.A., Bruno, J.F., Currin, C.A., Peterson, C.H., & Piehler M.F. (2015). Engineering away our natural defenses: an analysis of shoreline hardening in the US. *Frontiers in Ecology and the Environment* 13(6), 301–07.

Glasoe, S., & Christy, A. (2004). Coastal urbanization and microbial contamination of shellfish growing areas. *Puget Sound Action Team Publication (PSAT). Olympia, WA*, 04-09.

Herbert, R. A. (1999). Nitrogen cycling in coastal marine ecosystems. *FEMS Microbiology Reviews* 23, 563–590.

Hobbie, S. E., et al. (2017). Contrasting nitrogen and phosphorus budgets in urban watersheds and implications for managing urban water pollution. *Philosophical Transactions of the Royal Society B: Biological Sciences, The Royal Society* doi.org/10.1073/pnas.1618536114.

Holland Consulting Planners, Inc. (2008). *Town of Atlantic Beach Core Land Use Plan*. Wilmington, p.19.

Jassby, A. D., & Platt, T. (1976). Mathematical formulation of the relationship between photosynthesis and light for phytoplankton. *Limnology and Oceanography,* 21(4), 540-547. doi:10.4319/lo.1976.21.4.0540

Jin, G., et al. (2004): "Comparison of *E. coli*, enterococci, and fecal coliform as indicators for brackish water quality assessment." *Water environment research* 76(3), 245-255.

Johnson, D., Stocker, R. H. , Imberger, J., & Pattiaratchi, C. (2003). A compact, low-cost GPS drifter for use in the oceanic nearshore zone, lakes, and estuaries. *J. Atmos. Oceanic Technol.* 20 1880–1884.

Kaysner, C. A & DePaolo, A. (2004), "Laboratory Methods - BAM: Vibrio." *U S Food and Drug Administration Home Page*, Center for Food Safety and Applied Nutrition, www.fda.gov/food/foodscienceresearch/laboratorymethods/ucm070830.htm.

Kirby-Smith, W. B. (1994). Export of fecal coliform bacteria from freshwater into estuaries. Technical Report for North Carolina Department of Environment, Health, and Natural Resources.

Lefèvre, N., et al. (2013). "Modeling Carbon to Nitrogen and Carbon to Chlorophyll a Ratios in the Ocean at Low Latitudes: Evaluation of the Role of Physiological Plasticity." *Limnology and Oceanography* aslopubs.onlinelibrary.wiley.com/doi/abs/10.4319/lo.2003.48.5.1796.

Lewis, M., & Smith, J. (1983). A small volume, short-incubation-time method for measurement of photosynthesis as a function of incident irradiance. *Marine Ecology Progress Series* 13, 99-102. doi:10.3354/meps013099

Li, H., Sharkey, L. J., Hunt, W. F., & Davis, A. P. (2009). Mitigation of impervious surface hydrology using bioretention in North Carolina and Maryland. *Journal of Hydrologic*

Engineering 14(4), 407-415.
Li, W., Lewis, M., & Harrison, W. (2012). Multiscalarity of the nutrient–chlorophyll relationship in coastal phytoplankton. *Estuaries and Coasts* 33, 440-447.
LUMCON's Guide to Phytoplankton – An online taxonomic guide. (n.d.). Retrieved from https://phytoplanktonguide.lumcon.edu/
Mallin, M. A. (2013). Septic systems in the coastal environment: Multiple water quality problems in many areas. *Monitoring water quality, quality—pollution assessment, analysis and remediation* 81-102.
McMichael, A. J. (2015). "Extreme weather events and infectious disease outbreaks." *Virulence* 6(6),. 543-547.
Monsen, N.E., Cloern, J. E., & Lucas, L. V. (2002). A comment on the use of flushing time, residence time, and age as transport time scales. *Limnology and Oceanography* 47(5), 1545–1553.
Mõttus, M., Sulev, M., Baret, F., Lozano, R. L., & Reinart, A. (2011). Photosynthetically Active Radiation: Measurement and Modeling. *Encyclopedia of Sustainability Science and Technology*. doi:10.1007/springerreference_310766
Myers, S. S., Gaffikin, L., Golden, C. D., Ostfeld, R. S., Redford, K. H., Ricketts, T. H., Turner, W. R., & Osofsky, S. A. (2013). Human health impacts of ecosystem alteration. *Proceedings of the National Academy of Sciences of the United States of America* 110(47), 18753-18760.
National Ocean and Atmospheric Administration. (2013, March 26). What percentage of the American population lives near the coast?. http://oceanservice.noaa.gov/facts/population.html.
NCDEQ. (2018). *Recreational Water Quality*. [online] Available at: http://portal.ncdenr.org/web/mf/recreational-water-quality [Accessed 20 Nov. 2018].
Newell, R. I. (1988). Ecological changes in Chesapeake Bay: are they the result of overharvesting the American oyster, Crassostrea virginica. *Understanding the estuary: advances in Chesapeake Bay research* 129, 536-546.
Nichols, P. (2012). *Vertical Urban Reefs: A comparative analysis of Crassostrea virginica communities on different bulkhead materials* (Rep.).
NOAA/NOS/CO-OPPS (2018). Winds at 8656483, Beaufort, Duke Marine Lab NC (Meteorological Observations). Retrieved at https://tidesandcurrents.noaa.gov/met.html?id=8656483.
NOAA/NOS/CO-OPS (2018). Tide Predictions at 8656590, Atlantic Beach Triple S Pier NC. Retrieved at https://tidesandcurrents.noaa.gov/
North Carolina Office of State Budget and Management. (2017, October 15). *Projected Population of the State of North Carolina and North Carolina Counties by Age, Sex, Race, and Hispanic Origin for July 1, 2017 through July 1, 2037.* https://www.osbm.nc.gov/demog/county-projections
Ohrel, R. L., & Register, K. M. (2006). *Volunteer estuary monitoring: a methods manual*. Ocean Conservancy.
Onorevole, K.M., Thompson, S.P., & Piehler, M.F. (2018). Living shorelines enhance nitrogen removal capacity over time. *Ecological Engineering* 120, 238–248.
Paerl, H. W. (2009). Controlling eutrophication along the freshwater-marine continuum: dual nutrient (N and P) reductions are essential. *Estuaries and Coasts 32*(4), 593-601.
Paerl, H. W., Hall, N. S. Peierls, B. L., & Rossignol, K. L. (2014). Evolving paradigms and challenges in estuarine and coastal eutrophication dynamics in a culturally and climatically stressed world. *Estuaries and Coasts* 37(2), 243-258.
Palanisamy, A. & Gurugnanam, B. (2014). Evaluating the normalized difference vegetation index using Landsat data by by envy in Salem District, Tamilnadu, India. *International Journal of Development and Research* 4(9), 1845-1846.
Parker, J. K., McIntyre, D., & Noble, R. T. (2010). Characterizing fecal contamination in

stormwater runoff in coastal North Carolina, USA. *Water research* 44(14), 4186-4194.
Rao, Y. R., Keshari, A. K., & Gosain, A. K. (2013). Nitrogen Loading from Septic Tanks in the Coastal Plains. *Asian Journal of Water, Environment and Pollution* 10(4), 65-76.
Raquet, M., Williams, M., & Kucken, D. (2006). Chapter 10: Bacterial and Water Quality Impacts. In A Citizen's Guide to Water Quality Management in North Carolina (2nd ed.).
Redfield, A.C. (1963). The influence of organisms on the composition of seawater. *The Sea* 2, 26-77.
Riedel, T., Lettmann, K., Beck, M., and Brumsack, H. J. (2010). Tidal variations in groundwater storage and associated discharge from an intertidal coastal aquifer. *J. Geophys. Res.* 115, C04013, doi:10.1029/2009JC005544.
Riisgaard, H.U. (1988). Efficiency of particle retention and filtration rate in 6 species of Northeast American bivalves. *Marine Ecology Progress Series* 45, 217–223.
Ritts, D. & Larson, J. (1984). A Hydrological, Chemical, and Biological Study of the Pine Knoll Shores Canal.
Robertson, W. D., Cherry, J. A., & Sudicky, E. A. (1991). Ground□water contamination from two small septic systems on sand aquifers. *Groundwater*, 29(1), 82-92.
Sanctuary, F. K. (2011, April 07). Water quality describes the condition of the water, including chemical, physical, and biological characteristics, usually with respect to its suitability for a particular purpose such as drinking or swimming. Retrieved from https://floridakeys.noaa.gov/ocean/waterquality.html
Savenije, H. G. (2006). *Salinity and tides in alluvial estuaries*. Elsevier.
Schiavinato, L., & O'Hara, T. (2016). Nutrient pollution in North Carolina's waters: the innovation of numeric criteria as a management strategy. *Duke Environmental Law & Policy Forum* 26(2), 205-239.
Schueler, T. (2000). The importance of imperviousness. *Watershed Protection Techniques 1*, 100-111.
Schueler, T. (1995). The peculiarities of imperviousness. *Watershed Protection Techniques 2*, 233-238.
Selvakumar, A., & Borst, M. (2006). Variation of microorganism concentrations in urban stormwater runoff with land use and seasons. *Journal of Water and Health 4*(1), 109-124.
Sewers, S. D. G. (2000). Decentralized Systems Technology Fact Sheet.
Shergill, S. S. & Pitt, R. (2004). "Quantification of *Escherichia coli* and Enterococci levels in wet weather and dry weather flows." *Proceedings of the Water Environment Federation*, vol. 2004, no. 10 pp. 746–774., doi:10.2175/193864704784131446.
Smayda, T. J. (1997). Harmful algal blooms: Their ecophysiology and general relevance to phytoplankton blooms in the sea. *Limnology and Oceanography, 42*(5part2), 1137-1153. doi:10.4319/lo.1997.42.5_part_2.1137
Smith, V. H. (1990). Effects of nutrients and non-algal turbidity on blue-green algal biomass in four North Carolina reservoirs. *Lake and reservoir management* 6(2), 125-131.
Stumpf, R. P. (1983). The process of sedimentation on the surface of a salt marsh. *Estuarine, Coastal and Shelf Science* 17(5), 495-508.
Surface Waters and Wetland Standards. (2007). North Carolina Division of Environment and Natural Resources. Division of Water Quality Redbook, NC Administrative Code 15A NCAC 02B .0100, .0200 & .0300.
Taylor, B. L. (1993). The Influences of Wetland and Watershed Morphological Characteristics and Relationships to Wetland Vegetation Communities. *University of Washington*.
Temmerman, S., Meire, P., Bouma, T. J., Herman, P. M., Ysebaert, T., & De Vriend, H. J. (2013). Ecosystem-based coastal defence in the face of global change. *Nature* 504(7478), 79.
Theuerkauf, S. J., Burke, R. P., & Lipcius, R. N. (2015). Settlement, growth, and survival of eastern oysters on alternative reef substrates. *Journal of Shellfish Research* 34(2), 241-250.

UCMP (1997, September 7). Photosynthetic Pigments. Retrieved from http://www.ucmp.berkeley.edu/glossary/gloss3/pigments.html

U.S. Environmental Protection Agency (USEPA). (1986). Bacteriological Ambient Water Quality Criteria for Marine and Fresh Recreational Waters. EPA 440/5-84-002. EPA Office of Water. PB-86-158-045.

USEPA. (2002). "Method 1600: Enterococci in Water by Membrane Filtration Using Membrane Enterococcus Indoxyl Beta D Glucoside Agar (mEI)."

USEPA. (2016). *What Climate Change Means for North Carolina, US EPA* [online]. Available at https://19january2017snapshot.epa.gov/sites/production/files/2016-09/documents/climate-change-nc.pdf [Accessed Dec. 4, 2018].

USGS. (2009). High Resolution Orthoimagery: 3641663_OC6I037000206375022012, USGS EROS. [online] Available at: https://lta.cr.usgs.gov/high_res_ortho [accessed Sept. 14, 2018].

USGS. (2018). *Estimated Depth to Water, North Carolina*. USGS Open-File Report. [online] Raleigh: U.S. Geological Survey. Available at: https://www2.usgs.gov/water/southatlantic/publications/ofr01487/index.html#metadata [Accessed 16 Nov. 2018].

Withers, P. J., Jordan, P., May, L., Jarvie, H. P., & Deal, N. E. (2014). Do septic tank systems pose a hidden threat to water quality?. *Frontiers in Ecology and the Environment* 12(2), 123-130.

Yang, Z., Liang, T., Li, K., Zhang, Q., & Wang, L. (2016). The diffusion fluxes and sediment activity of phosphorus in the sediment–water interface of Poyang Lake. *Journal of Freshwater Ecology* 31(4), 521–531.

Zolch, T., Henze, L., Keilholz, P., Pauleit, S. (2017). Regulating urban surface runoff through nature-based solutions- An assessment at the micro-scale. *Elsevier* 157, 135-144.

Zweifel, U. L., Norrman, B. and Hagstrom, A. (1993). Consumption of dissolved organic carbon by marine bacteria and demand for inorganic nutrients. *Mar. Ecol. Progr. Ser.* 101: 23-32.